Department of Chemical Engineering

Green Biochar based Catalysts for the Cleaning of Syngas Produced from Solid-Fuels Gasification

Matthew Ian Witham

This thesis is presented for the Degree of
Doctor of Philosophy
of
Curtin University

December 2017

AUTHOR'S DECLARATION

To the best of my knowledge and belief this thesis contains no material previously published by any other person except where due acknowledgment has been made.

This thesis contains no material which has been accepted for the award of any other degree or diploma in any university.

Signature:  .....

Date: 13/12/17

DEDICATION

To my loving partner and family

ABSTRACT

In Australia, fossil fuels such as coal, oil, and gas are still playing vital roles in meeting the nation's energy demands. These sources of energy are cheap and readily available but their use is under scrutiny due to their significant contribution to greenhouse gas emissions, in particular carbon dioxide, which is known to be the main cause of global warming. As a result, there is extensive research being conducted in the area of renewable energy creating a renewed push for sustainable and cost-effective renewable energy methods to be commercialised. One such renewable energy source is biomass. In the south-west region of Western Australia, mallee eucalyptus is planted in a practice known as alley farming to reduce dry-land salinity. This biomass is fast growing and can easily be regrown from coppices and is produced on a large scale, therefore making it a prime candidate as a sustainable and cost-effective energy source.

Biomass gasification is a promising technology for harnessing the energy from biomass-based fuels. There are two challenges facing the conventional biomass gasification technologies. One is the production of a tar-containing syngas, which is detrimental to the downstream equipment. Cleaning methods such as using physical processes to remove the tar or adapting mineral based catalysts to crack the tar have been widely used. These methods can be problematic due to high costs and maintenance difficulties. The other is the disposal of spent catalysts when mineral based catalysts are used.

One approach to address these challenges is the use of a two-stage reactor featuring the pyrolysis of biomass in the first stage followed by the steam reforming of the tar-containing gas. Biochar-based catalysts, which can be prepared from the biochar produced in the pyrolysis stage, are used for syngas cleaning. The use of biochar-based catalysts offers several critical benefits including 1) eliminating the disposal issue associated with the spent biochar because the spent biochar can be returned to soil where the biomass is grown; 2) recycling nutrients in the biochar for compensating nutrients export due to biomass production; 3) amending soil quality because of the ability for the biochar to hold fertilisers and water; and 4) achieving carbon

biosequestration. This creates a carbon negative process and has economic benefits through the awarding of carbon credits due to carbon sequestration.

This thesis aims to develop a method to clean tar-containing syngas to a level where it is suitable for downstream applications using catalysts derived from biochar produced from biomass pyrolysis, whilst allowing the collection of the spent catalyst to be used as a soil amendment product. The specific objectives of are to: (1) analyse the pyrolysis of naphthalene over biochar-based catalysts loaded with different metallic species in order to evaluate the effectiveness of the catalyst loading and to better understand the reaction mechanism; (2) simulate a moving bed of biochar to study the steam reforming of naphthalene with increasing bed depth and to analyse the properties of the biochar collected from the outlet of the bed; (3) replace the naphthalene model compound with a tar-containing syngas produced from the continuous fast pyrolysis of biomass in order to determine whether the moving bed of catalyst can cope with real tar components and if it can be scaled up into a large-scale electricity production plant; and (4) test the agronomical benefits of adding the biochar into the soil where the biomass is regrown in order to enhance the growth properties of the soil, including increasing water holding capacity and nutrient concentrations.

Firstly, this study reports the naphthalene pyrolysis (the first step of catalytic naphthalene elimination) over biochars loaded with various metallic species at 900 °C. It was found that the raw biochar exhibits little catalytic ability for eliminating naphthalene in the gas stream under the conditions. However, such a catalytic ability is substantially increased when biochars are loaded with metallic species (K, Mg or Fe). An initial spike in the release of carbon monoxide is evident in the product gas upon a metal (K, Mg or Fe)-loaded biochar is exposed to naphthalene, at the expense of oxygen in the biochar. The process of oxygen depletion is accompanied with the losses of metallic species from the biochar-based catalysts. The results suggest that during naphthalene pyrolysis over biochars loaded with metallic species, naphthalene reacts with the oxygen in the biochar to produce hydrogen gas, H_2O and coke that deposits on the surface of biochar, leading to the catalyst deactivation. There was no evidence of large aromatic compounds in the outlet gas as the result of the polymerisation of naphthalene.

Secondly, even though naphthalene pyrolysis was observed over biochar based catalyst, it is not a sustainable method to clean syngas due to the deactivation of the catalyst. A simulated moving bed of biochar catalyst is an innovative and effective way to clean syngas under steam reforming conditions as the biochar is activated in the upper portion of the bed and can be removed once the catalyst is spent. It was shown by simulating a moving bed of K-Form biochar that the naphthalene concentration in the syngas can be reduced to 15 mg/m^3. The space time for the gas in the moving bed was 0.775 seconds. The steam utilisation efficiency of this process was 78% and the conversion of the carbon in the catalyst was limited to 26%. By studying the gas at the outlet of the moving bed it was found that the gas is formed at a rate of approximately 0.9 to 0.95 mmol per minute per gram of biochar on a dry ash free basis with hydrogen and carbon monoxide being the prominent components of the gas. Approximately 75% by volume of this gas coming from the steam reforming of naphthalene and the remaining from the steam gasification of biochar and the water-gas shift reaction. The lower heating value of this gas ranges between 215 to 225 J/min/g of biochar (daf basis). The concentration of methane was restricted to 700 ppm in the outlet gas. This is promising if the gas is to be used in Fisher-Tropsch synthesis. The primary use for the spent biochar is through the addition to the soil to increase the growing capabilities of the soil. The average H/C and O/C for the final product were 0.0781 and 0.0639 respectively. Hence the biochar is extremely stable when added to the soil. Through the steam gasification of the biochar, the surface area is increased from 20 to 700 m^2/g, potentially increasing the water holding capacity of the biochar.

Thirdly, based on the knowledge obtained in the previous chapter, an industrial scale process can be adopted where biomass undergoes pyrolysis to produce biochar, tar, and non-condensable gases followed by the reforming of the tar over the moving bed of biochar to produce a clean syngas. The first stage of this analysis is to create a pilot scale plant with the pyrolysis zone at 500 °C and the steam reforming at 830 °C. At a biomass addition rate of 0.2 g/min and a total gas flow of 2 L/min, the tar concentration in the gas at the exit in the absence of the biochar catalyst was 3600 mg/m^3. The components of this tar were benzene, toluene, naphthalene, acenaphthene, phenanthrene, and pyrene. After passing the tarry syngas through the moving bed of biochar, the tar content was reduced to 100 mg/m^3 with 80 % of the benzene, 95% of the toluene and naphthalene, and 99% of the acenaphthalene reformed and no evidence

of phenanthrene, and pyrene in the tar. The naphthalene concentration in the tar was 44 mg/m^3. By scaling these results up to 200 dry tons of biomass per day, a plant with an electricity output of 6.57 MW can be constructed at a capital investment of $AU 36.5M and a production cost of 10.201 AU¢ per kWh. The gas engine efficiency and biomass production/transport costs had the most effect on the electricity cost with the process being resilient to changes in carbon credit price.

Finally, introducing biochar to the soil is known to have many agronomical benefits; however, previous studies have only quantified the effect of using biochar prepared via pyrolysis. Biochar collected from the outlet of the moving bed reactor from previous studies have undergone partial gasification therefore it must be determined whether this process increases the benefits that the biochar has the regrowth of the biomass. Despite losses during the moving bed process, the leaching of sodium, potassium, magnesium, calcium, and chlorine is enhanced through partial gasification. After exiting the moving bed, all of the sodium, potassium, and chlorine in the biochar can be leached with only 3.75 and 5.05% of the magnesium and calcium respectively being unleachable. For all biochars, approximately 0.5% of the carbon is water leached, with there being no evidence of aromatic hydrocarbons being leached with water or an organic solvent. Increasing the pyrolysis temperature from 500 °C to 900 °C decreases the water holding capacity (WHC) from 4.10 to 1.07 g water per gram of biochar due to a decrease in oxygen content. Through increasing the surface area via partial gasification, the WHC is increased to 4.62 to 5.80 g water per g biochar. However, when taking into account the mass lost during the moving bed process, the WHC on per gram of biomass added is greater for the 500 °C biochar. Finally, after the inorganic species have been leached from the biochar, sites are available for the biochar to hold species contained in fertiliser such as phosphorus and potassium, known as the anion exchange capacity (AEC) and cation exchange capacity (CEC). The AEC after the steam reforming of naphthalene was 5.68 cmol per kg of biochar and the CEC was 17.3 cmol per kg of biochar. Much lower values were observed in biochars prepared via pyrolysis.

ACKNOWLEDGEMENTS

I gratefully acknowledge the Australian Research Council (ARC) and Australian Postgraduate Award (APA) provided by Curtin University for making this PhD possible.

I would like to give many thanks to my supervisor, Professor Hongwei Wu, for providing me with the opportunity to conduct this research, his continued support and devotion of time throughout my PhD, and for him challenging me to create the best thesis I possibly can. I also extend my thanks to Dr. Xiangpeng Gao for his guidance in the initial stage of my research and his continued support despite moving into another role at a different university.

I express my thanks to the Chemical Engineering Department lab staff Ms. Karen Hayes, Mr. Jason Wright, Mr. Araya Abera, Mr. Xiao Hau, Mr. Andrew Chan, Ms. Ann Carroll, Ms. Anja Werner, Dr. Roshanak Doroshi, Dr. Guanliang Zhou, and Ms. Melina Miralles for their assistance and technical support whilst in the laboratory completing my experimental work. Thank you to Mr. Steve Groves of Groves Manufacturing and Tooling for his fantastic work in constructing the reactor crucial in making this work possible.

Special thanks go to the current and former members of my research group Dr. Sui Boon Liaw, Dr. Mingming Zhang, Dr. Yun Yu, Dr. Mohammad Usman Rahim, Dr. Walter Ikealumba, Mr. Chao Feng, Mr. Bing Song, Ms. Wenran Gao, Ms. Yee Wen Chua, Mr. Yu Long, Dr. Syamsuddin Yani, Mr. Changya Deng and Mr. Xujun Chen for their willingness to share their knowledge and help me out with my experimental work and writing whenever called upon.

Finally I would like to thank my partner Sarah, my family, and my friends for their continued support and words of encouragement whilst completing my PhD.

LIST OF PUBLICATIONS

1. **Matthew Witham**, Xiangpeng Gao, Jun-ichiro Hayashi, Behdad Moghtaderi, Hongwei Wu. Pyrolysis of Naphthalene over Metal Loaded Biochars at 900 °C, to be submitted to Energy & Fuels

2. **Matthew Witham** and Hongwei Wu. Steam Reforming of Naphthalene over a Simulated Moving Bed of K-loaded Biochar, to be submitted to Fuel

3. **Matthew Witham** and Hongwei Wu. Two-Stage Fast Pyrolysis of Biomass and Steam Reforming of Tar over a Moving Bed of Biochar Catalyst: Proof of Concept and Economic Analysis, to be submitted to Energy & Fuels

4. **Matthew Witham** and Hongwei Wu. Environmental Benefits of Sequestering Biochar Collected from a Moving Bed Reactor, to be submitted to Fuel

TABLE OF CONTENTS

LIST OF FIGURES

LIST OF TABLES

CHAPTER 1 INTRODUCTION

1.1 Background and Motive

Australia's electricity needs are predominately supplied through fossil fuel sources with 82.7 - 94.2% supplied from coal, oil and gas [1, 2]. Such a high reliance on fossil fuels greatly contributes to the release of CO_2, which is known to contribute to global warming. With the global average temperature in 2017 increasing by up to 2 °C when compared to historical data [3], changes must be made in the nature of electricity production in Australia. In 2017, 5.8 - 17.3% of Australia's electricity production comes from renewable energy sources such as hydro, biomass, solar, and wind [1, 2]. Several targets have been set in regards to renewable energy production depending on the state or territory. The Australian Capital Territory has a target set of 100 % of the electricity produced from renewable energy sources by 2020, whilst Western Australia has yet to have a target set [1].

A promising source of renewable energy production in Australia is biomass with it contributing to 8.6% of renewable sources and 0.9 - 1.49% of the total electricity production [1, 4]. A possible source of biomass comes from the south-west region of Western Australia. Mallee eucalyptus previously dominated the landscape; however, it has been cut down to plant wheat and other crops. As a result the water table rose increasing the salinity in the soil therefore making it difficult to grow the crops. To combat the salinity in the soil, the mallee eucalyptus was replanted in a fashion known as alley farming, which integrates the mallee within the crops [5, 6]. These trees are fast growing and can be easily regrown from coppices [6]. As there is no competition in land dedication between the mallee and the crops and they are easily regrown, mallee eucalyptus in the south-west region is a promising second-generation renewable energy source [7-9].

The leading method used to utilise the energy contained within biomass is gasification using a gasifying medium such as steam, air, or carbon dioxide to produce a high energy syngas [10-14]. One issue related with this process is the presence of tar within the syngas. The nature of these tar components varies significantly depending on the

operating temperature and range from straight chain hydrocarbons to large aromatic ring structures [15-20]. The presence of tar in syngas is undesirable as it contributes to the corrosion of the equipment used to convert the syngas to electricity [21, 22]. The limit of how much tar in the syngas is acceptable depends on the use of the syngas. If the syngas is to be used in a gas engine, the concentration of tar in the syngas needs to be lower than 100 mg/m^3, whereas syngas designed to undergo Fischer-Tropsch synthesis requires a tar concentration of less than 1 mg/m^3 [23-25].

After gasification of biomass, tar concentrations in the syngas can range anywhere from 1 500 to 150 000 mg/m^3 depending on biomass feed and reactor configuration [24, 26-31]. Several methods exist to remove tar and produce a clean syngas. The simplest method to clean the syngas is through physical methods such as a cyclone or a filter; however these methods need regular cleaning increasing downtime in the process [29, 31, 32]. Mineral based catalysts can be used, with three common types employed; nickel based, dolomite based, and iron based [33]. These catalysts have been adopted in many process to clean syngas, however, they need to be purchased, often foul quickly, and need to be disposed of once they are spent. One alternative to mineral based catalysts are biochar-based catalysts [34-37]. The use of these catalysts are particularly attractive as they are produced in the gasification process and therefore do not need to be purchased. Biochar on its own is not considered a good catalyst and it often needs to be doped in order to be effective in cleaning syngas.

Another benefit of using biochar-based catalysts over mineral-based catalysts are how easily they can be disposed when spent. One such option for the spent biochar catalyst is further gasification to produce more syngas [38-41]. An alternative to gasification is adding the biochar into the soil where the biomass is grown. This results in the sequestration of carbon, therefore making the gasification process carbon negative. Other than carbon bio-sequestration, further benefits of adding biochar to the soil include the leaching of nutrients contained within the biochar [42-46], increased water holding capacity [47], and increased retention of fertilisers added to the soil [48, 49].

Despite there being extensive studies on the behaviour of tar species over biochar based catalysts, there are still significant research gaps in this area. There are few studies that study the fundamentals of the interaction that model tar compounds have with biochar catalysts, particularly in the absence of a gasifying agent. The study of

this interaction is crucial in developing an understanding of the tar reforming mechanism in order to improve the design of an effective method of cleaning syngas. The previous literature on the cleaning of syngas over biochar catalysts predominately focus on reforming over a fixed bed of biochar. This reactor configuration is impractical to adopt on a larger scale as a significant amount of downtime is needed to replace the catalyst when spent. Finally, the benefits that adding biochar as a soil amendment has on the growth of plants but the majority of the tests have been completed on biochar collected from pyrolysis and there is little information on the effect that partial gasification has on the agronomical benefits. A fundamental study is required to develop a continuous method of cleaning tar-containing syngas using a biochar based catalyst whilst allowing the spent biochar to be collected and recycled.

1.2 Scope and Objectives

The aim of this thesis is to investigate the fundamentals of tar reforming over biochar based catalysts. The conclusions made in the fundamental studies will then be used to develop a novel two-stage pyrolysis/reforming process to clean syngas over a moving catalyst bed and allow for the collection and recycling of the used biochar catalyst. The detailed objectives of this study are:

1. To develop an understanding of how the tar model compound naphthalene is cracked over several biochar based catalysts under pyrolysis conditions.

2. To investigate the effectiveness of a moving bed of biochar-based catalyst on the steam reforming of naphthalene and to quantify the influence the moving bed gasification and steam reforming of naphthalene has on the quality of the syngas produced.

3. To build on the conclusions in the steam reforming of naphthalene to determine whether a two-stage process of pyrolysis of biomass followed by the steam reforming of the produced tar over a moving bed of biochar catalyst can produce a clean, high energy syngas. The lab scale process will then be upscaled into an industrial scale process, which includes a detailed cost analysis.

4. To quantify the benefits of adding the biochar collected from the moving bed experiments to the soil where the biomass is grown.

1.3 Thesis Outline

Including this chapter, this thesis consists of 8 chapters, which is schematically represented in

Figure 1-1. The outline of this thesis is as follows:

- Chapter 1 introduces the significance of the research and outlines the scope and objectives of the thesis

- Chapter 2 serves as a review of the current literature available on the gasification of biomass to produce a syngas and the subsequent cleaning of the syngas from tar components. This section will also highlight the gaps in the literature and outline the detailed objectives.

- Chapter 3 provides details on the methodology used to achieve the objectives of this thesis including outlining the sample preparation, experimental rigs used, and the analytical techniques used to quantify the properties of the samples.

- Chapter 4 investigates the behaviour of naphthalene over four different biochar-based catalysts under pyrolysis conditions in regards to the extent at which it is cracked and how it is cracked.

- Chapter 5 employs a moving bed of biochar-based catalyst to determine the extent at which naphthalene is steam reformed over this catalyst configuration and to quantify the quality of the syngas produced from the steam reforming of naphthalene and steam gasification of biochar

- Chapter 6 expands on the results of chapter 5 by replacing the naphthalene model compound with a tar-containing syngas produced from the continuous fast pyrolysis of biomass. The results generated in the laboratory will then be up scaled into an industrial process and a detailed cost analysis completed on the process.

- Chapter 7 outlines the benefits that adding biochar to the soil has on the growth properties on the soil including quantifying the leaching capabilities, the water holding capacity, and the exchange capacities of the biochars collected from the exit of the moving bed.

- Chapter 8 summarises the current study and presents the recommendations for future studies

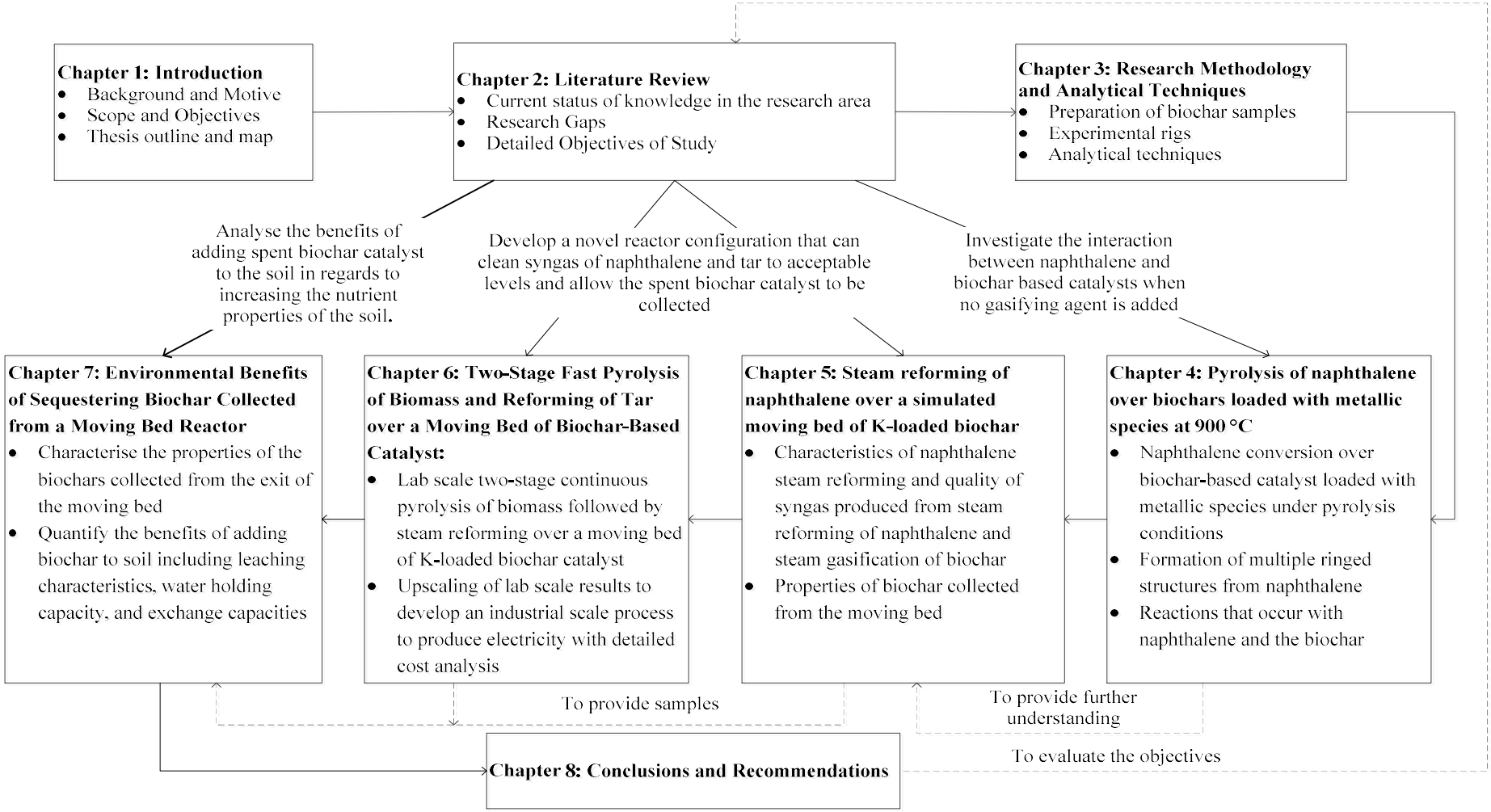

Figure 1-1: Thesis Map

CHAPTER 2 LITERATURE REVIEW

2.1 Introduction

Biomass as a steady and sustainable source of energy has a bright future in the South-West region of Western Australia [7-9]. Mallee Eucalyptus is planted in this area to reduce salinity in the soil and, as it regularly needs to be cut down, the biomass to energy process can take advantage of a pre-existing waste product [5, 6]. The energy contained within the biomass can be utilised by converting the solid to a syngas containing carbon monoxide and hydrogen, which can then be subsequently combusted. The process of converting biomass to syngas starts with pyrolysis, where the biomass is heated to temperatures between 450 and 500 °C in the absence of oxygen [50]. Pyrolysis of biomass produces three products; bio-oil, biochar, and syngas [51]. Bio-oil can be further treated to produce a liquid biofuel [52-57], where the biochar can be reintroduced to the soil to enhance the nutrient properties of the soil and aid in carbon sequestration [58-63], However, if an energy rich syngas is required, the bio-oil, biochar, and syngas undergo a process known as gasification. During gasification, the bio-oil and biochar are reacted with a gasifying agent (air, steam, oxygen, or carbon dioxide) to produce a syngas with high carbon monoxide and hydrogen concentrations [10-14]. During this process, the syngas often contains a significant amount of tar related compounds. Tar can be defined as anything with a molecular weight higher than benzene and condenses at ambient conditions [21, 22]. Tar should be limited to 100 mg/m^3 in combustion engines [23]. Two types of catalysts can be used to increase the reforming rate of tar contained in a syngas; mineral catalysts and biochar catalysts. Some examples of mineral catalysts include nickel based ores and iron contained within ilmenite [33, 64-68]. These are often used as they are inexpensive and easily sourced [22, 33]. Biochar based catalysts are an attractive alternative to mineral based catalysts as they are produced in the pyrolysis process and their catalytic activity can be easily maintained [34-37].

The aim of this chapter is to investigate the current literature available on the utilisation of biomass to produce an energy dense, clean syngas via pyrolysis and gasification, identify research gaps in the literature, and outline the intended research outcomes of

this thesis. The first part of this literature review will look into the importance of biomass as a fuel source. It will then move into the fundamentals of biomass pyrolysis and gasification to produce a syngas. During this discussion, the uses of biochar after pyrolysis/gasification will be mentioned. The next stage is to identify the problems associated with the pyrolysis/gasification of biomass. This will lead onto the comparison of biochar based catalysts to mineral based catalysts for the cleaning of syngas. Finally, the gaps in the literature will be identified, and the research objectives finalised.

2.2 Importance of Biomass as a Fuel

The use of fossil fuels as a source of energy is becoming increasingly concerning with the prevalence of global warming being at the forefront of this concern. A viable alternative to fossil fuels is biomass for the production of energy [69-71]. Depending on the source, biomass as a sustainable source of fuel will be carbon neutral and beneficial to the atmosphere in comparison to fossil fuels. If the biomass is cut down from existing forests, there is a significant addition of carbon dioxide to the atmosphere. However, if the biomass is sourced from waste or the trees are replanted, the process becomes carbon neutral [7]. Biomass is also beneficial to the atmosphere in comparison to fossil fuels as biomass contains little sulphur, hence there are minimal emissions of SO_x compounds [52]. Currently biomass contributes 0.9% of the energy production in Australia, with this number expected to increase to 4.4% by the year 2040 [4]. Depending on the location where the energy is required, the source of the biomass can vary drastically. Studies have been completed on the use of wood [72-74], sewage sludge [10, 75], algae [76], food waste [77], and sunflower seeds [78] as biomass based fuels for energy production.

In the south west of Western Australia, there is a potential gap in the market for the use of biomass as a sustainable source of energy [7]. Salinity is a massive issue in farming in this area as it can create issues in the growth of crops [8, 9]. To reduce the salinity in the soil, Mallee Eucalyptus (*E.loxophleba lissophloia*) is planted in a process known as alley farming [5]. The planting of trees in a farming environment is beneficial as they help maintain the water level to reduce the salinity in the soil. Mallee Eucalyptus is particularly beneficial as it is native to this region and, due to its outstanding coppicing ability, can be harvested every 3-7 years [6]. Despite the

significant potential for this biomass being used as a sustainable source of energy, it needs to be processed close to its source as there are major costs associated with the transport of the raw biomass [7, 79, 80].

Three major components of the mallee biomass are of importance when using it as a fuel; bark, wood, and leaf. A typical tree of mallee eucalyptus consists of 25, 40, 35 % by mass of bark, wood, and leaf respectively [79]. The composition of each of the components of the tree is shown in Table 2-1 [81-83]. All three components of the mallee biomass also contain a significant amount of metallic species present. These species are predominately the alkali and alkaline earth metals (AAEM's) sodium, potassium, magnesium, and calcium that have been absorbed into the tree from the salinity in the soil. The typical concentrations for these metallic species are given in Table 2-2 [82].

Table 2-1: Moisture content, proximate analysis, and ultimate analysis of different components of Mallee Eucalyptus biomass

		Proximate Analysis, wt% db[d]			Ultimate Analysis, wt % daf[e] basis				
Sample	Moisture[a] wt%	Ash	VM[b]	FC[c]	C	H	N	S	O[f]
Bark	4.9	5.5	67.7	26.8	52.0	6.4	0.39	0.05	40.9
Wood	5.3	0.4	80.7	18.9	49.0	6.7	0.19	0.02	44.1
Leaf	8.3	3.8	74.6	21.6	56.0	7.3	1.46	0.12	34.9

[a]moisture measured after air drying. [b]Volatile matter. [c]Fixed carbon. [d]Dry basis. [e]Dry ash free. [f]Calculated by difference

Table 2-2: AAEM species in Mallee Eucalyptus biomass

Element (wt % db)	Bark	Wood	Leaf
Na	0.2094	0.0212	0.5537
K	0.1105	0.0744	0.3797
Mg	0.0796	0.0364	0.1447
Ca	2.6591	0.1236	0.7652

Converting solid biomass into a form where its energy potential can be fully realised is often a complicated process. The simplest option for processing the biomass is the direct combustion of the raw biomass [84]. This option is not viable with Mallee Eucalyptus without any pre-treatment due to its high moisture content (approximately

45%) [79], low energy density [53], and poor grindability [5]. An alternative to the direct combustion of biomass is the co-firing of biomass with coal. However, due to the same reasons as with the direct combustion of biomass, approximately only 5 % of coal can be substituted with biomass [85, 86]. As a result of these restrictions with the combustion of mallee biomass, the following section will study the different thermochemical methods listed in the literature used to extract the energy from biomass.

2.3 Cost of Large Scale Biomass Treatment to Produce Electricity

As the conversion of biomass to another energy dense product is not a not a new process, therefore there are several large scale production facilities that are operated around the world. Currently there is 55 EJ/year of energy produced from biomass plants, with the majority of this produced in developing countries for cooking and heating [87]. By 2050, there is expected to be 120-160 EJ/year of energy produced from biomass, and this figure increased to 200-250 EJ/year by 2020 [88]. Generally, large scale facilities convert biomass to a liquid fuel, which is then often converted to electricity. Significant capital and operational costs are often associated with these facilities. Capital costs for electricity production from the gasification of biomass via proven technology, such as fixed bed and fluidised beds, are between $US 2140 to 5700 per kW [89]. Production costs for electricity generation at these plants range from $US 0.06 to 0.29 per kWh [89].

Energy production in Australia is a fledgling industry with 8.6% of Australia's renewable electricity coming from biomass sources [1]. One study has been completed at looking at constructing a biomass electricity plant in Australia. This study looked at three power plant capacities 1 MW, 5 MW, and 30 MW. The capital investment for these plants were calculated to be $AU 5.3M, $AU 12.5M, and $AU 47.4M respectively. The resulting electricity production costs in these production plants were 20 ¢AU/kWh, 14.4 ¢AU/kWh, and 10.7 ¢AU/kWh respectively.

Despite there being limited biomass based electricity production in Australia, there are several large scale facilities operational in the US. One study looks at the installation of a 200 dry tone per day biomass plant using corn stover as the feed to produce liquid transport fuel and electricity as a co-product, which is mainly used to power the plant

[90]. This resulted in an output of 193 MW of liquid fuel and 36 MW of electricity with a capital investment of $US 500-650M and an operating cost of $US 1.06-1.32 per litre of fuel. A similar study was completed looking at the same plant capacity (2000 dry tons per day), which produced 40 gallons of gasoline and 44 gallons of diesel per dry ton of biomass [91]. The total capital investment for this production plant was $ 700M with a minimum sale price of $US 0.896 per litre of gasoline. Studies on smaller capacity biomass plants in the US have been completed. A study on a 550 ton per day of wood chip biomass feed yielded a capital investment of $US 48M with a cost of $US 7.62/GJ of energy produced [92]. A similar capacity plant to this at 500 ton per day was calculated to have a capital investment of $US 78.5M [93] indicating there are some significant variations in costs depending on the biomass feed and the process used to convert the biomass to electricity.

A significant cost associated with biomass electricity production are the costs to transport the biomass to the production plant with studies showing that this can be up to 50-60% of the production costs [87]. Costs include the growth and harvesting of the biomass and the transportation of the biomass from the harvester to the bulk transporter and from the farm to the plant [94]. Factors such as farm size and distance from the farm to the plant can have a significant effect on the transportation costs. These costs can be particularly high in the south-west of Western Australia due to the sparse population [94] and consideration must be made in regards to the plant location to minimise these costs [95].

2.4 Pyrolysis of Biomass to Produce Bio-Oil and Biochar

2.4.1 Fundamentals of Biomass Pyrolysis

Based on the available literature, a common method of thermochemically treating biomass to extract the energy is the pyrolysis of biomass. In the context of biomass for fuel production, pyrolysis can be defined as the thermal degradation of solid products in the absence of an oxygenating species such as air or steam. Pyrolysis of biomass at high temperatures produces three products; bio-oil, non-condensable gases, and biochar solid [51]. There are two different forms in which the pyrolysis of biomass are conducted, slow pyrolysis and fast pyrolysis. Slow pyrolysis involves heating the biomass from ambient temperature to the pyrolysis temperature at a fixed heating rate. This method of heating can be advantageous if biochar is the desired product [73, 96].

The other method is fast pyrolysis, which involves heating up the biomass rapidly in a continuous manner. Generally fast pyrolysis is the preferred pyrolysis method as it can be maintained as a continuous process and produces a larger percentage of bio-oil [51].

During the fast pyrolysis of biomass, temperatures between 450-550 °C are generally used and the desired temperature depends on the biomass feed and the desired products ratio [50]. Typically, pyrolysis of Mallee Eucalyptus biomass is conducted at 500 °C [50]. At this temperature, the ratio of bio-oil to biochar to non-condensable gases is approximately 50, 20, and 30 wt% respectively [51]. Pyrolysis as a process is beneficial due to the increase in heating values of the three products in comparison to raw biomass. In the pyrolysis of Mallee Eucalyptus, the heating value is upgraded from 5 GJ/m^3 for raw biomass to 20 GJ/m^3 for the produced bio-oil [53] and 9 GJ/m^3 for biochar [38]. Completing this upgrade significantly reduces the transport costs associated with biomass.

Pyrolysis of biomass is an attractive process as all components of the biomass can potentially be utilised. The non-condensable gases, such as methane, ethane, and carbon monoxide can be used as a syngas or recycled back into the process [51]. Hydrogen is also produced during the pyrolysis process, however, it is at a such low concentration in the syngas it is often considered insignificant [51]. The main component after pyrolysis and, for the majority of the time is the most desirable product, is bio-oil. Bio-oil is a valuable product of the process due to its capability to be used as a liquid fuel [52, 54]. Finally, the solid biochar can be gasified with steam or oxygen as a further source of energy [38-41], used in carbon sequestration [59-63], or reintroduced to the soil providing many benefits in the soil growth properties [42-46].

2.4.2 Utilising Bio-Oil

As mentioned, the major product in the pyrolysis of biomass is bio-oil. Bio-oil is a complex mixture of organic chemicals produced from the thermal cracking of the cellulose, hemicellulose, lignins contained within the biomass. The composition of the bio-oil depends on the composition of the initial biomass but, more importantly, on the temperature at which the pyrolysis is conducted. At a temperature of 500 °C, typical of biomass pyrolysis, the bio-oil consists mainly of acetic acid and phenolic ethers [97]. Increasing the pyrolysis temperature thermally reforms the less refractory

compounds of the bio-oil [98]. At 800-900 °C, the bio-oil consists mainly of polyaromatic hydrocarbons (PAH's) such as naphthalene and phenanthrene [52, 97]. The large range of components within the bio-oil as well its variability with temperature means that there are a number of different uses available for the bio-oil.

Bio-oil from biomass pyrolysis has similar properties to diesel [55], hence there is the potential for it to be used a source of energy and heat. Due to the high content of water and acetic acid in bio-oil, an upgrading process needs to be completed before it can be used in this manner. This may be through further processing of the bio-oil to reduce these hazardous compounds [99] and/or through the modification of the diesel engine [100].

A predominant use of bio-oil is the production of a syngas that can be combusted as a source of energy [56, 57] or be further processed to form pure chemicals through Fischer-Tropsch synthesis [101]. Syngas from bio-oil consists of valuable components such as hydrogen, carbon monoxide, methane, and ethane and is formed through the gasification of the bio-oil with oxygen and/or steam. As there is no treatment required of the bio-oil before gasification, this process can be completed directly after the pyrolysis. The thermal properties of the syngas can be enhanced through the addition of catalysis to the gasification process [102-104]. Altering the process to promote the formation of hydrogen and carbon monoxide enhances the liquid hydrocarbons formed during Fischer-Tropsch Synthesis [25].

2.4.3 Utilising Biochar

As mentioned previously, a solid product remains after the pyrolysis of biomass known as biochar. Biochar is a highly porous solid with a large surface area consisting mainly of carbon. There are many uses for the remaining biochar, including gasification to produce syngas [38-41], as a specialised catalyst [105-108], or seeing its return to land as a soil amendment material, which enhances carbon bio-sequestration and leaches valuable nutrients into the soil [42-46]. The properties of the biochar as well as the location where the pyrolysis is completed and the desired outcomes have a major influence on how the biochar is used after the pyrolysis process.

Biochar Gasification

The biochar remaining after the pyrolysis to produce bio-oil has the potential to increase the fuel capabilities of the biomass if this energy can be efficiently utilised. One viable option for utilising the biochar is through mixing the biochar with the produced bio-oil to create a bioslurry. A large study was completed on the properties of bioslurries produced from the pyrolysis of Mallee Eucalyptus [5, 53, 109-113]. In this study, it was found that by completing the pyrolysis of biomass and combining the biochar and bio-oil into a bioslurry, the issues associated with the transport costs of the raw biomass are reduced. By combining the bio-oil with the biochar, the volumetric energy density could be increased from 5 GJ/m^3 with raw biomass to 23 GJ/m^3 with a 20 wt% blend of biochar in bio-oil. After the gasification or combustion of the bioslurry, the entire process can be considered carbon negative.

An alternative to creating a bioslurry is the direct gasification of the biochar in a similar process to the gasification of bio-oil discussed previously [38-41]. Due to the energy capabilities of the biochar, considerations have to be made in the pyrolysis process whether to optimise the production of bio-oil or biochar in order to decrease costs and maximise energy output [54]. The gasification of biochar can be completed with steam [11, 75] or carbon dioxide [12-14] to produce a syngas mainly consisting of hydrogen and carbon monoxide. Typically, the gasification of biochar is completed at a higher temperature than the pyrolysis with gasification temperatures ranging from 700-900 °C. Increasing the gasification temperature increases the rate at which the biochar is gasified [114]. The study conducted by Encinar et al. [114] showed that the partial pressure of the gasifying agent, in this case, steam has no influence on the gasification rate of biochar. This study also showed that the particle size of the biochar has very little influence on the gasification rate. It may be also necessary to adjust the conditions of the gasification to selectively produce or restrict the formation of one of the gaseous species. Methane is one of the products formed in the gasification process and can be detrimental to downstream equipment, particularly if the syngas is to be used in Fischer-Tropsch synthesis [115]. Hence, it may be necessary to suppress methane formation during gasification.

Along with the gasification parameters, the conditions of the pyrolysis process have a profound effect on the gasification reactivity of the biochar. A study by Cetin et al.

[116] showed that by using a fast heating rate in pyrolysis, the reactivity of the biochar is increased in comparison to a slow heating rate. This is due to the formation of more macropores in the pyrolysis process. Extensive studies have shown that surface area is known to influence biomass gasification rates [117]. The temperature of the pyrolysis also plays a significant role in biochar reactivity, with higher pyrolysis temperatures increasing the surface area and porous structure of the char, hence increasing gasification reactivity [40, 73, 118, 119].

Biochar as a Soil Amendment

An alternative use for the remaining biochar is its addition back to the soil where the biomass was grown to act as a soil amendment. Biochar is added into the soil at concentrations ranging from 5 - 50 tonnes per hectare [120, 121]. Re-introducing the biochar to the soil has many benefits including carbon sequestration, enhancing soil nutrient properties, and increasing soil water holding capacity [58]. The biochar also has the ability to hold nutrients in the soil, and hence can be useful when fertilisers are added to the soil. By evaluating these properties and comparing them with the available energy within the biochar, it can be determined whether the biochar is more suitable as a source of energy, a soil amendment, or a combination of both.

An important factor in determining the suitability of biochar as a soil amendment is the stability of the biochar when it is added to the soil. If the biochar degrades within the soil, the carbon sequestration potential of the biochar is lost as the regrowing trees will absorb the carbon from the soil opposed to that from the atmosphere. Other beneficial properties such as water holding capacity and cation exchange capacity will be lost over time if the biochar structure changes within the soil [121]. The stability of the biochar can be quantified through the O/C elemental ratio. Organic materials with an O/C greater than 0.6 have a half-life of approximately 10 years within the soil [122, 123]. With a growth cycle of 3-7 years, the O/C ratio of the soil amendment for Mallee Eucalyptus is important. Reducing the O/C ratio to 0.2 increases the half-life of the soil amendment material to 1000 years. Typically, raw biomass has an O/C ratio of more than 1 [122], indicating that it will be not suitable to add back to the soil in terms of carbon sequestration as it will degrade rapidly. After the pyrolysis process, the O/C ratio is reduced to below 0.6 [122], with this ratio decreasing to 0.1 in some instances [124].

As it has been proven that biochar can be extremely stable when added to the soil, biochar produced from the pyrolysis has fantastic potential in terms of carbon sequestration [59-63]. Typically during the pyrolysis process, approximately 50% of the carbon in the biomass is maintained within the biochar whilst the remainder is present in the bio-oil [125]. In the case of the pyrolysis of biomass and subsequent gasification of the biochar as a source of energy, all of the carbon in the biomass is converted into carbon dioxide. This means that the process is carbon neutral as all of the carbon absorbed by the biomass during its growth is released to the atmosphere [79]. If the biochar produced after pyrolysis is to be returned to the soil, the process becomes carbon negative [126]. That is the carbon that is removed from the atmosphere in the growth of the biomass is more than what is released during energy production.

Along with the negative carbon emissions, the returned biochar also has the potential to absorb further carbon dioxide [62, 127]. The further sequestration of carbon dioxide is achieved through the reaction with CO_2, water, and the aromatic groups on the surface of the biochar [62]. A study from Hansen et al. [124] showed that, as well as there being a sorption of carbon dioxide by biochar in the soil, the biochar can reduce the carbon dioxide concentration during the pyrolysis process through binding with the calcium and magnesium present in the char. As well as the potential to further reduce the carbon dioxide content in the atmosphere, the addition of biochar to the soil has also been shown to reduce nitrous oxide and methane contents in the atmosphere [126, 128]. This is particularly important as nitrous oxide and methane are 300 and 23 times respectively more potent greenhouse gases compared to carbon dioxide [126].

Along with the carbon sequestration potential, the use of biochar as a soil amendment has the potential to enhance the nutrient properties within the soil. As shown in Table 2-2, there is a large amount of metallic species present in biomass. The study from Yip et al. [115] showed that 80-90 % of these metals contained within Mallee Eucalyptus biomass are retained within the biochar after pyrolysis. There is also the possibility of metallic species being added to the biomass before pyrolysis to act as a catalyst. This will be discussed in further detail later in this chapter. When added to the soil, these metals and other inorganic compounds can leach out from the biochar into the soil through the washing of the biochar with rainwater [42-46]. Three main contributors to

plant growth that are present in biochar are potassium, nitrogen, and phosphorous [120, 121, 129-132]. As can be seen in Table 2-2, there is a large amount of potassium available to be leached in the biochar even with no further addition of metallic species. Phosphorous and nitrogen are also present in biomass, however, they do not have a high retention in biochar during the pyrolysis process and that which does remain is difficult to leach with water [121]. Other compounds present in biochar, such as calcium, sodium, magnesium, and chlorine are also known to enhance the fertility of the soil [133, 134].

As the inorganic compounds present in the biochar are beneficial to the soil, it may be necessary to consider altering the biochar properties to enhance the leaching capabilities. This can be through changing the pyrolysis conditions [135], altering the raw biomass properties, or through the partial gasification or other treatment of the biochar [136]. A study by Wu et al. [82] showed that through water leaching, all of the potassium and sodium present in the biochar produced from the pyrolysis of Mallee Eucalyptus biomass can easily be removed. However, the magnesium and calcium are not leached to the same extent. This is due to how the inorganic species are bonded on the biochar. It was proposed that the leachable Na and K are bonded to ion-exchangeable carboxylate groups present on the surface of the biochar, whilst the Mg and Ca are bonded to the water insoluble carboxylates. A further study by this research team showed that there is a difference in the leaching characteristics of biochars depending on whether the biochar is produced via slow or fast pyrolysis [135]. Fast pyrolysis biochars have a lower Na and K leachability but an increased Mg and Ca leachability. This is associated with the access that the water has to these surface groups. By increasing the surface area and porosity of the biochar through partial gasification (approximately 5-10% of the carbon in biochar), the access to these inorganic compounds can be increased and the leaching properties enhanced [136].

Along with the inorganic compounds present in biochar, a small amount of the carbon can be leached into the soil. Recent studies have shown that less than 1.5% of the carbon present in biochar is leached into the soil [82, 136]. This leaching will be beneficial as the carbon can aid in the growth of new plants [137]. However, aromatic compounds are often present in this leachable carbon [42, 136], and are particularly hazardous to plant growth and can make their way into water ways, posing a hazard to

human health [138]. Through the partial gasification of the biochar, the biochar becomes free of leachable aromatic compounds [136].

After the leaching of the metallic and anionic species into the soil, active, charged surface groups remain present on the surface of the biochar. Upon the addition of fertilisers to the soil, the positive and negative charged compounds present in the fertilisers, such as potassium and phosphorous, can bond with the available surface groups [121]. What this means is that the fertilisers will be held in the soil at a greater extent and will be more readily available for plant growth. The ability for the biochar to hold the nutrients in the soil can be quantified as properties known as cation and anion exchange capacities [48, 49]. Increasing the anion exchange capacity (AEC) allows the biochar to retain valuable anionic compounds such as phosphorous and chlorine, whilst increasing the cation exchange capacity means the biochar can retain metallic ions such as potassium and magnesium [139, 140]. CEC and AEC are quantified as cmol/kg, meaning the centimoles of bonded anion or cation on the surface of the biochar per kilogram of biochar [141].

The anion and cation exchange capacity of biochar are dependent on the porous structure of biochar, aromatic surface structures, and oxygen containing surface groups [59]. The metallic species, such as K^+, Na^+, Ca^{2+}, and Mg^{2+}, are bonded to the negatively charged surface groups that are prevalent on the surface of the biochar such as COO^- an O^- [142, 143]. AEC is enhanced through the presence of the oxonium group ($C\text{-}O^+$) bonding with the anionic compounds [144]. As expected, the pH of the soil plays a role in the AEC and CEC of biochars, however, the addition of biochar to the soil can potentially double the CEC [59]. Biochar typically has a CEC in the range of 15-25 cmol/kg [145].

The final benefit of the addition of biochar as a soil amendment is the potential increase in water holding capacity (WHC). The WHC capacity is simply defined as the ability of the soil to retain the water. Sandy soils often have a low WHC and any water added to the soil is quickly washed away and not held in the soil. The addition of biochar to the soil will increase the WHC and promote efficient water use and plant growth [47]. As with AEC and CEC, the WHC is dependent on the surface area, pore size, surface carbon structure, and surface functional groups in biochar [145-147]. The functional

groups associated with increasing WHC are the oxygenated polar groups such as carboxylate (COOH) bonding with the water [148].

2.5 Syngas Production from the Gasification of Biomass

2.5.1 Fundamentals of Biomass Gasification

Section 2.4 in this literature review discussed how biomass can be converted to valuable products in bio-oil and biochar via pyrolysis. A thermochemical treatment process that can be conducted concurrently with the pyrolysis of biomass is gasification. Gasification involves the reaction of the solid carbon in the biochar with an oxygen containing gasifying agent to produce several gaseous products. Where gasification of biomass differs from combustion is that gasification increases the energy within bonds, hence is an endothermic process, where combustion releases this bonding energy and is therefore an exothermic process. Direct combustion of biomass is an inefficient way to harness its energy due to its high energy content and low energy density [7, 79, 80]. Gasification of biomass produces a syngas typically containing hydrogen, methane, carbon monoxide, and carbon dioxide [149]. This syngas is typically combusted as a source of energy but can also be converted into specialty chemicals [24, 25, 150].

There are three stages in the gasification process; drying, thermal decomposition and gasification [149]. The first stage in the process is drying where the water entrained in the biomass is evaporated. Drying is generally completed just above 100 °C, a temperature not high enough to decompose the organic compounds in the biomass [51]. After the biomass is dried, it undergoes thermal degradation. Direct gasification of the biomass is kinetically unfavourable, hence the thermal degradation stage is completed under pyrolysis conditions [151]. Pyrolysis of biomass was discussed in detail in the previous section however briefly, the biomass is converted in the absence of oxygen into bio-oil, biochar, and non-condensable gases. These three products are then carried into the final stage of the reactor where the gasifying agent is added. In this stage, the thermally cracked biomass products are then gasified into a syngas containing the valuable non-condensable gases leaving behind the ash consisting of oxides of the metallic species present in the biomass. The pyrolysis of biomass occurs much faster than the gasification process, hence gasification is the rate-limiting step [98]. Gasification has the advantage over pyrolysis as it produces a syngas with a

greater concentration of hydrogen, a gas with a much higher calorific value than the other compounds formed. The gasification process is generally completed at a temperature between 600 – 1000 °C depending on the feed stock and desired products [152].

Three common gasifying agents are used in biomass gasification, air/oxygen [153, 154], carbon dioxide [12, 155, 156], and steam [157, 158]. Air/oxygen is a common gasifying agent as it can be cheaply and efficiently sourced from the atmosphere. The intake of air must be monitored closely as when the equivalence ratio is too high, the biomass will be combusted rather than gasified. Typical equivalence ratios for gasification with air/oxygen range 0.01 to 0.45 [159]. Another attractive gasifying agent is carbon dioxide as it can be potentially recycled from the flue gas produced in syngas production. Doing so will reduce the carbon footprint of the process. However, this practice is not typically implemented as the reaction rate for carbon dioxide gasification is often 6 times in magnitude slower than with air or oxygen [160]. The gasifying agent with the biggest potential in biomass gasification is steam. The steam can be added externally, sourced from the biomass itself during the drying process, or a combination of both. Steam has the advantage over air and carbon dioxide as it produces a syngas with a higher hydrogen content [149]. This means the syngas produced with steam has a higher heating value, typically 10-15 MJ/m^3, compared to that gasified with air, 3-6 MJ/m^3 [152]. Methane is often an undesirable product in syngas and its presence can be reduced in steam gasification compared to gasification with air/oxygen and carbon dioxide [115]. Due to these advantages, steam gasification will be the focus for the remainder of this literature review.

Steam gasification is simply not just the reaction of biomass with steam, there are many competing reactions occurring. Hence ample care must be taken in optimizing the reactor conditions. The major reactions that take place during the gasification process are outlined in Table 2-3. Reactions 1 and 2 revolve around the steam gasification of the biomass. Reaction 1 is the simple gasification of the carbon contained in the biochar to produce carbon monoxide and hydrogen. In reaction 2, the remaining hydrocarbon products formed in the pyrolysis of biomass that have not yet been thermally cracked can react with the steam to again produce hydrogen and carbon monoxide.

Table 2-3: Reactions occurring during the steam gasification of biomass

Reaction Number	Reaction
1	$C + H_2O \rightarrow CO + H_2$
2	$C_mH_n + mH_2O \rightarrow mCO + (m + \frac{n}{2})H_2$
3	$CO + H_2O \leftrightarrow H_2 + CO_2$
4	$C + CO_2 \leftrightarrow 2CO$
5	$C + 2H_2 \leftrightarrow CH_4$
6	$2CO + 2H_2 \leftrightarrow CH_4 + CO_2$
7	$CH_4 + H_2O \leftrightarrow CO + 3H_2$

An important reaction in the gasification is the water gas shift reaction [149]. This is outlined in reaction 3 and involves the reaction of the steam with the carbon monoxide produced in reactions 1 and 2 to produce hydrogen and carbon monoxide. This reaction consumes carbon monoxide, which is a valuable product for energy production, and steam, which is used to gasify the biochar and bio-oil, and produces carbon dioxide that has no benefits in energy production. However, the reaction produces hydrogen, which is very important in energy production due to the high calorific value of hydrogen. As this is a reversible reaction, the conditions can be altered in order to tailor the products depending on what is required. Reaction 4 shows the gasification of the carbon in the biochar with the carbon monoxide produced in the water gas shift reaction. This is known as the Boudouard equation. At temperatures typical of gasification, the forward reaction is dominant; hence there will be a gasification of carbon by carbon dioxide [161].

Methane is also formed in the process of pyrolysis and gasification [149]. Equations 5 and 6 show the formation of methane through the reaction of carbon and hydrogen in equation 5 and carbon monoxide and hydrogen in equation 6. Equation 7 shows how steam can react with the produced methane. Even though methane has a high calorific value it can be potentially hazardous to downstream equipment, especially if the syngas is to be used in Fischer-Tropsch synthesis [115]. Hence, it may be necessary to tailor the conditions of gasification in order to minimise methane production.

Despite hydrogen being a valuable product in the gasification of biomass, its presence in the syngas can be detrimental at a certain concentration. Hydrogen is well known to restrict the gasification process [162-165]. The restriction in gasification is due to the chemisorption of hydrogen onto the active carbon sites on the surface of the biochar [166]. As a result, the steam cannot access the carbon and hence the rate of gasification decreases.

2.5.2 Reactor Configurations

Multiple reactor types are available for biomass gasification. Depending on the situation where gasification is required and the nature of the biomass feedstock, the design of the reactor may vary greatly. The reactor configuration may be as simple as a fixed bed reactor to the more complex dual fluidised bed reactor. The following section outlines the different reactor configurations that can be used in the gasification of biomass. Table 2-4 summarises the advantages and disadvantages of all of the discussed reactor configurations.

Moving Bed Reactor

The simplest type of reactor used in biomass gasification is the moving bed reactor. In this configuration, the biomass is added into a heated furnace and an inert carrier gas is added containing the gasifying agent to produce a syngas. The carrier gas flow rate is restricted as not to fluidise the biomass bed. Fluidised bed reactors will be discussed later in this section. It is known as a moving bed reactor as the biomass is added through the top on a continuous basis and then the reactor typically contains a grate at the bottom where the ash can be removed after the biomass gasification is complete. Three types of moving bed reactors exist, updraft gasifier (Figure 2-1), downdraft gasifier (Figure 2-2), and crossdraft gasifier (Figure 2-3) [167].

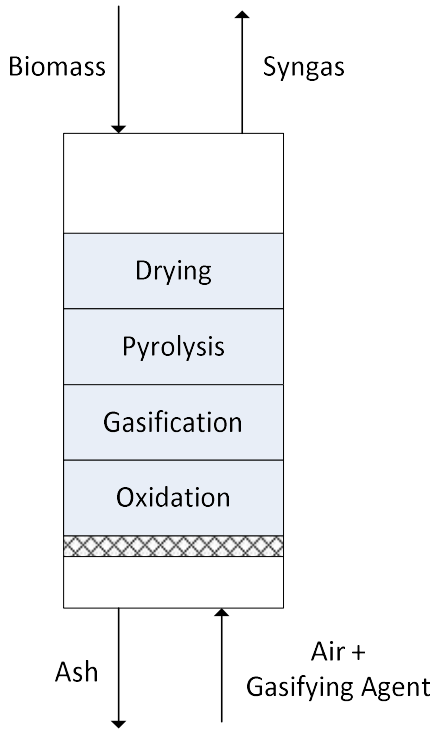

Figure 2-1: Updraft Moving Bed Biomass Gasifier

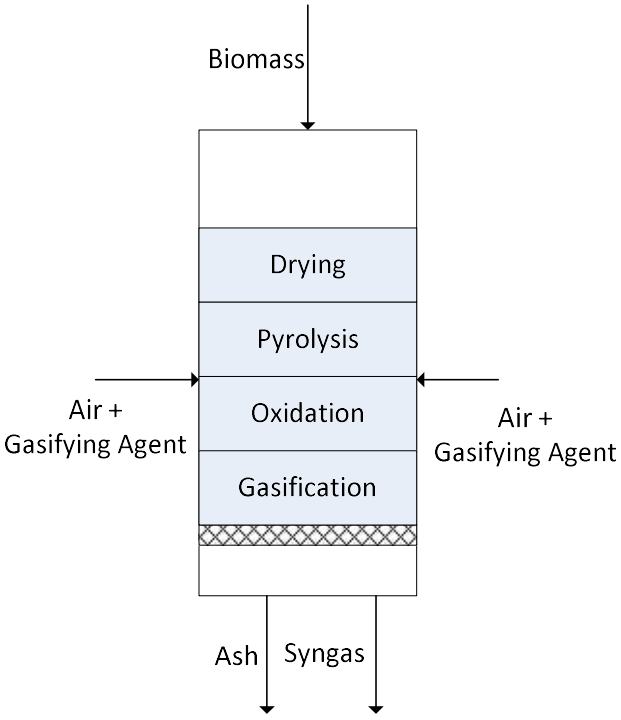

Figure 2-2: Downdraft Moving Bed Biomass Gasifier

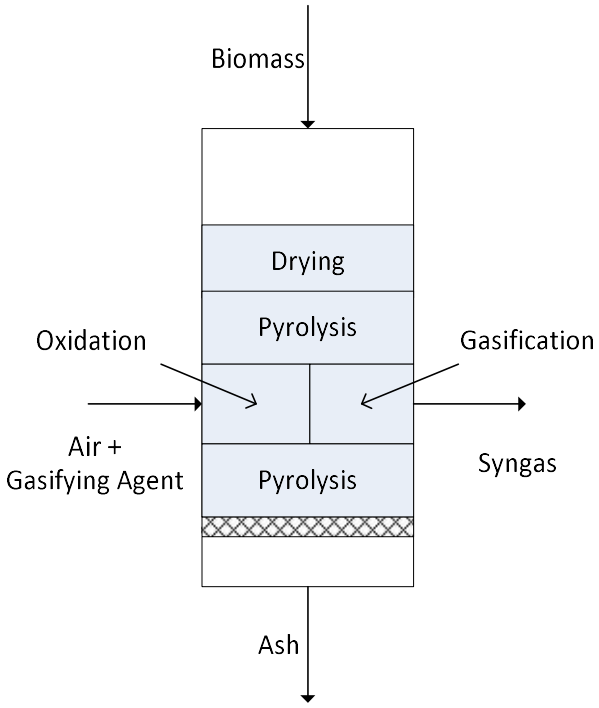

Figure 2-3: Crossdraft Moving Bed Biomass Gasifier

The simplest form of a moving bed reactor is the updraft gasifier, where the biomass is added through the top and the gasifying agent with the inert carrier gas added underneath [168]. The syngas is collected from the top and the ash removed out the bottom. This reactor configuration is particularly attractive when being used on a small scale as it is simple in design and construction and can handle varying biomass feeds with a high ash and moisture content. However, the syngas produced is often crude and dirty meaning it may be unsuitable for certain downstream applications [167]. These reactors also usually include a combustion zone that is used to provide the heat required to maintain the gasification temperature [169]. This form of reactor is often the reactor of choice when completing laboratory based studies such as kinetic analysis of the gasification process as they are easy to construct and the conditions can be easily controlled and monitored.

Downdraft and crossdraft reactors have similar constructions where the air and gasifying agent are added into the side of the reactor after the drying and pyrolysis stages [167]. In the downdraft gasifier, the syngas is collected at the bottom with the ash, whilst in the crossdraft it is collected from the side. Both of these reactor configurations provide a cleaner syngas than that from the updraft gasifier, however,

the heat transfer efficiency is lost; hence more of the valuable syngas needs to be combusted to maintain the gasification temperature [167].

Fluidised Bed

More complex reactor classifications for biomass gasification are fluidised bed reactors. Fluidised bed reactors are preferred on a medium production scale as they produce a cleaner syngas [167]. However, there will need to be a pre-treatment of the biomass before being added to the reactor to ensure it can be fluidised within the reactor. The simplest fluidised bed reactor is the bubbling fluidised bed reactor, as shown in Figure 2-4 [170]. This reactor has a similar construction to the updraft moving bed reactor, with the major difference being that the gas flow is high enough to fluidize the bed of biochar. This reactor configuration has the advantage of its simplistic design and tolerance for variance in feedstock, however, the syngas is often low in energy density and contains a high amount of entrained solids [98].

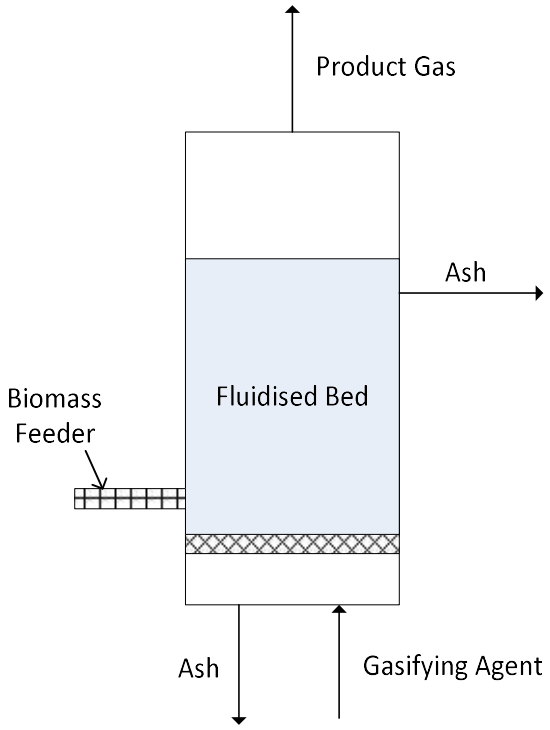

Figure 2-4: Bubbling Fluidised Bed Biomass Gasifier

An upgraded form of the bubbling fluidised bed is the circulating fluidised bed, as shown in Figure 2-5 [171, 172]. In this reactor configuration, the syngas is recycled back through the bed. As the gas flow rate to achieve the fluidization of the bed is often

high, the energy density of the syngas can be low due to the presence of the inert gas. By circulating the syngas until the concentrations of hydrogen and carbon monoxide have been maximised mitigates this issue. The circulating loop also allows for the capture and recycle of solid particles entrained in the syngas. This minimises the impact on downstream equipment and increases the efficiency of the process.

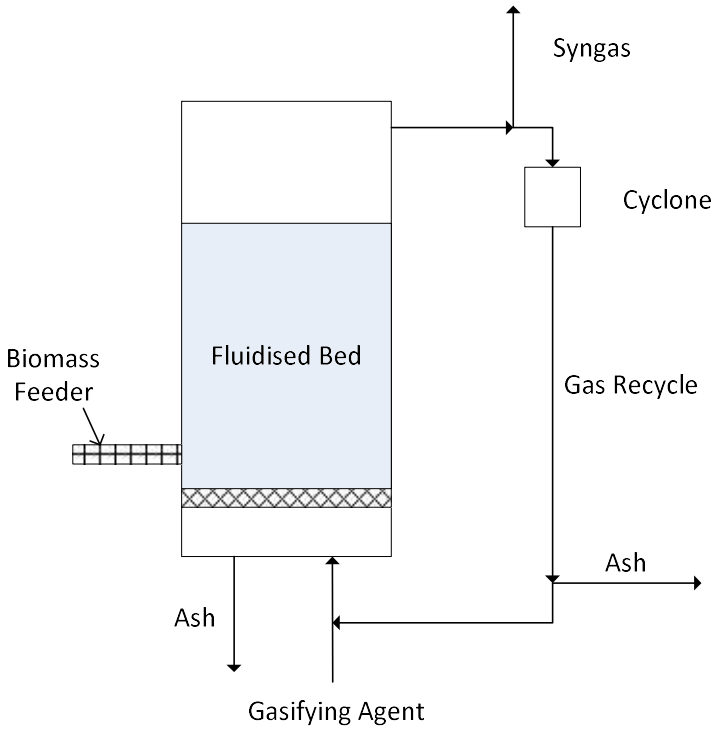

Figure 2-5: Circulating Fluidised Bed Biomass Gasifier

As biomass gasification is an endothermic reaction, there can often be issues with maintaining the temperature of the reactor. Instead of maintaining the temperature with an external heating source, a two stage dual fluidised bed reactor can be used, as shown in Figure 2-6 [173-175]. The first stage involves the gasification of the biomass to produce the syngas. Some of the biochar and syngas is then transferred into the second fluidised bed where combustion occurs to provide the heat to maintain the reaction. This reactor system has the advantage of producing a clean, high energy density syngas, however, as this is a complex design the capacity of this reactor needs to be high in order for its potential to be realised [98].

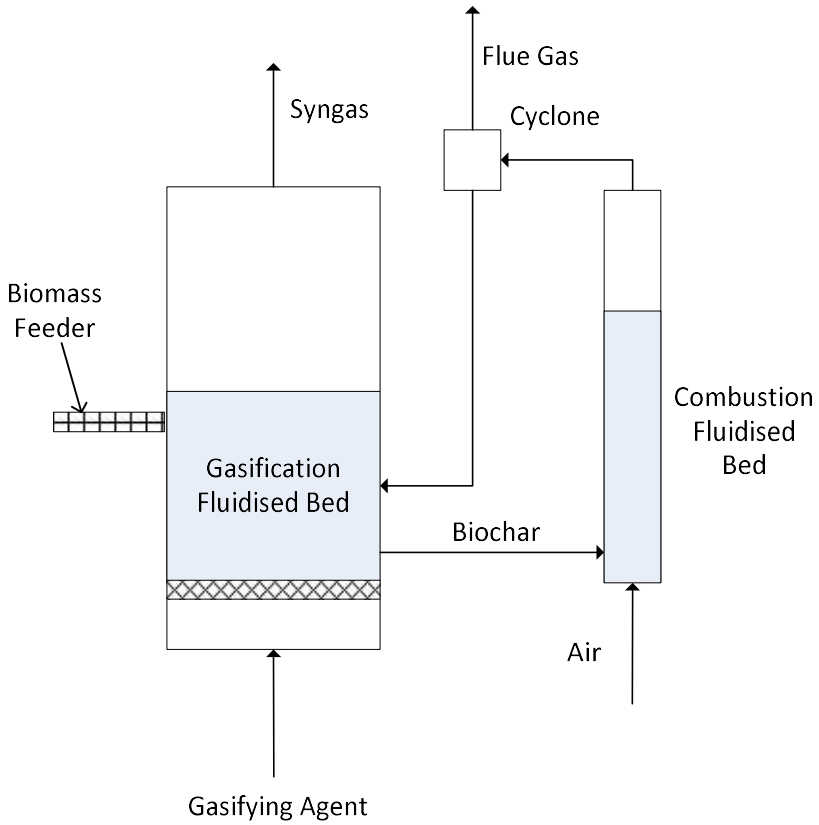

Figure 2-6: Dual Fluidised Bed Biomass Gasifier

There have been several studies on the modelling and optimisation of fluidised bed reactors for the gasification of biochar [166, 176-183]. In these studies, it was shown that the interaction between the volatiles, both those produced from the biomass gasification and those added to gasify the biochar, and the biochar is very important to ensure optimum gasification efficiency [184, 185]. This shows that the gasification reaction in a fluidised bed is controlled by gas-solid interactions; hence good mixing is required and special consideration needs to be made in designing the gasifier [172]. Other variables that need to be considered when designing a fluidised bed reactor include gasification temperature, steam to biomass ratio (equivalence ratio), and feed stock pre-treatment [186, 187].

Table 2-4: Summary of reactors used in biomass gasification

Reactor Configuration	Type of Reactor	Gas Flow	Advantages	Disadvantages
Updraft	Moving Bed	Counter current	Simplest design Can handle varying feed quality	Produces low quality syngas
Downdraft/ Crossdraft	Moving Bed	Co-current Cross current	Produces higher quality syngas than updraft reactor	Requires increased combustion of biomass to maintain temperature
Bubbling	Fluidised Bed	Counter current	Simplest fluidised bed design	Low density syngas produced
Circulating	Fluidised Bed	Counter current	High density syngas Solid particles captured	Difficulty maintaining reactor temperature
Dual Bed	Fluidised Bed	Counter current	Produces the highest quality syngas	Complicated design

2.5.3 Catalytic Enhancement from Metallic Species

It is well known that the gasification stage of the biochar is the rate determining step in biomass gasification [165]. As a result, it is often necessary to enhance the gasification process through the addition of catalysts to the process. Increasing the rate of gasification will allow for the higher input of biomass feedstock and higher energy production capacity. Not only does the addition of a catalyst enhance the rate of gasification, it provides a reduction in the methane content in the syngas [149]. The most common form of catalysts are metal based catalysts [33, 64-68]. The metal catalysts used to enhance gasification can be classified into two sections; mineral based catalysts that are dry mixed with the biomass and alkali and alkaline earth metal (AAEM) based catalysts that are loaded onto the surface of the biomass, often through wet impregnation [33]. Biomass often contains a large amount of AAEM's, as seen in Table 2-2, however, it is sometimes necessary to add further AAEM species to enhance the reaction rate.

Mineral based catalysts are an attractive catalyst to enhance biomass gasification as they are easily sourced, often inexpensive, do not undergo volatilisation in the gasification process, and can be easily removed from the reactor once spent [33, 64-68]. Dolomite ($MgCO_3.CaCO_3$) is often used as a catalyst in biomass gasification. Studies from Orio et al. [188] and Delgado et al. [189] showed that the mixing of dolomite with biomass during gasification can increase the gas yield by 10-20% and the heating value of the gas by up to 15%. Nickel based catalysts can also be used with similar success in increasing the quality of the syngas produced during gasification [190]. These metal catalysts can also be valuable in the reduction in methane concentration in the syngas with Paksoy et al. [191] showing that a Co and Ce doped ZrO_2 catalyst can provide significant reforming of methane.

More commonly, AAEM catalysts are used in biomass gasification. These catalysts are loaded onto the biomass or biochar before gasification through the wet impregnation of water soluble salts of the desired metal. The addition of K, Ca, Mg, or Na or a combination of these metals significantly increases the rate of gasification under both steam [192-194] and carbon dioxide [12, 14] gasification conditions. The addition of these catalysts not only increases the rate of gasification but increases the yield of gas and increased the syngas heating value [195, 196]. A study by Yip et al. [115] showed that the addition of potassium has the greatest increase in gasification rate under steam conditions followed by sodium and finally calcium. The same trend was concluded by Kim et al. [192] when looking at carbon dioxide gasification.

The gasification of biomass/biochar process can be divided into two parts, non-catalytic and catalytic gasification [117, 197]. Non-catalytic gasification is the direct reaction between the steam and the carbon of the biochar, whilst during catalytic gasification, the metal catalyst is involved with the reaction. The addition of the metal catalyst not only increases the reaction rate but also increases the gas yield from gasification as the metal provided additional active sites on the surface of the biochar [114]. A study by Kajita et al. [165] proposed mechanisms for both catalytic and non-catalytic gasification. These reaction schemes are shown in Table 2-5. Under non-catalytic gasification, the carbon active sites react with steam to form hydrogen gas and oxygen bonded to carbon (C(O)). The C(O) is then released as carbon monoxide gas. In catalytic gasification, the steam reacts with the metal to form hydrogen gas and

a metal oxide. The oxygen is then transferred to a carbon active site to form C(O) that is then released as carbon monoxide.

Table 2-5: Reaction mechanisms for catalytic and non-catalytic gasification of biomass/biochar [165].

Reaction Number	Equation
Reaction 1	$C( ) + H_2O \rightarrow C(O) + H_2$
Reaction 2	$C( ) + H_2 \rightarrow C(H_2)$
Reaction 3	$C(O) \rightarrow CO$
Reaction 4	$M + H_2O \rightarrow M(O) + H_2$
Reaction 5	$M(O) + C( ) \rightarrow M + C(O)$
Reaction 6	$(O) + C(O) \rightarrow M + CO_2$

2.6 Problems Associated with Syngas Production

2.6.1 Presence of Tar in Syngas

A major issue in the gasification of biomass is the presence of tar in the syngas remaining after the gasification process. In the literature, there is no set definition of tar in the context of biomass gasification, however, the consensus varies between two definitions. The first is tar is a mixture of volatiles, excluding water, that are condensable at room temperature [21], whilst the second definition states that tar is any compounds of higher molecular weight than benzene [22]. During the pyrolysis of biomass, there is a release of a large variety of volatile organic compounds [15-17]. As mentioned in Section 2.3, these volatile compounds are formed through the decomposition of the organic compounds contained in the biochar including ligins, cellulose, and hemi-cellulose [98, 198]. The majority of these compounds are reformed in the gasification process into carbon and hydrogen through thermal cracking (Equation 2.1) and reactions with steam that occur on the surface of the biochar (Equation 2.2). At 800 °C, a temperature typical of biomass gasification, it is often difficult to reform many compounds and they remain in the gas stream as tar. Depending on the gasification conditions, the tar composition can vary, however tar generally consists of polyaromatic hydrocarbons (PAH's) [18-20]. These range from small one ringed structures, such as benzene and toluene, to PAH's consisting of 5 rings [187]. At a gasification temperature 800 °C, the major components of tar are benzene (22 %), toluene (24 %), and naphthalene (15 %) [199]. These three

components of tar are often the most talked about when discussing tar formation in biomass gasification as they are the most refractory compounds [151]. What this means is that high temperatures are required to reform these tar components if the reaction is not catalytically enhanced.

$$C_mH_n \rightarrow mC + \frac{n}{2} H_2 \quad 2.1$$

$$C_mH_n + mH_2O \rightarrow mCO + (\frac{n}{2} + m) H_2 \quad 2.2$$

Table 2-6 shows the typical tar concentrations after gasification in different reactor configurations [24, 26-31]. As can be seen the tar concentration not only varies depending on the reactor configuration used, but also differs significantly within each of the configurations. The variations can be attributed to the type of biomass feed, the temperature of gasification, rate of biomass addition, and inert gas flow rate.

Table 2-6: Typical tar compositions in different reactor configurations during biomass gasification

Reactor Configuration	Typical Tar Concentration (mg/m^3)
Updraft Moving Bed	10 000 – 150 000
Downdraft Moving Bed	10 – 6 000
Bubbling Fluidised Bed	1 500 – 9 000
Circulating Fluidised Bed	9 000- 10 000

When syngas is used in downstream applications, it is often cooled down and pressurised to increase its energy capabilities. As a result of this, tar content in gas is undesirable as during this process, it condenses and deposits on the surface of downstream equipment [200]. PAH's of two rings or higher are particularly concerning as they condense at high temperatures. Based on this issue, it is necessary to set limits of the tar concentration in syngas to minimise damage to downstream equipment. These limits vary depending on the application of syngas. In an internal combustion engine, the limit of tar can be as high as 100 mg/m^3 [23]. This is because the syngas does not often need to be cooled down and is often combusted immediately after gasification, and hence condensation is limited. If the syngas is to be used in a gas turbine, the tar concentration needs to be much lower with the limit set at 5 mg/m^3 [200-202]. This lower concentration limit is due to the abrasion that occurs to the

turbine blades from the presence of these tars [31]. Finally, the tar concentration needs to be lower than 1 mg/m^3 if the syngas is to be used in Fischer-Tropsch (FT) synthesis to produce liquid hydrocarbons [24, 25]. In FT synthesis, there are generally complex and expensive catalysts used that can foul easily in the presence of tar, hence the tar concentration needs to be kept at a minimum [24, 25].

There are many different methods to reduce the tar concentration in syngas produced from biomass gasification. The cleaning methods can be split into two different categories, primary cleaning and secondary cleaning [175]. Primary cleaning of tar takes place within the gasifier, whilst secondary cleaning takes place downstream in dedicated processing equipment. The most common method in both primary and secondary cleaning is the addition of a catalyst [22, 194]. Catalytic cracking of tar compounds will be discussed in further detail in the remaining sections in this chapter. Besides catalytic cracking, primary methods of cleaning of tar include increasing the extent of gasification, modifying the biomass feedstock, changing the gasifying agent, and increasing the equivalence ratio [203].

Secondary methods that do not employ the use of a catalyst primarily consist of physical separation methods [31]. One common method of physical separation is through a cyclone [31]. Cyclones separate the light syngas from heavy tars and particulate matter, which settle at the bottom of the cyclone. A further method of physical separation is through filtration. Filter materials can range from activated carbon, fabric, ceramic and sand [29, 32]. These physical separation methods provide a simple and effective way to remove tar from syngas; however, there is often rapid fouling occurring from the deposition of the tar on the cyclone walls or surface of the filter, which can be an extensive exercise to clean. Thus, a catalyst often needs to be added in gasification in order to reform the tar.

2.6.2 Release of Inorganic Compounds from Biomass

Along with the release of tar, during gasification of biomass, there is a release of many other compounds that can be lumped into the category of inorganic compounds. These consist of SO_x, NO_x and other nitrogen containing gas compounds, non-metallic compounds such as chlorine, and metallic compounds that are contained within the biochar. The presence of all of these species in the syngas is to be avoided as they can all potentially be poisonous or hazardous to downstream processing equipment.

During the gasification of coal, the emission of SO_x and NO_x compounds is significant. The addition of these compounds into the atmosphere should be avoided as they are known to cause smog and acid rain [204]. The nitrogen contained within the coal can also be released in the form of ammonia and hydrogen cyanide, two potentially hazardous compounds. Biomass has the advantage over coal as the feedstock contains significantly less nitrogen and sulphur, 0.23 and 0.03 wt% respectively, compared to coal, 0.71 and 0.26 wt% respectively [205]. Even though the majority of the sulphur from biomass is released during gasification [206], as the sulphur concentration is low in the biomass feed, it is not of concern. Catalysts can also be added to the gasification process to reduce the emission of NO_x and other nitrogen containing gases [207].

Despite there being little nitrogen and sulphur contained in biochar, there is often a large amount of chlorine present, particularly in Mallee Eucalyptus grown to reduce salinity. The chlorine concentration in biomass can be up to 0.42 wt% [205]. During biomass gasification, up to 94% of the chlorine can be gasified and contained within the syngas, whilst the remainder is stored within the solid ash [208]. Chlorine within the syngas is either bonded to metallic compounds that are also gasified to form salts or in the form of hydrochloric acid [208]. Both chlorine salts and hydrochloric acid can be hazardous to downstream equipment as they cause corrosion and deposition of ash, which can reduce heat transfer capacity [209-211]. As the presence of chlorine in biomass gasification is potentially hazardous, it may be necessary to alter gasification conditions or pre-treat the biochar to reduce the chlorine presence in the syngas.

Finally, as shown in Table 2-2, there is often a lot of metallic species present in the biomass feed. As discussed in section 2.5.3, there can also be metallic species added to the biomass feedstock to increase gasification rates. A large number of studies have been completed on the volatilisation of metallic species during the pyrolysis and gasification of both biomass and coal [185, 212-224]. These studies showed the monovalent AAEM's, sodium and potassium, are volatised at a much faster rate than the divalent AAEM's calcium and magnesium. The metals not volatised remain in the ash after gasification. Other variables that effect volatilisation of metallic species include gasification temperature and heating rate. As with chlorine and tar, metallic species within the syngas should be avoided as they can potentially cause ash related issues to downstream equipment. If the presence of metallic species in the syngas is of

a concern, their concentration in the biomass feed can be minimised by washing the biomass before gasification [205, 208].

2.7 Cleaning of Syngas Using Inert Catalysts

By comparing the typical tar concentrations shown in Table 2-6 to the limits discussed in Section 2.6, the tar concentration from each of the gasification reactors needs to be reduced in order for the syngas to be used in any downstream application. Section 2.6 discussed that the most common method of reducing the tar concentration is through the addition of catalysts. This process is known as catalytic cracking of tar. The catalysts used in the cracking of tar can be divided into two categories; biochar based catalysts, which will be discussed in further detail in Section 2.8, and inert catalysts. Inert catalysts are called as such as they do not react with the gasifying agent to a significant extent during the cracking process.

Inert, or mineral based, catalysts have significant potential to be used in the tar reforming process [33, 64-68]. These catalysts are an attractive way to promote cracking of tar as they are cheap and readily available [203, 225, 226]. There are three common types of mineral based catalysts; nickel based, dolomite based, and iron based [33]. Generally, inert catalysts are employed in a secondary manner, i.e. the cracking of tar occurs downstream from the gasification process, however, they can be added into the gasification reactor in a primary manner [31, 33]. For a catalyst to be suitable for the process, it should effectively remove tar whilst; being inexpensive, is resistant to fouling, and can be easily regenerated [22, 33].

Table 2-7 to 2-10 summarise the current literature on mineral catalysts used for the removal of tar from a gas stream. As can be seen, there is a wide range of studies available that vary drastically in regards to the catalyst used and also with the reaction conditions. There is also a wide range in the effectiveness of the catalysts with several studies reporting that all of the tar can be removed from the gas stream, whilst other studies report a conversion as low as 23%. One commonality between the studies is the use of a model compound with the most common being naphthalene, toluene and benzene. These compounds are selected because, as discussed in Section 2.6, these are the most common tar components at common gasification temperatures and are notoriously difficult to remove [151]. Model compounds are used opposed to a real tar

system as they it can be assured that the model compounds are pure and a model compound allows for a consistent concentration to be added to the gas stream, where an in-situ production of tar can often be inconsistent. A full summary of some of the studies reported in Table 2-7 to 2-10 are provided in the sections below.

Table 2-7: Summary of nickel based catalysts used for cracking of tar contained in syngas from literature (continuing in next page)

Nickel Based Catalysts					
Catalyst	**Temperature**	**Reaction Time**	**Conversion**	**Comments**	**Reference**
Alumina-supported nickel catalysts	700-900 °C	0.0004-0.0237 kg_{cat} h/m^3	Naphthalene – 80%	Studies model compounds: Benzene, Toluene, Naphthalene, Anthracene, Pyrene Reactivity: benzene>toluene>>anthracene>>pyrene>naphthalene	[227]
Ni supported on SiO_2, Al_2O_3, MgO, CaO, and K_2O	750 °		Reduces tar yield by a factor of 5-10	Combination of primary and secondary catalysts	[16]
Ni-Ca-Al	650 °C		70%	Toluene as a model compound. Variation in nickel, calcium, and aluminium ratios	[228]
Y-Zeolite NiMo	550 °C		100%	1-methyl naphthalene as a model compound	[229]
Nickel Oxide	740-820 °C	1500-6000 h^{-1}	>99%	Three different catalysts tested	[230]
Nickel Monolith	900 °C	1 s	100%	Also looks into ammonia destruction	[231]
Ni + MnO_x/Al_2O_3	600 °C		100%	Used real tar system and toluene as a model compound	[232]
Nickel	400-900°C	0.26 s	100%	Benzene and naphthalene model compounds	[233]
Co/MgO Ni/MgO		2 s residence time	23%	Naphthalene model compound	[234]
NiO/CaO/MgO/Al_2O_3	750-900 °C	0.5 s	99.8%	Studies different catalyst structures	[235]

Nickel Based Catalysts					
Catalyst	**Temperature**	**Reaction Time**	**Conversion**	**Comments**	**Reference**
Palygorskite-supported Ni-Fe	800 °C		70%	Toluene and naphthalene model compounds	[236]
Olivine supported nickel	750-800 °C		75%		[237]
Ni/Ru-Mn/Al_2O_3	673-1073 K		100%	Toluene model compound	[238]
Ni	750-900 °C		100%	Naphthalene model compound. Nickel activated candle filter	[32]
Ni/Mayenite	700-800 °C		90%	Also observe reduction in methane concentration in syngas	[239]
Ni/Ca-Fe-Al	550-800 °		80%	Toluene model compound	[240]
Ni	650-900°C		100% Benzene, Toluene 80% Naphthalene	Benzene, Toluene, and Naphthalene model compounds	[241]
Ni/Olivine	560-850 °C	9 kg_{cat} h m^{-3}	100%	Toluene model compound	[242]
Ni/Cordierite	750-900 °C		94.1 %	Toluene model compound	[243]

Table 2-8: Summary of iron based catalysts used for cracking of tar contained in syngas from literature

Iron Based Catalysts					
Catalyst	**Temperature**	**Reaction Time**	**Conversion**	**Comments**	**Reference**
Iron Oxide	600 °C		100%	Tar produced from the gasification of untreated wood. Aluminium oxide added to reduce the deactivation of the catalysts	[244]
Ilmenite	500-850 °C		95%	Showed that carbon deposited on the catalyst from tar cracking can be gasified through the addition of steam	[81]
Metallic Iron/Fe_3O_4	700-900 °C		100 %	Studies total tar conversion as well as individual naphthalene, toluene, and benzene	[245]
Olivine	900 °C	0.3 s	>80%	Looks into the importance of pre-treatment of catalyst. Naphthalene as a model compound	[246]
Ilmenite	825 °C		50 %	Primary addition of catlyst to reduce tar concentration	[247]
Olivine	750, 800 °C		90%	Compares calcined and untreated olivine	[248]

Table 2-9: Summary of dolomite based catalysts used for cracking of tar contained in syngas from literature

Dolomite Based Catalysts					
Catalyst	**Temperature**	**Reaction Time**	**Conversion**	**Comments**	**Reference**
Calcined Dolomite	800-880 °C	0.08-0.32 kg_{cat} h/Nm^3	100%	Biomass produced tar studied	[249]
Dolomite/Sand	800-900 °C	0.3 s 7.4 kg_{cat} h m^{-3}	63%	Compares dolomite and olivine catalysts	[250]
Dolomite/Limestone	900 °C	0.1-1.5 s	100%	Studies variation in Mg and Ca concentration	[251]
Dolomite	700-800 °C		70%	Compares dolomites from different locations	[252]

Table 2-10: Summary of other non-biochar based catalysts used for cracking of tar contained in syngas from literature

Other Catalysts					
Catalyst	**Temperature**	**Reaction Time**	**Conversion**	**Comments**	**Reference**
Co/MgO	600 °C		23% Carbon converted to gas	Naphthalene as a model compound. Focuses on amount of carbon converted to gas opposed to deposited on catalyst	[253]
ZrO_2	600-900 °C		90%	Naphthalene model compound	[254]
MgO/CaO	650 °C	8 s	90%		[255]
ZrO_2 and Al_2O_3 doped with Ni, Cr, Fe, Ce, Co, and Pt	450-800 °C		90-100%	Naphthalene model compound	[256]
Ion Exchange Polymers	1040 °C		80-95%		[257]

2.7.1 Nickel Based Catalysts

Nickel based catalysts have been studied in great detail in the literature. The reason for which is due to these nickel based catalysts being relatively inexpensive and easy to source [22]. Nickel based catalysts generally consist of an active catalyst, a promoter, and a support [22]. The nickel is the active component in the removal of the tar, a promoter increases the catalytic ability of the catalyst, and the support provides a high surface area. The variation in ratios of these three components can have a profound effect on the ability of these catalysts to remove tar from the gas stream. A study by Ashok et al. [228] varied the ratios of nickel (active component), calcium (promoter), and aluminium (support). The study found that a Ni-Ca-Al ratio of 8:62:30 has the highest activity for tar removal due to its enhanced strength and resistance towards agglomeration. Koike et al. [232] showed that addition of a manganese oxide promoter can enhance the catalytic ability of a Ni/Al_2O_3 catalyst and reduce the amount of coking on the surface.

The deposition of carbon on the surface of the nickel based catalyst due to the cracking of the tar, i.e. coking, is a significant issue for mineral based catalysts. If not controlled, it can deactivate the catalyst rapidly. One method of minimising coking is through the addition of an additive to the catalyst to promote the tar to form carbon monoxide gas opposed to solid carbon. Quitete et al. [258] showed that through the addition of a barium hexaluminate to a nickel catalyst will minimise the carbon deposition. An alternative method to adding often expensive substances to the catalyst is to increase the steam in the gas flow to gasify the deposited carbon. According to Coll et al. [227] the steam to carbon ratio required to prevent deposition can range from 2.5 to 8.4 depending on the composition of the tar.

Often, to increase the activity of the catalyst, the catalyst is preheated in a process called calcination [259, 260]. In nickel based catalysts, the nickel salts loaded onto the support are converted to nickel oxide. Depending on the catalyst, the calcination temperature and time can have significant effects on the catalyst activity. A study from Swierczynski et al. [242] on nickel/olivine catalyst showed that a calcination temperature of 1100 °C for a period 4 hours was required for the catalyst to reach full activity. Furusawa et al. [234] loaded a nickel nitrate salt on a magnesium oxide

support and discovered that a temperature of 600 °C was required to convert the nickel nitrate to nickel oxide.

2.7.2 Dolomite Based Catalysts

An alternative to nickel based catalysts are dolomite based catalyst. Dolomite based catalysts are often used over nickel based catalysts as they are often cheaper, however, need temperatures much higher than the nickel catalysts to remove the tar [249]. Dolomite catalysts also have the ability to withstand these high temperatures for a significant amount of time with Delgado et al. [249] finding that a calcined dolomite catalyst can remove tar for up to 14 hours at over 850°C without showing any signs of deactivation. Devi et al. [250] showed that at a temperature of 900 °C, the addition of dolomite to sand can remove up to 90 % of tar from the gas stream. Particular focus in this study was placed on the conversion of individual components of tar with polyaromatic hydrocarbons being the most difficult compounds to reform.

Dolomite consists of magnesium and calcium carbonate, with varying ratios of magnesium and calcium. For the dolomite to have any catalytic ability in removing tar, it needs to undergo calcination to convert the carbonates to magnesium and calcium oxide [259, 260]. As with nickel based catalysts, the calcination time and temperature is important in determining the activity of the catalyst. Studies by Simell et al. [251] and Yu et al. [252] discussed that a temperature of 900 °C was required to calcine the catalyst, with calcination times ranging from 1.5 - 4 hours.

2.7.3 Ilmenite/Iron Based Catalysts

The final types of metal based catalyst used in tar reforming are iron based catalysts. Iron based catalysts are beneficial over nickel based catalysts as they are often cheaper and are non-poisonous, whilst they have the advantage over dolomite catalysts as a lower temperature is required to achieve full tar conversion and calcination is not required [244]. There are many different forms of iron based catalysts including metallic iron, iron oxide, and naturally occurring ilmenite. A study by Azhar Uddin et al. [244] showed that iron oxide (Fe_3O_4) was able to gasify more than 90% of the volatiles produced from the steam gasification of biomass at a relatively low temperature of 600 °C. Metallic iron can also be used as a catalyst with Nordgreen et al. [245] proving that 100% of tar can be removed at 900 °C using metallic iron in the

presence of steam. Finally, naturally occurring ilmenite ($FeTiO_3$) can be used as a catalyst with the potential of significantly reducing the tar content produced from biomass gasification [81].

2.8 Using Biochar as a Catalyst to Remove Tar

2.8.1 Benefits of using Biochar as a Catalyst

Despite there being many benefits associated with mineral based catalysts, these catalysts can have many disadvantages when being used in the reforming of tar. These issues include:

- If non-ideal operating conditions are used, the catalysts foul quickly, hence lose their catalytic ability and need to be disposed of and replaced.
- Even with optimised operating conditions, the catalyst eventually loses its activity through deposition of solid carbon and poisoning from compounds such as H_2S produced during the gasification of biomass. When the catalyst is spent, it needs to be disposed of and replaced.
- Nickel is a poisonous metal; hence it cannot be simply recycled back from where it came from once it is spent. Money needs to be spent to safely recycle the spent catalyst.
- These mineral based catalysts are often sourced naturally; hence their composition can vary depending on the source.
- If the process causes the catalyst to foul rapidly, expenses associated with sourcing the catalyst as it is not produced in the process.

Many of the issues listed above associated with mineral based catalysts can be solved through replacing the catalyst with a biochar based catalysts [34-37]. Biochar based catalysts eliminate the costs associated with sourcing mineral catalysts as they are already produced in the process of biomass pyrolysis, as discussed in Section 2.4. Biochar catalysts are also easily disposed of once they are spent through either gasification to produce a syngas or recycled back into the soil to improve the agronomical properties of the soil. These were discussed in detail in Sections 2.5 and 2.4 respectively. Finally, the issues with catalyst poisoning and fouling are non-existent in biochar as the deposited carbon on the biochar is simply gasified through

the steam already present in the process. There is a significant amount of literature on the use of biochar based catalysts to reform tar, which is summarised in Table 2-11 and will be discussed in detail in this chapter.

Table 2-11: Summary of biochar catalysts used for cracking of tar contained in syngas from literature (continued on next page)

Biochar Treatment	Reactor Configuration	Temperature	Reaction Time	Tar Conversion	Comments	Reference
None	Fixed Bed	700-900 °C	0.3 s	100 % Phenol 99.6% Naphthalene	Model compounds phenol and naphthalene. Phenol dominated by thermal cracking, naphthalene by catalytic conversion. Showed biochar has similar catalytic capabilities to nickel and is more efficient than dolomite, olivine and sand	[226]
None	Two Stage Pyrolysis/Reforming Fixed Bed	800-850 °C	0.34-0.4 s	Reduced to <100 mg/m^3	Steam gasification and partial oxidation	[151]
Ni and Fe(III) Loaded Charcoal	Two Stage Pyrolysis/Gasification Fluidised Bed/Fixed Bed	500- 850 °C		100 % Ni 96% Iron	Also studies reaction kinetics	[261]
Fe(III) Loaded Mallee Biochar	Two Stage Pyrolysis/Reforming Fixed Bed	800 °C		97%	Fast pyrolysis of mallee wood to produce a tar that is then steam reformed over the catalyst	[23]
Untreated Charcoal	Fixed bed	700-900 °C	15-45 mm Bed Depth	98 %	Benzene, Naphthalene, Phenol, Pyrene, and Phenanthrene model compounds. Charcoal had a surface area of 740 m^2/g. Showed that the loss in activity in the catalyst as the surface area and pore size decreases due to the deposition of carbon.	[262]

Biochar catalyst crushed and sieved to 212-420 µm	Packed Bed	600-900 °C		94 %	Toluene as a model compound	[263]
Pre-activated with CO_2	Fixed Bed	850-1050 °C	0.8 s	100 %	CO_2 Gasification. Benzene as a model compound	[264]
Fe(III) loaded	Two Stage Pyrolysis/Gasification Fluidised Bed/Fixed Bed	800 °C		Reduced to <100 mg/m^3	Showed that surface area and pore volume were not the determining factors in tar reforming, number of active sites are more important	[265]
None	Fixed Bed	750-950 °C	0.3s	Up to 100%	Naphthalene and toluene model compound. Compares three different kinds of biochar	[266]
Fe(III) Loaded	Packed Bed	600-900 °C		100%	Maintained full activity for up to 16 hours	[199]
NiO Loaded	Fixed Bed	650-850 °C	0.1-1.2 s	97%	NiO loaded onto biochar at 15 wt% showed the highest activity	[267]
None	Fixed Bed	850 °C	0.32s		Phenol as a model compound	[268]
Ni-Loaded	Fixed Bed	700-900 °C		80%	Showed that Nickel loaded catalysts initially shows a higher activity but is deactivated quickly where raw biochar shows greater longevity. Naphthalene used as a model compound	[269]
K-Loaded	Two-Stage Downdraft Gasifier	700-800°C	0.24 s	93 %	Loading potassium significantly increases the catalytic ability of the biochar	[270]

2.8.2 Importance of Treating Biochar Based Catalysts before Reforming Process

Biochar on its own is not a good catalyst in reforming of tar; hence it is often necessary to treat the biochar before it is to aid in tar reforming. In order to increase the catalytic ability of the biochar, two common methods are used: increasing the surface area of the biochar or loading the biochar with active components. The most common way of enhancing the catalytic biochar is through the addition of metallic species. Depending on the source of the biomass, the biochar has an inherent amount of Na, K, Mg, and Ca already present [82], however, it is often necessary to load more of these metals onto the biochar in order to reach peak catalytic ability. The metallic species are generally loaded onto the biochar as metal salts or metal oxides. The biochar then acts as a carbon reductant at high temperatures to convert these salts or oxides to its metallic species [37]. These metallic species act as active sites for the tar to be reformed. They are often bonded to negatively charged surface groups contained on the biochar. The roles of these surface groups will be discussed later in this section. Zhang et al. [270] showed that by loading potassium on the biochar catalyst, the formation of naphthalene can be restricted in the gasification process, hence increasing the catalytic ability of the biochar.

Non AAEM species such as Ni, Co, Cu, Zn, Fe, and Al are also known to increase the catalytic ability of the biochar [261, 271]. These metals are generally mixed with the biochar in their oxide forms as they often occur in their oxide from naturally. A study by Han et al. [271] looking into several biochar supported catalyst. The study found that, in respect to tar reforming, the catalytic activity was in the order of Co-char, Ni-char, Cu-char, and Zn-char. A further study by Min et al. [261] found that, through the addition of iron (III) and nickel to the biochar significantly increases the ability of the biochar to reform tar contained within an inert gas.

Another way of increasing the catalytic ability of the biochar is through the increase in surface area of the biochar. The reforming of tar on biochar consists of two main mechanisms. The first stage is through the adsorption of the tar components onto the surface of the biochar. Basic surface functional groups such as $–NH_2$ can combine with Lewis acid components of the tar such as phenol [37]. However, biochar is often low in nitrogen [81-83] and therefore does not include an abundance of these functional

groups. Hence, the tar is more likely to adsorb on the –OH, -C-O, and C=O functional groups ever-present on the surface of biochar [37]. Increasing the surface area opens up the pores of the biochar, allowing further access of the tar to the active surface groups. This process also brings inherent metallic species contained in the biochar to the surface. As discussed previously, these metals significantly increase the catalytic ability of the biochar to reform tar, hence the second mechanism involved in tar reforming.

There are two common methods of increasing the surface area. The first is through the reduction in particle size of the biochar. This is done through the grinding of either the biomass fed into the rector or the biochar [38, 272]. Through the analysis of the surface properties of the biochar, Mani et al. [263] showed that the crushing of the biochar directly increases the surface area, and hence increases its ability to reform toluene, a model compound of tar. The other common way of increasing surface area is through the pre-activation of the biochar. By treating the biochar with steam, carbon dioxide or oxygen at high temperatures, the carbon is gasified, and hence the surface area increases. Gasification of the biochar not only opens the pores, but also forms new active surface groups on the biochar [273, 274]. By activating a wood based biochar with carbon dioxide before using it to reform tar, Burhenne and Aicher [264] found that the surface area of the biochar can increase from 126 m^2/g up to 870 m^2/g. This in turn meant that the conversion of benzene increased from just 20% to 100%. Despite these studies showing that surface area impacts catalytic ability, the surface area is not the determining factor in the reforming of tar. It is in fact the access of tar to active surface groups. If the surface area and pore size increase without increasing the number of surface groups, the catalytic ability of the biochar will not increase [265].

2.8.3 Reforming Model Compounds over Biochar-Based Catalysts

To test the ability of a biochar to catalytically reform tar, a model compound is often used in replace of a real tar. The methodology behind using a model compound opposed to a real tar is associated with the properties of the biomass. As biomass is often of inconsistent properties, it is difficult to create a tarry syngas from the pyrolysis of biomass with a constant tar consistency and flow rate. Also, if it is necessary to compare the performance of one biochar with that from a previous study, it may not be possible to do so with a real tar system. Hence, a model compound is often use as

it can be as pure as required and can be added at a constant rate. The most common model compounds used in biochar/tar reforming tests are toluene, naphthalene, and benzene as they are the most often the most difficult to reform [151].

There are several studies that look into the reforming of model compounds over a bed of biochar. Typically, these studies are completed over a fixed bed of biochar. By using model compounds naphthalene and phenol, Abu El-Rub et al. [226] compared biochar based catalysts with inert mineral based catalysts under steam gasification conditions. It was discovered that biomass has a similar activity to nickel based catalysts in regards to reforming these model compounds and outperforms dolomite, sand, and olivine catalysts. The activity of biochar catalysts to reform naphthalene has been confirmed by Zhang et al. [269] and Fuentes-Cano et al. [266] with these studies showing good conversion of naphthalene contained within syngas using biochar based catalysts.

The longevity of biochar activity in a fixed bed reactor configuration is often a concern. As a result of the reforming of these model compounds, carbon is deposited on the surface of the biochar, decreasing the activity of the biochar by blocking access to active surface groups. The deposition of carbon can be counteracted with the addition of steam, however, this steam will also react with the biochar eventually consuming the catalyst. A study by Hosokai et al. [262] confirmed that the activity of the char catalyst can be maintained by closely matching the rate of deposition with the rate of carbon gasification. Through such consideration of replenishing the catalytic capabilities of the biochar, Kastner et al. [199] showed that a biochar supported iron catalyst can effectively reform 100 % of toluene contained within a syngas for a period of 16 hours.

2.8.4 Reforming of Biomass Generated Tar and Reactor Configuration

Along with using model compounds for tar reforming, there are several studies looking into using a complex tar system. [23, 151, 270] To create the tarry syngas, biomass is undergoes pyrolysis or gasification in the first section of the reactor. This gas is then transferred to the second section to reform the tar and create a syngas. This is what known as a two-stage reactor. A diagrammatical representation of this two stage reactor is shown in Figure 2-7. The biochar catalyst used in the reforming section can be from an external source or from the biochar produced in the pyrolysis process in

the first stage of the reactor. By having the two sections separated, it allows for the biochar to be pre-treated before being added into the reforming section.

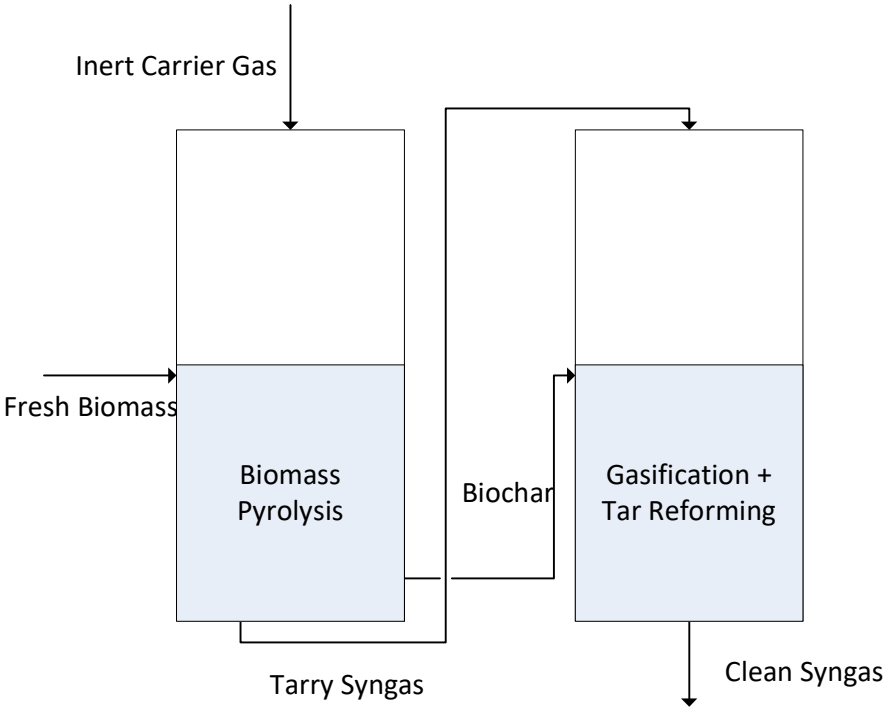

Figure 2-7: Two-Stage Pyrolysis of Biomass/Gasification and Reforming of Tar

A study by Hosokai et al. [151] looked at reforming of tar over a fixed bed of biochar catalyst in a two stage reforming process. The first stage of the reactor featured the pyrolysis of a Japanese cedar to produce a tarry syngas. Through a combination of steam gasification and partial oxidation (air to steam ratio of 0.115) in the reforming section, the tar content in the syngas can be effectively reformed over a biochar catalyst. By looking at the individual components in the tar, it was found that the naphthalene concentration can be reduced to 12 mg/m^3. Similar results were discovered in Dong et al. [23] were tar could be reduced to 82 mg/m^3 using a biochar catalyst under partial oxidation conditions. However, it is often inefficient to reform the tar under partial oxidation conditions as the oxygen will react with the hydrogen and carbon monoxide, decreasing the calorific value of the syngas.

2.8.5 Summary of Desirable Biochar Properties

The following is a list of the properties that make a good biochar catalyst used to clean a tar containing syngas.

- Simple and inexpensive production from a readily accessible biomass source
- High initial surface area or can easily have the surface increased through gasification pre-treatment.
- Resistance from fouling through in-situ regeneration of the biochar.
- Inherent metallic species present in increase the catalytic ability of the biochar.
- If the biochar has minimal inherent metallic species, any loaded metals should be retained on the biochar during its use.
- The biochar should not release any hazardous materials during its lifetime
- The catalyst should be easily disposed and potentially have a positive effect on where it is disposed.

2.9 Conclusions and Research Gaps

Through the utilisation of a pre-existing waste product, the South-West of Western Australia is a potential location to implement a process to convert biomass to a sustainable energy source. [7-9] The biomass is converted to syngas through the pyrolysis of the biomass and subsequent gasification of the bio-oil and biochar. The major issue in this process is the tar content within the syngas, which is often of a much higher concentration that is acceptable for downstream applications. [23] To clean the syngas of these tars, a mineral catalyst such as nickel or iron can be used to increase the reforming rate of these tars. [33, 64-68] However, the use of these catalysts are not ideal in some situations as they can be easily poisoned, they are deactivated quickly if the conditions are not ideal, and there are difficulties in their disposal once they are spent. [34-37] To counteract these issues, a biochar catalyst can be used. An important study by Hosokai et al. [151] showed that the tar concentration can be reduced to 12 mg/m^3 of a char catalyst. However, this study was completed under partial gasification conditions, potentially decreasing the calorific value of the syngas compared to what would be achieved using steam gasification. As a result of this literature review, the

following research gaps exist in the pyrolysis/gasification of biomass to produce a clean syngas.

1. Further studies are required on the behaviour of tar over a biochar based catalyst in the absence of oxygen (pyrolysis), focusing on the addition of metallic species to enhance the catalytic ability of the biochar. This will allow for a study on initially how effective the catalyst is in reforming tar contained within a gas stream, determine the mechanism involved in the reforming of tar, study the change in the surface morphology of the biochar during exposure to tar, and estimate when the biochar catalyst becomes deactivated. The mechanism of tar reforming can be represented by studying the reforming properties of a tar model compound.

2. The majority of the studies in the literature on the reforming of tar over a biochar catalyst are performed in a fixed bed reactor. As the biochar is consumed in the process via gasification and can become deactivated, using a fixed bed reactor becomes a batch process. A new reactor configuration needs to be developed that allows for the effective reforming of tar over a biochar catalyst that can be adapted into a continuous process.

3. Previous studies showed that partial oxidation is required in order to effectively reform the tar over biochar catalysts. However, partial oxidation conditions may need to be avoided as the oxygen can react with the syngas and reduce the calorific value of the syngas. It is unclear whether steam only gasification conditions can effectively reform the tar produced from biomass pyrolysis.

4. Studies in literature are generally concerned with the final concentration of tar after the gas stream has passed through the full bed of biochar. There are few studies on the amount of tar reforming experienced at different bed depths, hence calculating the rate of tar reforming with respect to bed depth. Particular focus can be placed on the reforming of the individual components of the tar.

5. Finally, the studies completed on the addition of biochar back into the soil as a remuneration product are on biochars produced directly from pyrolysis/gasification of biomass. There have been minimal studies on adding

biochar back to the soil after it has been used as a tar reforming catalyst and has undergone partial gasification.

2.10 Research Objectives

Based on the gaps in the literature discussed in Section 2.9, the following are the research objectives for this thesis. These objectives attempt to fill the major research gaps identified; however, it is to be acknowledged that there are gaps in the literature that will not be discussed in this thesis.

1. To study the reforming of a tar model compound (naphthalene) over a fixed bed of metal loaded biochar under pyrolysis conditions in order to determine the reforming mechanism.

2. To develop a reactor configuration that allows for the continuous removal of spent biochar and addition of fresh biochar to create a continuous process of tar reforming under steam gasification conditions.

3. To create a process that creates a tarry syngas from the pyrolysis of biomass and then allows for the in-situ cleaning of the syngas over a continuous bed of biochar. Focus will be placed on the reforming rate of the individual tar components.

4. To ensure that this process is cost effective in terms of electricity production compared to other methods.

5. To quantify the benefits of adding spent biochar catalyst to the soil in regards to increasing the nutrient properties of the soil.

CHAPTER 3 RESEARCH METHODOLOGY AND ANALYTICAL TECHNIQUES

3.1 Introduction

Section 2.10 outlined the research objectives for this thesis, hence this chapter will outline the methodology required to achieve these research objectives. Detailed descriptions of the research methodologies and analytical techniques used in this thesis will be discussed here

3.2 Research Methodology

Several research objectives were outlined in Section 2.10 with the overall aim being to create a biochar based catalyst that can effectively reduce the tar content in a syngas down to a suitable level whilst being suitable to be returned to the soil in order to enhance the growth potential of the soil. In order to achieve this overall aim, the following set of experiments was completed.

- Slow pyrolysis of mallee wood biomass to produce a biochar, which is subsequently treated in order to produce the biochar catalysts required to complete the following experiments.
- Pyrolysis of naphthalene entrained in argon, hence in the absence of oxygen, over a fixed bed of biochar catalyst at 900 °C in order to determine the conversion of naphthalene. Four biochar based catalysts will be tested; Raw Biochar, K-Form Biochar, Mg-Form Biochar, and Fe(III)-Form Biochar.
- Steam reforming of naphthalene over a moving bed of K-Form Biochar catalyst at 830 °C to again determine the conversion of naphthalene over the catalyst bed
- Repeat the above experiment using the moving bed of biochar but replace naphthalene with tar produced from the fast pyrolysis of mallee biomass at 500°C.
- Quantify the potential benefits of adding the spent biochar catalysts back into the soil by measuring the leaching kinetics of compounds such as potassium

and chlorine, water holding capacity, cation exchange capacity, and anion exchange capacity of the biochars used in all moving bed reactor experiments.

- Analysis of the properties of the biochar catalysts via several analytical techniques to determine properties such as surface morphology, proximate analysis, and elemental composition.

The above research methodology is summarised in Figure 3-1. To ensure experimental integrity, the experiments were completed in at least duplicate. For all of the data points provided in this thesis, the average value is reported with error bars included.

3.2.1 Fixed Bed Pyrolysis

To study the interaction naphthalene has with biochar, a fixed bed configuration was used. This study was completed under inert conditions in order to eliminate any steam reforming/gasification reactions. Naphthalene was used as a model compound to represent the tar produced during the pyrolysis and subsequent steam reforming of biomass as it is known to be one of the most refractory compounds. To do this, biochar catalyst was prepared through the pyrolysis of biomass followed by acid washing of the biochar to remove the inherent metallic species followed by the loading of chlorine salts of different metallic species. The pyrolysis of naphthalene was tested by adding the biochar catalyst to a quartz reactor and heating to 900 °C in a furnace. Once the temperature was stabilised, a steady stream of naphthalene was added to the reactor. Experiments were completed where naphthalene was not added to the reactor to study the effect temperature has on the biochar properties. The unreacted naphthalene was captured in order to calculate the conversion and the properties of the biochar analysed before and after the exposure to naphthalene. The data gathered is presented and discussed in Chapter 4 in order to achieve Objective 2.

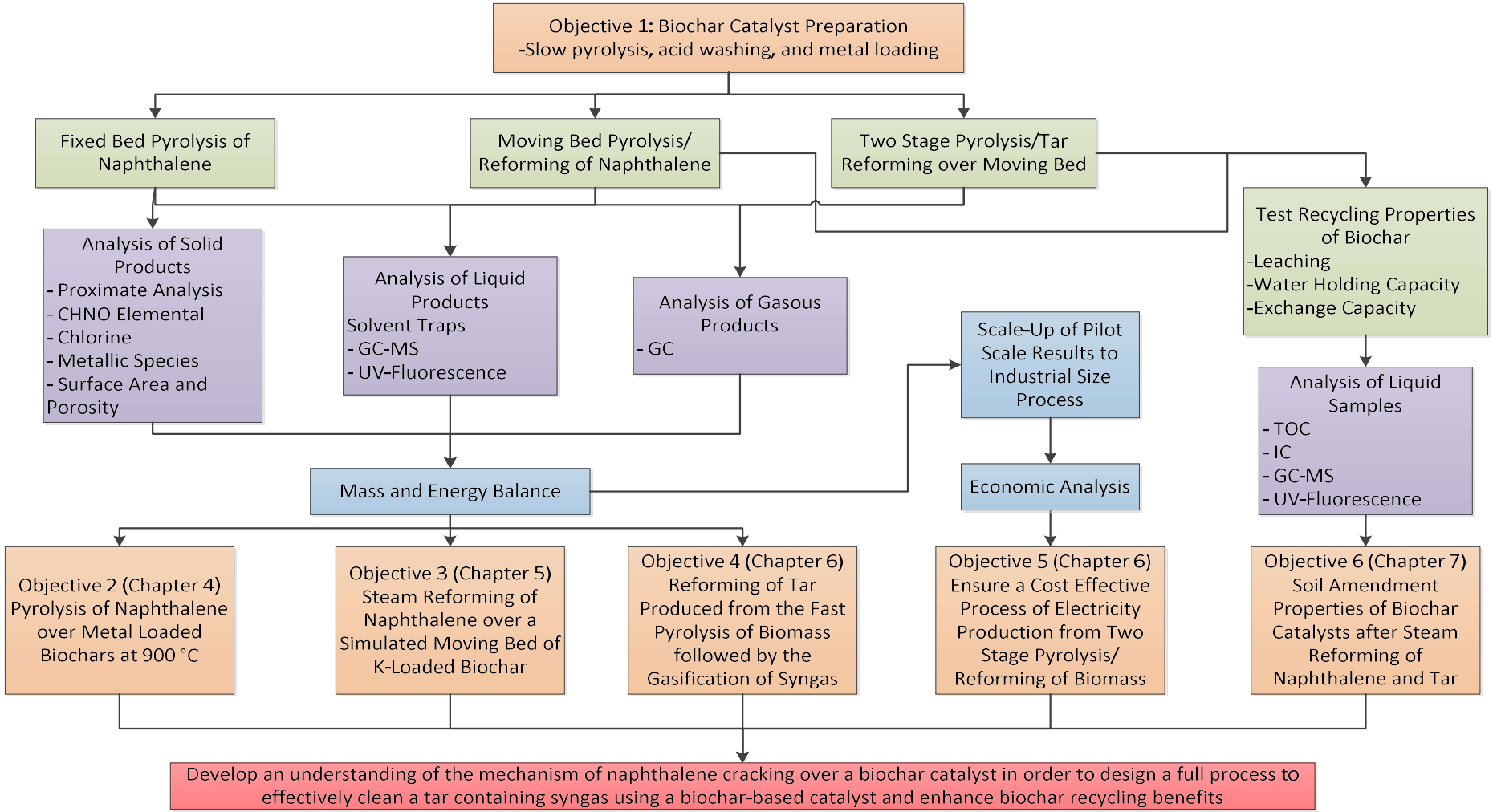

Figure 3-1: Overall Research Methodology

3.2.2 Moving Bed Reforming

To achieve the third and fourth objectives in this study, a moving bed of biochar was created. As moving beds are difficult and expensive to construct as well as difficult to control on a small scale in order to get a consistent flow of solid catalyst, the moving bed had to be manually simulated. To do so, a specific amount of biochar was added to a stainless steel basket, which was designed in order to hold the biochar but allow the gas to flow through. The biochar containing basket was then added to the stainless steel reactor and the experiment completed. Once the reactor was cooled, another basket containing fresh biochar was added on top of the stack and the procedure completed until there were 10 baskets on the stack. At this point, the process was completed a further four times with the biochar bottom basket collected each time and fresh biochar added into a basket and on top of the stack in order to study the variations in results at the maximum bed depth. In Chapter 5, a naphthalene model compound was used once again, with this time steam added in order to study the steam reforming of naphthalene over the moving bed of biochar. For Chapter 6, the naphthalene model compound was replaced with a tar-containing syngas produced from the fast pyrolysis of biomass. In this reactor, the pyrolysis and steam reforming section were separated to ensure that no biochar from pyrolysis reaches the moving bed and there is no steam gasification in the pyrolysis section.

To achieve Objective 5, the experimental results achieved from Objective 4 were scaled up to a size indicative of current industrial processes used to convert biomass to electricity. It was assumed there was no change in composition of the biochar or the syngas when increasing the size of reactor from the laboratory size to industrial size. The cost analysis was completed on the size of the equipment and biomass addition rate required to maintain the industrial size process. Historical data collected to complete the cost analysis was converted to Australian dollars ($AU) adjusted to 2017 value.

3.2.3 Soil Amendment Tests

To achieve Objective 6, several tests were completed in relation to the benefits that the addition of biochar has on the regrowth of biomass when added to the soil. It needs to be determined whether the moving bed steam gasification of biochar is beneficial or detrimental to the agronomical capabilities of the biochar when compared to the

biochar collected from only the pyrolysis of biomass. The water leaching of valuable AAEM species as well as carbon from the biochar was tested in a batch process. An organic solvent was used to determine the organic species present on the surface of the biochar. The water holding capacity, the anion exchange capacity, and cation exchange capacity of the biochar collected after the pyrolysis of biomass and from the exit of the moving bed reactor were quantified using methods outlined in Section 3.3.6.

3.3 Experimental

3.3.1 Biomass Samples

Mallee Eucalyptus (*E.loxophleba lissophloia*) sourced from Narrogin in Western Australia will be the primary source of biomass for this set of experiments. The individual components (wood, leaf, and bark) where physically separated from the tree, however, only the wood component will be utilised. The wood was then subsequently dried in an oven for 24 hours at 40 °C before being reduced in size using a cutting mill (model: Fritsch Cutting Mill Pulverisette 15). The cut wood biomass was collected and sieved into two size fractions; 1.0-2.0 mm and 150-250 µm. The 1.0-2.0 mm particle size biomass was used in the preparation of biochar catalysts, discussed in detail in Section 3.3.2, whilst the 150-250 µm biomass was used in the two-stage moving bed experiments to produce a tar-containing syngas, discussed in detail in Section 3.3.5. The difference in particle sizes is associated with the limitations of the two-stage reactor to take large particle sizes in the top pyrolysis zone. This will be discussed in further detail later in this section. When not in use, the biomass was stored in plastic bottles at a temperature of -9 °C.

3.3.2 Preparation of Biochar Based Catalysts

The first step in preparing the biochar catalyst is the slow pyrolysis of the biomass sample to produce biochar. To do this, firstly approximately 20 g of biomass wood (1.0-2.0 mm) was dried in an oven at 40 °C overnight. This biomass was then added to the fixed bed quartz reactor shown in Figure 3-2. A quartz frit is included in the reactor in order to prevent the biomass leaving the reactor. The reactor was weighed before and after the biomass was added in order to know exactly how much biomass was added. This is important in order to determine the biochar yield. After the biomass was added, the reactor was lowered into an electrically-heated furnace and purged with

argon (ultrahigh-purity, 1 L/min) for 15 minutes to ensure the biomass is not exposed to oxygen. The furnace was then switched on and heated at 10 °C/min to a final temperature of 900 °C with 15 minutes of holding once the final temperature was reached. The bed temperature was measured by situating a thermocouple just above the top of the biomass bed. After the holding time, the reactor was immediately lifted out of the furnace and allowed to cool to room temperature with the argon continuing to flow through the reactor to aid in cooling and to ensure the biochar is not exposed to oxygen. The reactor was weighed to measure the amount of biochar remaining, and hence calculate the yield of biochar based on the biomass feed. Finally, the biochar was collected and will be dedicated the name Raw Biochar.

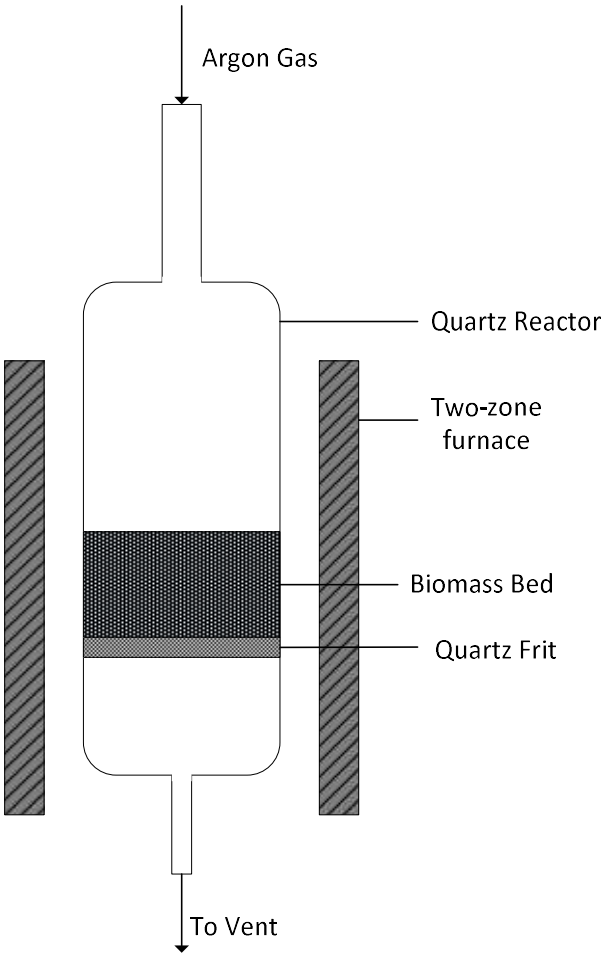

Figure 3-2: Schematic for the fixed bed quartz reactor vessel used to produce biochar from biomass through slow pyrolysis. The internal diameter of the section of reactor holding the biomass is 60 mm.

One of the aims of this thesis is to determine the catalytic effects of different metallic species. To isolate the effects of these metallic species, firstly the metallic species

contained within the biochar need to be removed, and then the new species added to the biochar. The alkali and alkaline earth metals (AAEM's) contained in the biochar were removed by soaking the biochar in 3 M hydrochloric acid for 24 hours. The HCl was heated to 50 °C and stirred constantly. After the 24 hour period, the HCl was separated from the biochar via vacuum filtration. To remove the residual HCl from the biochar, it was soaked in approximately 200 mL of ultrapure water (resistivity >18.2 MΩ-cm) for 15 minutes and then vacuum filtered. This process needed to be completed 25 times to remove all of the HCl. The acid and water washed biochar was collected and dried in the oven overnight at 40 °C.

The desired metallic species were loaded onto the biochar via wet impregnation. To do this, the acid washed biochar was mixed with a small amount of ultrapure water and KCl (Sigma-Aldrich, >99.0%), $MgCl_2$ (Aldrich, >98%) or $FeCl_3$ (Sigma-Aldrich, >97%), to prepare a set of KCl-, $MgCl_2$-, or $FeCl_3$- loaded biochars. The concentrations of K, Mg, and Fe (III) in these metal-loaded biochars were 6.160, 3.690, and 7.860 wt%, respectively, on a dry basis. This corresponds to having equimolar concentrations of each of the metallic species. The biochar was the dried in an oven overnight at 40 °C and then stored for future use.

3.3.3 Fixed Bed Pyrolysis of Naphthalene

The reactor set-up for the pyrolysis of naphthalene over a fixed bed of biochar is shown in Figure 3-3. Firstly, enough biochar was added to the quartz reactor in order to achieve a bed depth of 30 mm then the reactor was lowered into an electrically-heated furnace. The reactor was purged with argon (ultrahigh-purity, 1 L/min) for 30 minutes and then heated to 900 °C at a heating rate of 10 °C/min. Before adding the naphthalene and steam, the biochar was held at 900 °C for 5 minutes to ensure that the bed temperature had stabilised. Once the temperature reached 900 °C, the majority of the Cl was released from the biochars. Thus, the metals (i.e., K, Mg and Ca) retained in the biochars are in forms other than chlorides and these biochars are denoted as K-form biochar, Mg-form biochar and Fe (III)-form biochar, respectively.

To generate a steady stream of naphthalene at a constant concentration, ~0.9 L/min of argon was flowed over a flat plane of naphthalene (Sigma-Aldrich; >99%), taking advantage of naphthalene's sublimation property. The naphthalene concentration in the argon can be controlled by varying the temperature of the naphthalene. At the inlet

of the reactor, a further 0.1 L/min of argon was added and, at a naphthalene temperature of 54 °C, a concentration of 4500 mg/m^3 naphthalene was achieved. All gas lines were preheated to prevent naphthalene condensation. To collect the condensable reaction products, including the unreacted steam and naphthalene, the outlet gas was passed through a series of three condensers containing a 20:80 by volume methanol:chloroform solvent. The first condenser, containing 100 mL of solvent, was placed in an ice bath, whilst the second and third condensers, both containing 50 mL each, were placed in a dry ice bath. The non-condensable gases were then collected using gas bags for a period of one minute every three minutes.

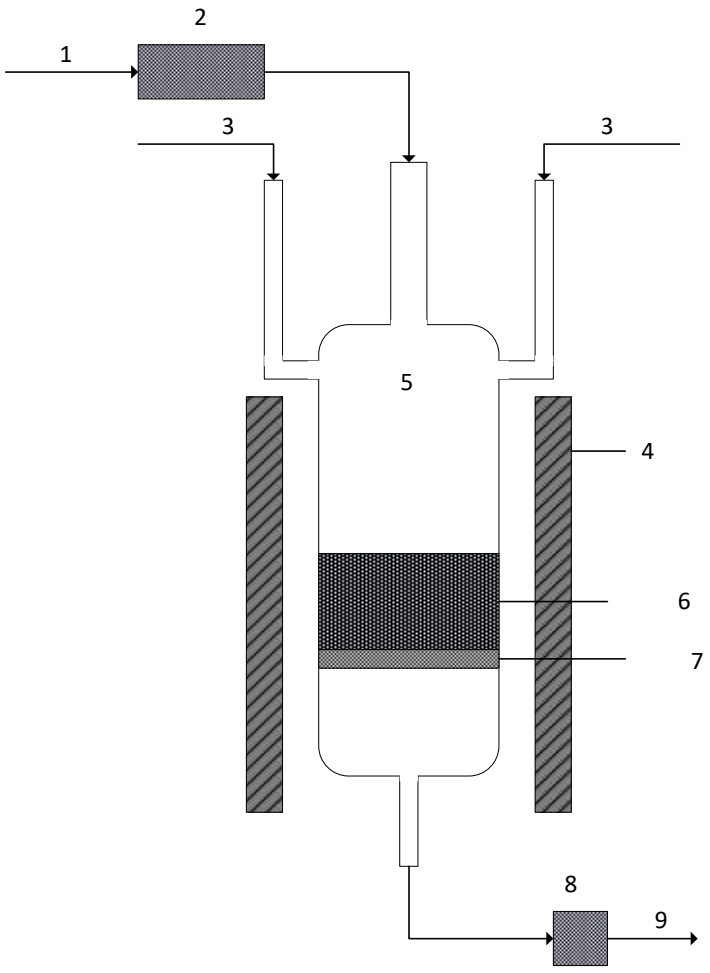

Figure 3-3: Schematic for the fixed-bed quartz reactor for the pyrolysis/steam reforming of naphthalene over biochar catalyst. The internal diameter of the reactor was 40 mm. 1 – argon; 2 – naphthalene vapour generator; 3 – argon + steam; 4 – furnace; 5 – fixed-bed quartz reactor; 6 – biochar catalyst bed; 7 – quartz frit; 8 – solvent traps; 9 – outlet for gas collection.

Once the allotted experiment time was complete (47 minutes), the naphthalene addition was shut off and the reactor immediately lifted out of the furnace. To aid in the cooling and to prevent any oxidation of the sample, the argon continued to flow through the reactor. Once the biochar had cooled to room temperature, the reactor was weighed and the biochar collected for further analysis.

3.3.4 Steam Reforming of Naphthalene over a Moving Bed of Biochar

The experimental set-up for the moving bed reactor explored in Chapter 5, as shown in Figure 3-4, is similar to that of the fixed bed pyrolysis/steam reforming set-up, as shown in Figure 3-3, with the major difference being in the reactor configuration. To simulate a moving bed of biochar, approximately 1.3 g of potassium loaded biochar was placed in a stainless steel basket and then placed into the stainless steel reactor. This amount of biochar corresponds to a bed depth of 3.8 mm of biochar. The baskets featured a mesh bottom to allow for the gas to flow through the bed but not allow the biochar to move from one basket to another. The reactor was constructed from SS316 and could be opened to allow access to easily remove the baskets. Before each experiment, the reactor was tested to make sure it was properly sealed.

Once the basket containing the biochar was added, the reactor was purged with argon at 1 L/min for 15 minutes. The reactor was then lowered into a preheated electric furnace and once the temperature reached 830 °C, the naphthalene and steam flow was started. For the pyrolysis experiments the steam was not added. The reaction time was 7 minutes. Once the reactor was cooled, a new basket containing another 1.3 g of potassium loaded biochar was placed on top of the previous basket in the reactor and the process repeated. This was completed until there were 10 baskets in the reactor signalling maximum bed depth. This process both simulated the moving bed of biochar and allowed for analysis of the reaction to be completed at different bed depths. Once the process was completed, each basket containing the biochar was weighed and the biochars collected from further analysis. The other reaction products were collected in the same manner as discussed in Section 3.3.3.

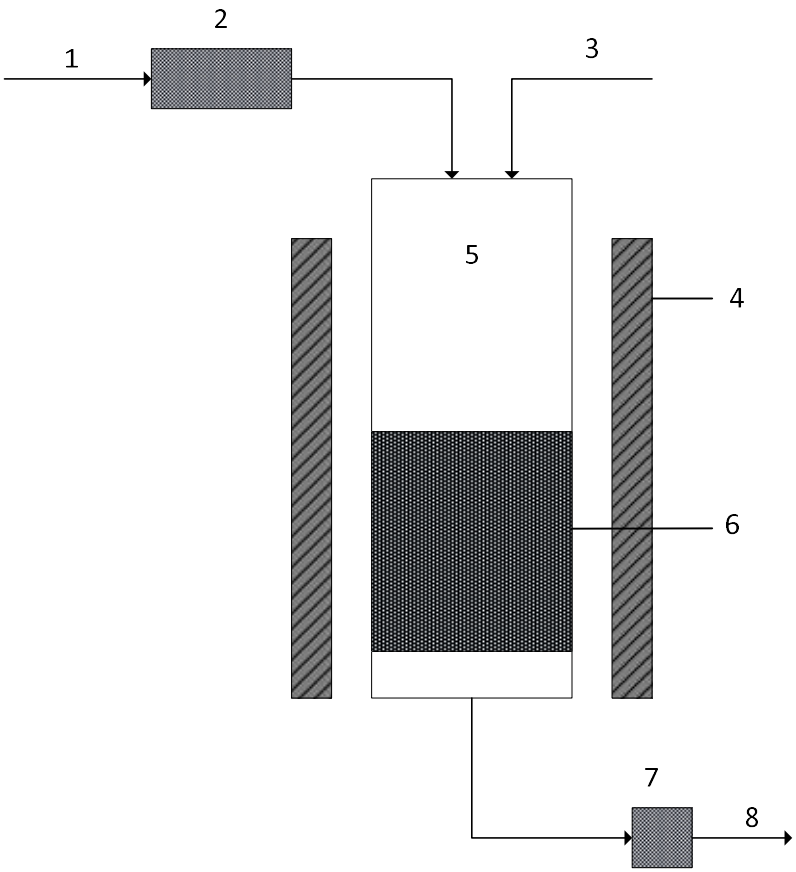

Figure 3-4: Schematic diagram for naphthalene pyrolysis/reforming over a moving bed of biochar. The internal diameter for the reactor was 40 mm. 1 – argon; 2 – naphthalene vapour generator; 3 – argon + steam; 4 – furnace; 5 – stainless steel reactor; 6 – moving bed including ten stainless steel baskets; 7 – solvent traps; 8 – outlet for gas collection.

3.3.5 Fast Pyrolysis of Biomass followed by Reforming of Tar over a Moving Bed of Biochar

The steam reforming of a real tar over a moving bed of biochar catalyst that will be studied in detail in Chapter 6, requires a two stage reactor. Fast pyrolysis of biomass was completed in the top section of the reactor, the tar and non-condensable gases produced were then carried into the second section of the reactor containing the moving bed of biochar. To manufacture the two-stage reactor, the moving bed reactor was modified to allow the pyrolysis section to be screwed on top. The full experimental set-up for the two-stage reactor is shown in Figure 3-5.

In this process, the moving bed is prepared via the same method discussed in Section 3.3.4. In this case, 1.85 g of potassium loaded biochar was added to each basket. Once the biochar catalyst was added and the reactor purged with argon it was lowered into the furnace. As the pyrolysis and reforming sections need to be at different

temperatures, two electrically heated furnaces placed on top of one another were used. The top furnace was set to provide a pyrolysis temperature of 500 °C whilst the bottom furnace a reforming temperature of 830 °C. Insulation was placed between the furnaces to ensure that the temperatures remained stable.

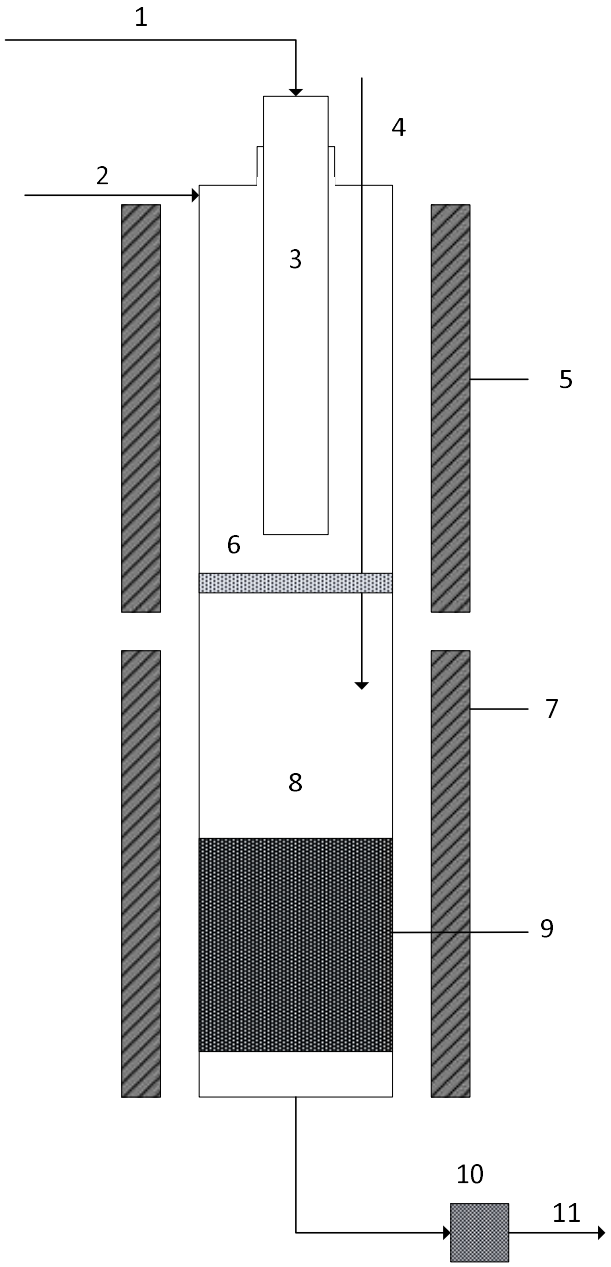

Figure 3-5: Schematic for two-stage fast pyrolysis/tar reforming over a moving bed of biochar reactor. The internal diameter of the reactor was 40 mm. 1 – argon + biomass; 2 – argon; 3 – water cooled feeding tube; 4 – argon + steam; 5 – top furnace; 6 – stainless steel mesh; 7 – bottom furnace; 8 – stainless steel reactor; 9 – moving bed including ten stainless steel baskets; 10 – solvent traps; 11 – outlet for gas collection.

Figure 3-6: Photograph of the top of the two-stage fast pyrolysis/tar reforming over a moving bed of biochar reactor as used in the laboratory.

Once the temperatures were stabilised, the biomass (Wood component of Mallee Eucalyptus, 150-250 μm) was added to the top of the reactor at 0.2 g/min. As the biomass is added at a continuous rate into a preheated reactor it undergoes fast pyrolysis. The biomass was entrained in a 1 L/min flow of argon via a screw feeder. To prevent the biomass undergoing pyrolysis before it reaches the bottom of the reactor, the inlet was fitted with a water jacket. The biochar was stopped from reaching the reforming section of the reactor through the addition of a stainless steel mesh, still allowing the tar and non-condensable gases through. Dead spots at the top of the reactor were prevented through the addition of a further 0.5 L/min of argon. Steam was added into the reforming stage of the reactor using a HPLC pump at a rate to create a final concentration of 10 vol%. A further 0.5 L/min of argon was added with the steam to ensure it stayed within the reforming section and didn't flow up into the pyrolysis section. As a result, the total argon flow was 2 L/min.

The fast pyrolysis/reforming process was completed for 10 minutes for each basket added to the reactor. This corresponds to a total reaction time of 100 minutes and a total of 20 g of biomass and 18.5 g of potassium loaded biochar added. The reaction

products were collected as described in Section 3.3.3. Each basket was individually weighed after each experiment and collected for further analysis once the entire experiment was complete. After each run, the biochar produced in the fast pyrolysis section was removed from the reactor.

3.3.6 Testing Recycling Properties of Biochar

The following are all of the tests required to quantify the benefits that the addition of biochar into the soil will have on the soil properties. The results of these experiments will be discussed in detail in Chapter 7.

Water Leaching

The water leaching capabilities of the biochar was tested in a batch process. The biochar was leached in water after the experiments were completed in the moving bed reactor experiments. All of the baskets were tested for biochar gasification with no naphthalene, naphthalene reforming over biochar, and tar reforming over biochar. Approximately 0.5 g of biochar sample was placed in 1 L of ultrapure water (resistivity >18.2 MΩ-cm) and continuously stirred. 20 mL samples of the water were taken at 15 mins, 30 mins, 1 hour, 3 hours, 6 hours, 12 hours, 1 day, 2 days, 3 days, and finally, every second day up to 15 days. Each sample was centrifuged at 4700 rpm for 5 minutes and the water collected for analysis of Na^+, K^+, Mg^{2+}, Ca^{2+}, Cl^-, and total carbon concentrations. The settled solid was then added back to the leaching sample with 20 mL of fresh ultrapure water approximately 5 minutes after the sample was taken to maintain the water level at 1 L.

The leaching kinetics were calculated by assuming a pseudo-second order model adapted from previous studies [136, 275-278]. The leaching model is shown in equation 3.1.

$$\frac{dC_t}{dt} = k(C_s - C_t) \qquad 3.1$$

Where C_t is the concentration (mgL^{-1}) of the species at any time t, C_s is the equilibrium concentration (mgL^{-1}), and k is the leaching rate constant ($mgL^{-1}day^{-1}$). The values for Cs and k are calculated by creating a plot of t/C_t versus t. Equation 3.2 is used to calculate the initial leaching rate (h, $mgL^{-1}day^{-1}$) when t is approaching 0.

$$h = kC_s^2 \quad 3.2$$

Organics Leaching

Leaching of the organic compounds contained within the biochar was measured by adding approximately 0.05 g of the biochar sample to 5 mL of 20:80 by volume methanol:chloroform. The biochar was soaked in the solvent for 24 hours before the liquid was collected for analysis of organic compounds. As with the water leaching, all biochars tested in the moving bed reactor experiments were tested for organics leaching.

Water Holding Capacity

The water holding capacities of all of the biochars tested in the moving bed experiments were tested using the device shown in Figure 3-7. In the middle section of the device, approximately 0.5 g of biochar was mixed with approximately 70 g of silica sand. A blank experiment was also completed just using sand. Into the tops section, 100 mL of water was added and allow to slowly flow down into the middle section through perforations in the bottom of the top section. The device was then sealed allowed to stand for 24 hours. The water holding capacity of the biochar was measured by comparing the amount of water added, the increase in mass of the middle section through the capture of water, and the amount of water let through into the bottom section.

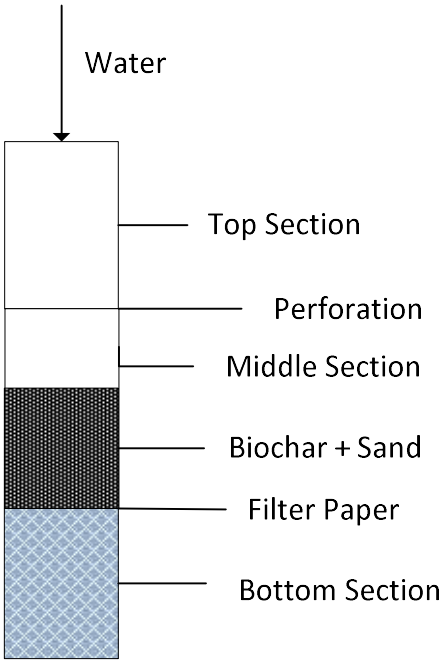

Figure 3-7: Schematic for vessel to measure water holding capacity of biochar.

Exchange Capacities

The measurement of biochar exchange capacities were developed by adapting the procedures as described in previous studies [279]. The exchangeable bases, anion exchange capacity, and cation exchange capacity were tested for all biochars tested using the moving bed reactors. Firstly, approximately 0.1 g of biochar sample and 0.9 g of silica sand was added to a 15 mL centrifuge tube. The soluble salts were removed by washing the biochar/sand by adding 10 mL of 70 % (w/w) aqueous ethanol and shaking for 30 minutes. The sample was centrifuged at 4700 rpm for 5 minutes and the ethanol removed. The procedure was then repeated once more with 70 % (w/w) aqueous ethanol followed by 20 % (w/w) aqueous glycerol.

The exchangeable bases in the biochar were measured by adding 10 mL of 0.1 M $BaCl_2$/0.1 M NH_4Cl solution to the washed biochar/sand. The solution was mechanically shaken for 2 hours, centrifuged, and the supernatant collected. The supernatant solution was analysed for Na^+, K^+, Ca^{2+}, and Mg^{2+} concentrations.

The anion exchange capacity (AEC) and cation exchange capacity (CEC) were measured by first removing the NH_4^+ by adding 10 mL of 0.05 M $BaCl_2$ solution. The mixture was then stirred for 1 hour, centrifuged, and the supernatant removed by

suction. The ionic strength of the biochar was reduced by washing with 3X10 mL portions of 0.002 M $BaCl_2$. After the final wash, the sample was centrifuged and the supernatant collected and analysed for Cl- concentration. The exchange capacities were measured by exchanging the entrained Ba^{2+} with Mg^{2+} and the Cl^- with SO_4^{2-}. To do this, 10 mL of 0.005 M $MgSO_4$ solution was added to the sample. The solution was mixed thoroughly and allowed to stand for an hour. The sample was then centrifuged and the supernatant collected for analysis of Mg^{2+} and Cl^-. The process was then repeated twice more with the supernatant analysed each time.

3.3.7 Economic Analysis

The base case for the large-scale production plant will be 200 dry ton per day of biomass. The moisture content of the biomass was assumed to be 45% [95, 280]. When scaling up, it was assumed that the syngas and biochar composition was the same as measured in the pilot-scale operations. The energy output was calculated based on the lower heating value of the syngas. The energy available in the biomass feed was calculated using equation 3.3 [87].

$$HHV_{d.b.} = 0.3491 * C + 1.1783 * H + 0.1005 * S - 0.0151 * N - 0.1034 * 0.0211ASH \ (\frac{MJ}{kg}) \quad 3.3$$

Where C, H, S, N, O, and ASH are the content of carbon, hydrogen, sulfur, nitrogen, oxygen, and ash of the biomass in wt% on a dry basis.

This economic analysis was carried out based on Australian dollars ($AU) adjusted to 2017 value. The Chemical Engineering Cost Index, as shown in equation 3.4, was used to convert historical pricing to the corresponding value in 2017 [281, 282].

$$Present\ Cost = Original\ Cost(\frac{index\ value\ at\ present}{idex\ value\ at\ time\ original\ cost\ was\ obtained}) \quad 3.4$$

This economic analysis was based around the production model of Mallee Eucalyptus (*E.loxophleba lissophloia*) in the south west of Western Australia.[94, 95] For this study, it was assumed that the biomass is produced at a rate of 60 green tonne per hectare per harvest cycle [95]. The initial harvest cycle was 5 years followed by 3 year coppice harvest cycles. The mallee production system was assumed to have a production lifetime of 50 years. Equation 3.5 was used to calculate the average transport distance of the biomass [95, 283].

$$r_b = \frac{1}{6}\tau\sqrt{\frac{P\times 330}{(1-\omega)\times 100\times M\times l}}\left(\sqrt{2}+\ln\left(1+\sqrt{2}\right)\right) \quad 3.5$$

Where r_b is the average transport distance, τ is the tortuosity factor (assumed to be 1.3 based on a previous study) [94], P is the processing capacity of the plant (dry tons per day), ω is the moisture content (45%), M is the mallee productivity (20 gt per hectare per year), and l is the land coverage of mallee planting (2%).

Equation 3.6 was used to adjust the capital and operating costs when taking capital costs from other sources and performing the sensitivity analysis on plant size

$$C_2 = C_1\left(\frac{P_2}{P_1}\right)^n \quad 3.6$$

Where C_1 and C_2 are the capital costs of the original and new plant respectively, P_1 and P_2 are the capacities of the original and new plant respectively and n is the scale factor, 0.6 will be used in this study

3.4 Instrument and Analytical Techniques

3.4.1 Proximate and Ultimate Analysis of Biomass and Biochar Samples

The proximate analysis of all biochar samples was completed using a thermogravimetric analyser (TGA, Model: Mettler Toledo STARe). The proximate analysis determines moisture content, ash content, volatile matter, and fixed carbon. To do this, approximately 10 mg of sample was added into the TGA at 40 °C and purged with argon for 15 minutes. The temperature was increased to 110 °C at 10 °C/min and held for 20 minutes; the weight loss at this stage was the total moisture in the sample. The temperature was then increased at 50 °C/min to 950 °C and held for 20 minutes followed by reducing the temperature at 25 °C/min to 600 °C; the weight loss here is the volatile material. Finally, the char was exposed to 100 mL/min of air for 30 minutes; the weight loss here is the fixed carbon content and the remaining material is ash.

The contents of carbon (C), hydrogen (H), and nitrogen (N) in biochar were quantified via an elemental analyser (Perkin Elmer 2400 Series II). Chlorine (Cl) content was measured using the conventional Eschka method as specified in AS 1038.8.2. [284]. The sulphur (S) content of biochar was tested following the method specified in

AS1038.6.3.1. [285]. The oxygen (O) content was then determined by the difference from carbon, hydrogen, nitrogen, chlorine, and sulphur contents on a dry and ash-free (daf) basis.

3.4.2 Quantification of Inorganic Species in Biochar

The quantification of alkali and alkaline earth metallic (AAEM) species was adopted from a method described in a previous study [111]. To analyse the AAEM species in biochar approximately 15 mg of biochar was placed in a platinum crucible and ashed in a muffle furnace with a temperature program designed to prevent the loss of ash-forming species. The ash was then digested in a mixture of concentrated HF/HNO_3 (1:1 ratio by volume) for 16 hours followed by the evaporation of the acid. The Na, K, Mg, and Ca was then quantified by digesting the residue in 0.02 M methasulphonic acid and analysing the solution using an ion chromatograph (IC) as detailed in Section 3.4.6. The Fe(III) content was then analysed by digesting a separate sample of the residue in 0.1 M HNO_3 and analysing the solution using an inductively coupled plasma optical emission spectrometer (ICP-OES) as detailed in Section 3.4.6.

The remainder of inorganic species (P, Si, Al) in biochar was quantified by following the borate flux method [115]. The fluxed biochar was then washed in 30 mL of 5% nitric acid and stirred for 24 hours at 50 °C. The acid solution was then analysed for P, Si, Al via inductively coupled plasma optical emission spectrometry (ICP-OES, Perkin Elmer Optima 8300).

3.4.3 Non-Condensable Gases in Syngas

The concentrations of the non-condensable gases H_2, CH_4, CO, and CO_2 in the syngas collected during the pyrolysis and reforming experiments were analysed using two gas chromatographs (GC). The first GC used to analyse H_2 was a Perkin Elmer AutoSystem XL consisting of a molecular sieve column and argon as the carrier gas. The CH_4, CO, and CO_2 concentrations were measured on a Perkin Elmer AutoSystem GC with a molecular sieve/Porapak-N dual column system with helium as the carrier gas.

3.4.4 Determination of Naphthalene and Tar Concentration in Solvent Traps

The unreacted naphthalene and tar captured in the methanol/chloroform solvent solutions as well as the solvent from organics leaching were quantitatively and semi-quantitatively analysed using a gas chromatography mass spectrometer (GC-MS, Agilent 7890B/5977A). The program used to analyse for naphthalene is as follows: initial temperature of 180°C, heating rate of 50 °C/min, final temperature of 240 °C, helium gas flow of 1 mL/min through the column, and a split ratio of 100. The concentration of naphthalene was quantitatively analysed by comparing the peak area of the samples to those of standards of known concentration prepared using naphthalene (Sigma-Aldrich; >99%) dissolved in methanol/chloroform solution (1:4 by volume). The program to analyse tar is as follows: initial temperature of 40°C, heating rate of 10 °C/min, final temperature of 240 °C, holding time of 5 minutes, helium gas flow of 1 mL/min through the column, and a split ratio of 100. The tar content was semi-quantitatively analysed by comparing the GC-MS outputs of different samples.

The larger aromatic ringed structures in the methanol/chloroform solvent traps, water leached samples, and organic leaching samples were analysed via UV-Fluorescence (Perkin Elmer LS55).

3.4.5 Surface Area and Pore Volume Analysis

The data required to measure the surface area and pore volume of the biochar was analysed on a Micrometrics Tri-star II model 3020 using N_2 adsorption. A typical adsorption isotherm gathered from the instrument is shown in Figure 3-8. To do so, approximately 150 mg of the biochar was added to the sample tube and degassed for 12 hours at 150 °C. The analysis was then completed using N_2 gas at the temperature of liquid N2. The surface area was calculated using the Brunauer-Emmett-Teller (BET) method [286] and the pore volume calculated using the Dubinin-Astakhov method [287].

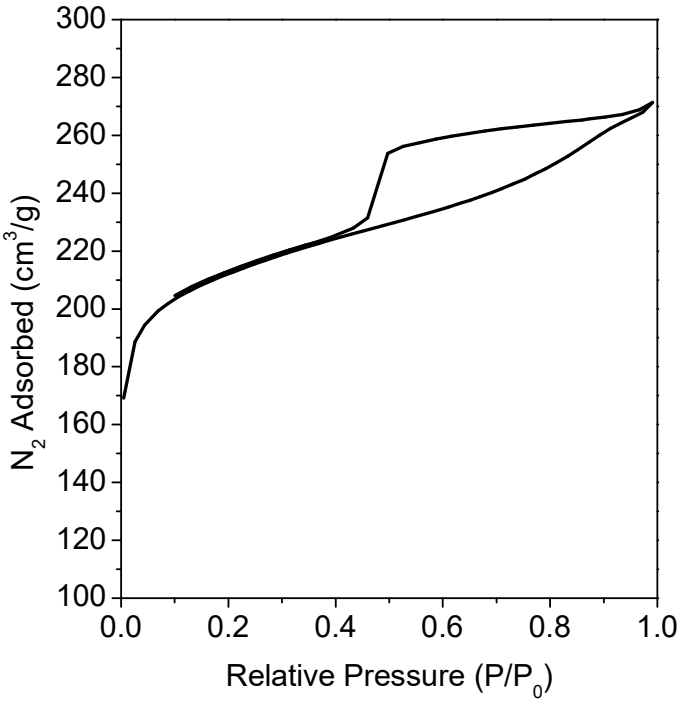

Figure 3-8: Typical adsorption isotherm from a surface area/pore volume analysis on a biochar sample collected from the moving bed reactor.

3.4.6 Analysis of Inorganic and Organic Species in Liquid Samples

The measurement of AAEM species in liquid samples was adopted from a previous study [111]. The concentration of the AAEM species (Na, K, Mg, and Ca) in the solutions collected from acid digestion, leaching, and exchange capacity were quantified using an ion chromatograph (IC, DIONEX ISC-3000) equipped with suppressed conductivity detection system using 0.02 M methanesulphonic acid as the eluent. The chlorine content was quantified using another IC system (DIONEX ISC-1100). In this case, 0.045 M sodium carbonate 0.014 M sodium bicarbonate solution was used as the eluent. The Fe(III) concentration was quantified using an ICP-OES (Perkin Elmer Optima 8300).

3.4.7 Specific Reactivity of Biochar

The specific reactivity of the biochar was measured using a TGA (Mettler Toledo STARe). A detailed procedure of reactivity measurement is outlined in a previous study [184]. Briefly, approximately 8 mg of biochar sample was loaded into a sample pan and placed in the TGA at 40 °C. The temperature was increased to 110 °C in an argon atmosphere and held for 30 minutes to remove the moisture contained in the

biochar. This was followed by heating to 425 °C at 50 °C/min. Once the temperature reached 425 °C, air was introduced and the reactivity calculated from this point using the following equation:

$$R = -W\frac{dW}{dt} \quad (3.7)$$

where W is the weight of the sample at any time t. The change in weight over time (dW/dt) was calculated using the software used on the TGA. The conditions for the reactivity measurements were chosen to ensure the measurement is completed under a chemically controlled regime and the diffusion effect has been eliminated.

3.4.8 Errors, Mass Balances, and Repeatability

The main source of error in these experiments is associated with the heterogeneous nature of the biochar samples. This results in the measured properties of the biochar varying depending on the amount of biochar collected for analysis. To minimise the errors associated with the heterogeneous nature of the biochar, the analysis of the biochar, such as the proximate and ultimate analysis, where measured in triplicate and the average value used. Any values that were considered unusual were repeated and the value discarded if necessary. Mass balances were conducted on each of the experiments conducted taking into account the gas flows and composition as well as the changes in composition and mass in the biochar. Any inconsistencies in the mass balance resulted in the repeat of the experiment.

3.5 Summary

Biochar catalyst was prepared via the pyrolysis of mallee wood biomass at 900 °C followed by acid washing and subsequent loading of potassium, magnesium, or iron (III) via their chloride salt. The catalytic capability of the different biochar-based catalysts to crack naphthalene was tested in a fixed bed capacity under inert conditions. These results also allowed for the analysis of the interaction between the biochar and the naphthalene. The potassium loaded biochar was then adopted as a catalyst in a moving bed operation to study the steam reforming of naphthalene as a model compound as well as the steam reforming of tar contained in a syngas produced from the pyrolysis of biomass. A scale-up to an industrial size plant and subsequent cost analysis was conducted based on the results achieved from the two-stage pyrolysis of

biomass and steam reforming of the tar-containing syngas. Finally, the benefits of adding the biochar collected from the outlet of the moving bed reactor to the soil were quantified. The properties tested included leaching of AAEM species, water holding capacity, anion exchange capacity, and cation exchange capacity.

CHAPTER 4 PYROLYSIS OF NAPHTHALENE OVER METAL LOADED BIOCHARS AT 900 °C

4.1 Introduction

Tarry substances in syngas produced from biomass gasification can be notorious for downstream applications [21, 31]. For example, the tar content in syngas must be less than 100 mg/m^3 in a gas engine [67] and 50 mg/m^3 in a gas turbine [66]. Mineral-based catalysts [7, 81, 173, 229, 254, 256, 262, 263, 267, 288-291] are considered to be effective in eliminating tars for syngas cleaning. The major drawbacks of such mineral-based catalysts are issues associated with catalyst deactivation, regeneration and disposal. An alternative is biochar-based catalysts, which provide many benefits over mineral-based catalysts. For example, biochar can be produced from the pyrolysis of biomass that can be the same feedstock for gasification. Spent catalyst disposal is also easy because it can be gasified for energy recovery or possibly returned to soil for carbon sequestration and inorganic nutrients recycling [136].

Naphthalene is regarded as the most prevalent and refractory aromatic hydrocarbon [21, 253, 254], which typically contributes to 15% of the tar in syngas [199]. It is known that tar elimination over biochar-based catalysts is dictated by the net effect of coke deposition on biochar surface and the competitive coke gasification reactions [151]. Therefore, it is critical to understand the behaviour of naphthalene pyrolysis that is the first step of naphthalene gasification. There is still considerable scope in understanding the fundamental reaction mechanisms on naphthalene pyrolysis over biochar-based catalysts. Therefore, this chapter aims to carry out a systematic investigation into the pyrolysis behaviour of naphthalene over various biochar-based catalysts at 900 °C including biochar and biochars loaded with potassium, magnesium and iron (III).

4.2 Conversion of Naphthalene over Biochar-based Catalysts during Pyrolysis

Figure 4-1 represents the conversion of naphthalene with or without catalysts. In absence of a catalyst, there is little conversion of naphthalene under the conditions. However, it should be noted that there was visual evidence of traceable coke deposited on the wall of reactor after the experiment. Via a combustion method (i.e. passing oxygen through the reactor at 900 °C then quantifying the released CO and CO_2 using GC), the results show that the deposited coke contributes to < 0.7% conversion of naphthalene in the experiments. Such conversions are very small and within the experimental errors of naphthalene recovery quantification (see Figure 4-1).

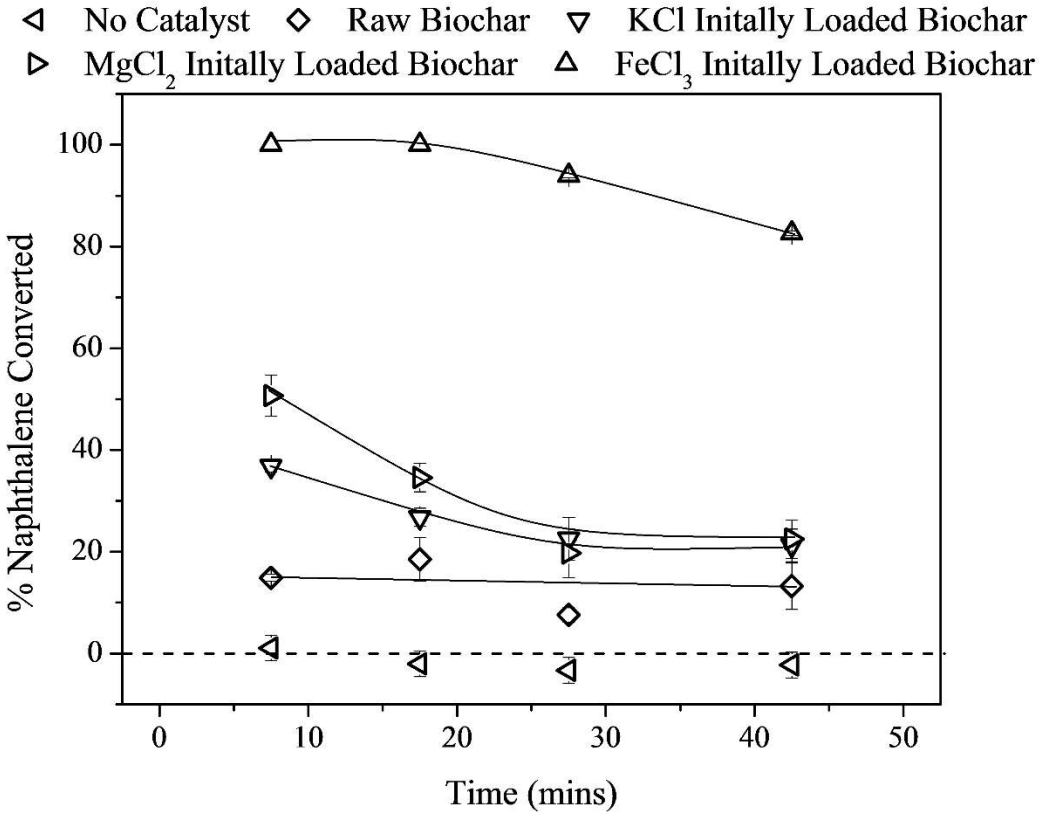

Figure 4-1: Naphthalene conversion over time at 900 °C after being passed over the four different biochar based catalysts as well as in the absence of biochar catalyst. The naphthalene was captured in the methanol/chloroform traps for 5 minutes; hence the average conversion is taken at the median point in time.

Figure 4-1 further demonstrates the conversion of naphthalene over the four different biochar catalysts. One immediate finding is that the conversion of naphthalene over

the raw biochar is as low as ~7−18%. The conversion of naphthalene increases with the addition of metallic species on the biochar. The reforming of naphthalene increases to 36.8 to 50.7 % for the K-form biochar and Mg-form biochar respectively after 7.5 minutes of reforming. Potassium chloride and magnesium chloride, as loaded onto the biochar are ineffective catalysts. The K and Mg need to bond with the biochar and subsequently release chlorine [215]. By studying the chlorine ratios provided in Table 4-1, it can be seen that the metal to chlorine ratio before and after reforming is much lower than 2 for Mg-form biochar but closer to 1 for K-form biochar. This suggests that Mg is bonded to the biochar, either directly or to surface groups, to a greater extent than K therefore explaining its higher activity. The addition of $FeCl_3$ to the biochar results in 100% conversion of the naphthalene in the first 20 minutes. The higher activity of the Fe(III)-form biochar is because the Fe forms Fe_3O_4 on the surface, a highly active catalyst [215, 261, 292, 293]. The metal to chlorine ratio in the supplementary material for Fe(III)-form biochar is much lower than 3, confirming that iron is present on the biochar in other forms opposed to $FeCl_3$ during reforming. It has also been found previously that Fe_3O_4 will be evenly distributed on the surface of the biochar [261] whereas K and Mg for a loose patchwork structure, resulting in an uneven distribution and lower activity [12].

Table 4-1: Metal to chlorine ratio for biochars tested

	KCl-Loaded Biochar	**$MgCl_2$-Loaded Biochar**	**$FeCl_3$-Loaded Biochar**
Untreated	1	2	3
900 °C - 0 mins	1.08	0.317	0.184
900 °C - 47 mins	0.621	0.239	0.190

The ability of each biochar catalyst studied to remove naphthalene decreases over time. The conversion of naphthalene over Fe (III)-form biochar remains at 100 % for 20 mins before it begins to decrease. Its conversion over K-form and Mg-form biochars decreases up until 30 mins and then levels off.

4.3 Release of Gases during Naphthalene Pyrolysis

To understand how the naphthalene interacts with the biochar catalysts and influences the syngas composition during pyrolysis at 900 °C, it is important to investigate the

release of typical gaseous products such as hydrogen (H_2) and carbon monoxide (CO) in the absence and presence of naphthalene. Figure 4-2 and Figure 4-3 illustrate the rates of H_2 and CO released during pyrolysis with and without naphthalene, which were calculated from the concentration of H_2 or CO in the syngas and the flow rate of the syngas. As expected, for both the H_2 and CO released in the absence of naphthalene, the rate decreases over time. The H_2 released is greatest in the raw biochar and the smallest in Mg-form biochar, whereas the CO released is greatest in the Fe(III)-form biochar and the smallest in the Mg-form biochar. The differences in H_2 and CO release rates due to thermal cracking can be attributed to the interaction of the metallic species with the surface groups on the biochar. During the slow heating process, the positively charged metallic species bond with the negatively charged carboxylate groups releasing hydrogen. Hence, when the temperature reaches and is held at 900 °C, there is less hydrogen available to be released. The bonds with the metallic species also restrict the thermal cracking of these groups to form CO due to the increased strength of the bond. These results can be confirmed by looking at the hydrogen and oxygen content the biochar in Table 4-2. The amount of hydrogen and oxygen lost when held at 900 °C without naphthalene per gram of biochar is highest in raw biochar.

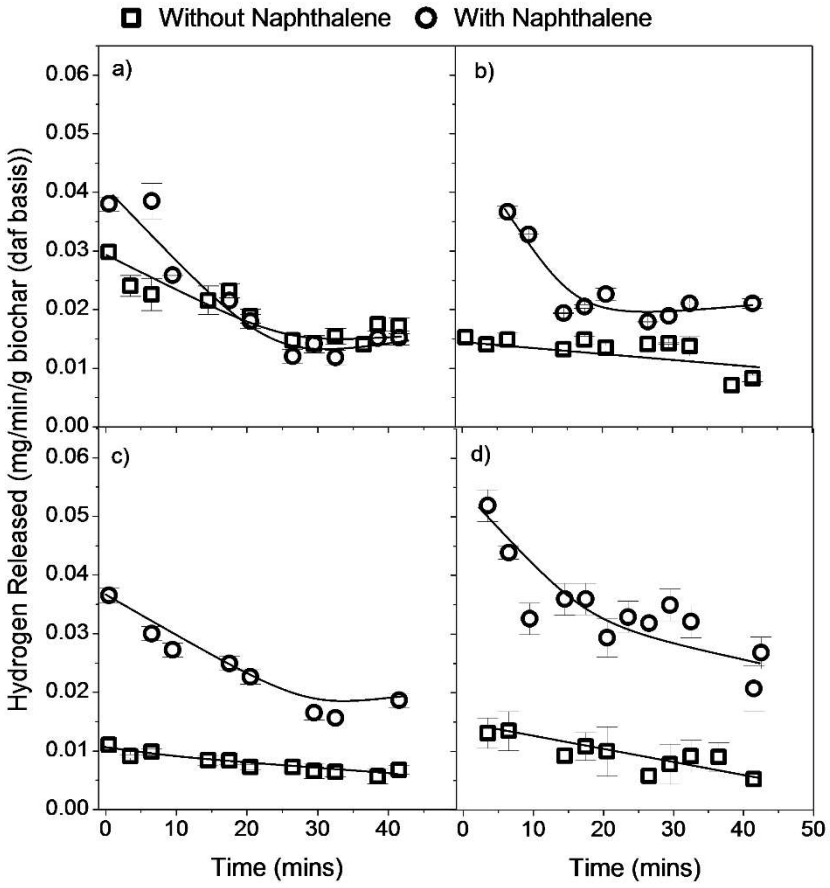

Figure 4-2: Rate of hydrogen released per gram of biochar (daf basis) for a) Raw Biochar b) K-Form Biochar c) Mg-Form Biochar d) Fe(III)-Biochar with and without the addition of naphthalene

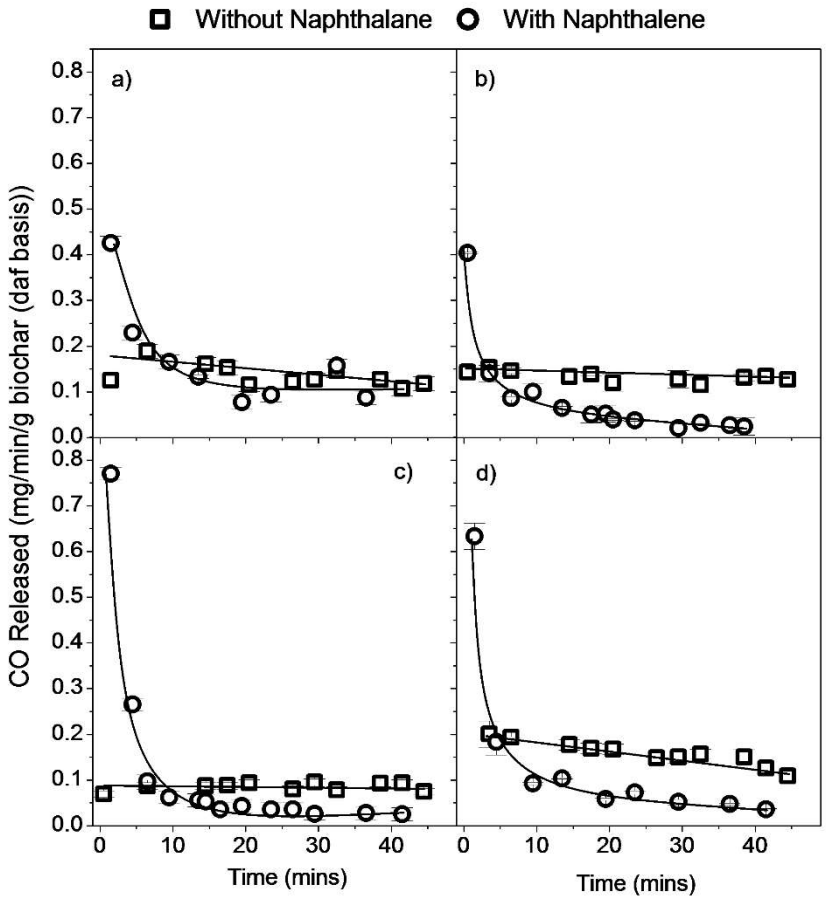

Figure 4-3: Rate of carbon monoxide released per gram of biochar (daf basis) for a) Raw Biochar b) K-Form Biochar c) Mg-Form Biochar d) Fe(III)-Biochar with and without the addition of naphthalene

In the presence of naphthalene, the releases of H_2 and CO follow significantly different trends than seen without naphthalene. The hydrogen released during the pyrolysis over K-form, Mg-form and Fe(III)-form biochars follows a linear trend similar to that released in the absence of naphthalene. For raw biochar, the amount of H_2 released from the catalyst and naphthalene increases slightly over time. However, for periods of time, the rate of H_2 released in the presence of naphthalene is less than in the absence of naphthalene, in despite of a large conversion of naphthalene, which is expected to produce hydrogen (see Figure 4-1). For the other two catalysts, the rate of H_2 released is larger during naphthalene pyrolysis due to the much larger naphthalene conversion (see Figure 4-1).

Table 4-2: Properties of biochar-based catalysts in this chapter

sample	proximate analysis (wt%, db[b])				elemental analysis (wt % daf [c])						inorganic analysis (wt%, db[b])				
	moisture (ad[a])	Ash	VM[d]	FC[e]	C	H	N	O[f]	S	Cl	Na	K	Mg	Ca	Fe
Raw biochar	4.1	2.3	7.9	89.7	91.1	1.30	0.32	7.3	0.01	0.02	0.09	0.257	0.132	0.681	0.000
Acid-washed biochar	5.1	2.3	8.6	89.1	90.3	1.2	0.27	6.6	0.01	1.61	0.06	0.142	0.101	0.402	0.000
KCl-loaded biochar	7.4	10.5	13.4	75.3	81.9	0.66	0.27	8.8	0.01	8.34	0.06	5.046	0.105	0.313	0.000
$MgCl_2$-loaded biochar	18.0	6.9	19.5	73.7	78.4	2.30	0.30	8.0	0.01	10.99	0.05	0.116	2.663	0.242	0.000
$FeCl_3$-loaded biochar	14.2	9.5	21.2	69.4	71.5	1.60	0.23	12.1	0.01	14.56	0.06	0.095	0.090	0.263	9.524
biochar-based catalysts															
Raw biochar	5.2	2.3	7.4	90.3	89.8	0.92	0.32	8.9	0.01	0.01	0.10	0.262	0.138	0.696	0.000
K-form biochar[g]	6.5	2.5	8.3	89.2	89.5	0.89	0.36	7.7	0.01	0.87	0.01	3.63	0.061	0.400	0.000
Mg-form biochar[g]	5.5	4.6	7.5	87.9	89.2	0.78	0.33	9.1	0.01	0.65	0.01	0.043	2.03	0.357	0.000
Fe-form biochar[g]	1.8	5.2	8.3	86.5	88.4	0.96	0.29	9.9	0.01	0.46	0.01	0.047	0.096	0.413	3.930
biochar-based catalyst after reactions															
Raw without naphthalene	5.1	2.9	7.3	89.9	90.4	0.83	0.51	8.5	0.01	0.03	0.08	0.272	0.136	0.670	0.000
Raw with naphthalene[i]	3.0	2.5	6.7	90.8	90.7	0.77	0.57	8.1	0.01	0.03	0.10	0.263	0.138	0.607	0.000
K-form without naphthalene [h]	3.2	3.2	8.3	89.3	90.5	0.85	0.48	7.5	0.01	0.44	0.02	2.33	0.051	0.320	0.000
K-form with naphthalene [i]	3.3	4.7	8.4	87.4	91.4	0.77	0.52	6.8	0.01	0.76	0.03	1.893	0.089	0.312	0.000
Mg-form without naphthalene [h]	3.6	3.3	7.1	89.6	89.8	0.72	0.39	8.7	0.01	0.52	0.02	0.122	1.595	0.266	0.000
Mg-form with naphthalene [i]	4.5	5.3	8.4	86.3	90.8	0.63	0.54	7.7	0.01	0.60	0.02	0.105	1.571	0.299	0.000
Fe-form without naphthalene [h]	1.0	5.6	6.3	88.1	89.2	0.89	0.35	9.6	0.01	0.50	0.01	0.015	0.052	0.198	3.566
Fe-form with naphthalene [i]	1.0	5.0	7.3	87.7	91.7	0.66	0.44	7.1	0.01	0.67	0.02	0.063	0.044	0.360	2.911

[a]Air dried basis. [b]Dry basis. [c]dry and ash-free basis. [d]Volatile matter. [e]Fixed carbon. [f]By difference, Cl contributes to 70% of ash and was taken into account in this calculation. [g]Biochar exposed to 900 °C for 0 min in the absence of naphthalene. [h]Biochar exposed to 900 °C for 47 min in the absence of naphthalene. [i]Biochar exposed to 900 °C for 47 mins in the presence of naphthalene

The release of CO in the presence of naphthalene follows a much different trend than the H_2 released. For all of the biochar catalysts, the rate of CO experiences a spike immediately after the naphthalene is added, followed by a significant decrease. After 5 minutes, the rate of CO released during naphthalene pyrolysis is less than that released from the biochar in the absence of naphthalene for all catalysts. The initial spike in the rate of CO released shows that the naphthalene reacts with the oxygen contained in the biochar. The significant decrease in rate of CO released points toward the depletion of oxygen available to react with naphthalene.

4.4 Formation of Multiple Ringed Aromatic Structures

The previous sections showed that naphthalene can be removed from the gas stream to different extents using biochar catalysts (Section 4.2) and converted to H_2 and CO under pyrolysis conditions (Section 4.3). One further possible mechanism for naphthalene to undergo during pyrolysis is the polymerisation into larger ringed polycyclic aromatic hydrocarbons (PAHs). The presence of these large PAH's in the gas stream can be just as, if not more, detrimental to downstream equipment as naphthalene as they can readily deposit on the surface of critical equipment. As with the naphthalene conversion and H_2 captured, the baseline must be established to determine the release of large ringed PAHs from biochar in the absence of naphthalene. Figure 4-4 shows the normalised intensity from UV-Fluorescence based on per gram of biochar. It can be seen there are very little ringed compounds released from biochars at 900 °C in the absence of naphthalene.

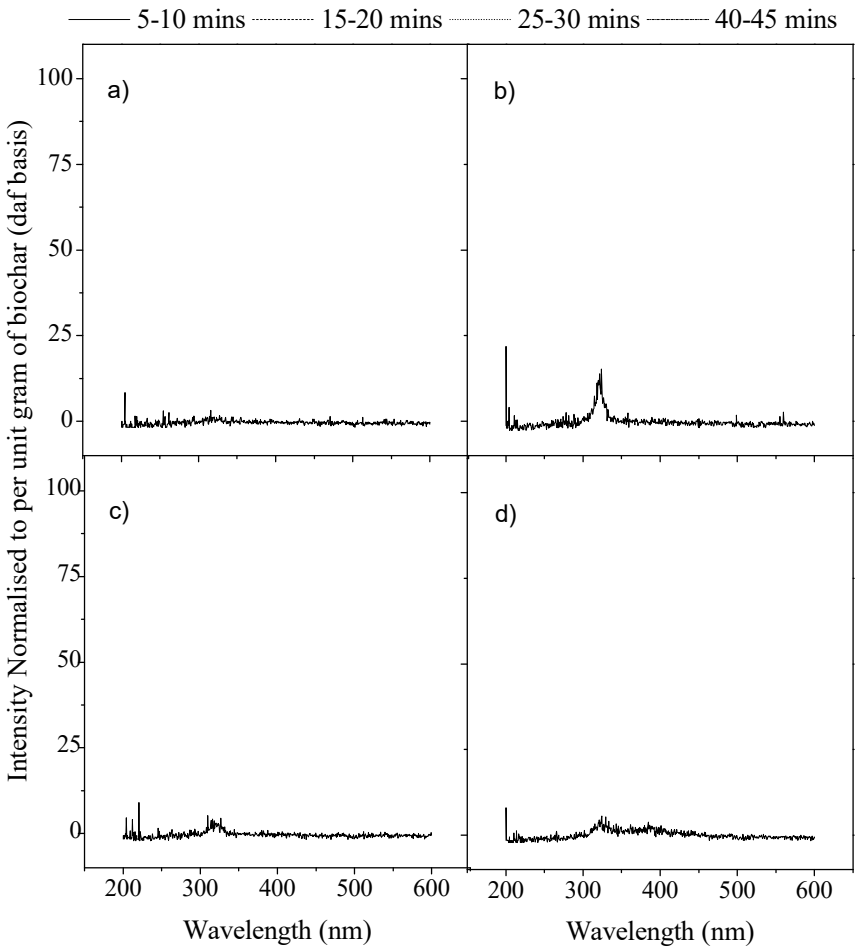

Figure 4-4: Normalised UV-Fluorescence Intensity of Gases Captured in Methanol/Chloroform Traps Released from Biochars in the Absence of Naphthalene a) Raw Biochar b) K-Form Biochar c) Mg-Form Biochar d) Fe(III)-Form Biochar. The intensity was normalised to per gram of biochar (daf basis).

Figure 4-5 compares the normalised UV-Fluorescence data from the pyrolysis of naphthalene in the absence of biochar to that with each of the biochars. The methanol/chloroform traps were analysed; hence it can be determined whether there is a presence in the gas stream. The intensity was normalised against the amount of naphthalene converted for the 5 mins the gas was exposed to the methanol/chloroform traps to allow for a semi-quantitative comparison of each of the biochars tested. By comparing each of the biochars tested with the peaks obtained from the pyrolysis of naphthalene in the absence of biochar, the peaks decrease in intensity as the conversion increases. For the analysis where no catalyst was present, i.e., with a low conversion, a large peak can be seen for naphthalene at 300-350 nm and also other peaks at a higher wavelength showing the formation of 3-5 ringed hydrocarbons. When catalysts are added, and the conversion of naphthalene increases, there is less evidence of 3-5 ringed PAH's being formed in the gas stream. When the conversion is 100% in the Fe (III)-

Form Biochar, there is no evidence of polymerisation. Hence the polymerisation mechanism during the pyrolysis of naphthalene is not dominant when a catalyst is used and the conversion is high.

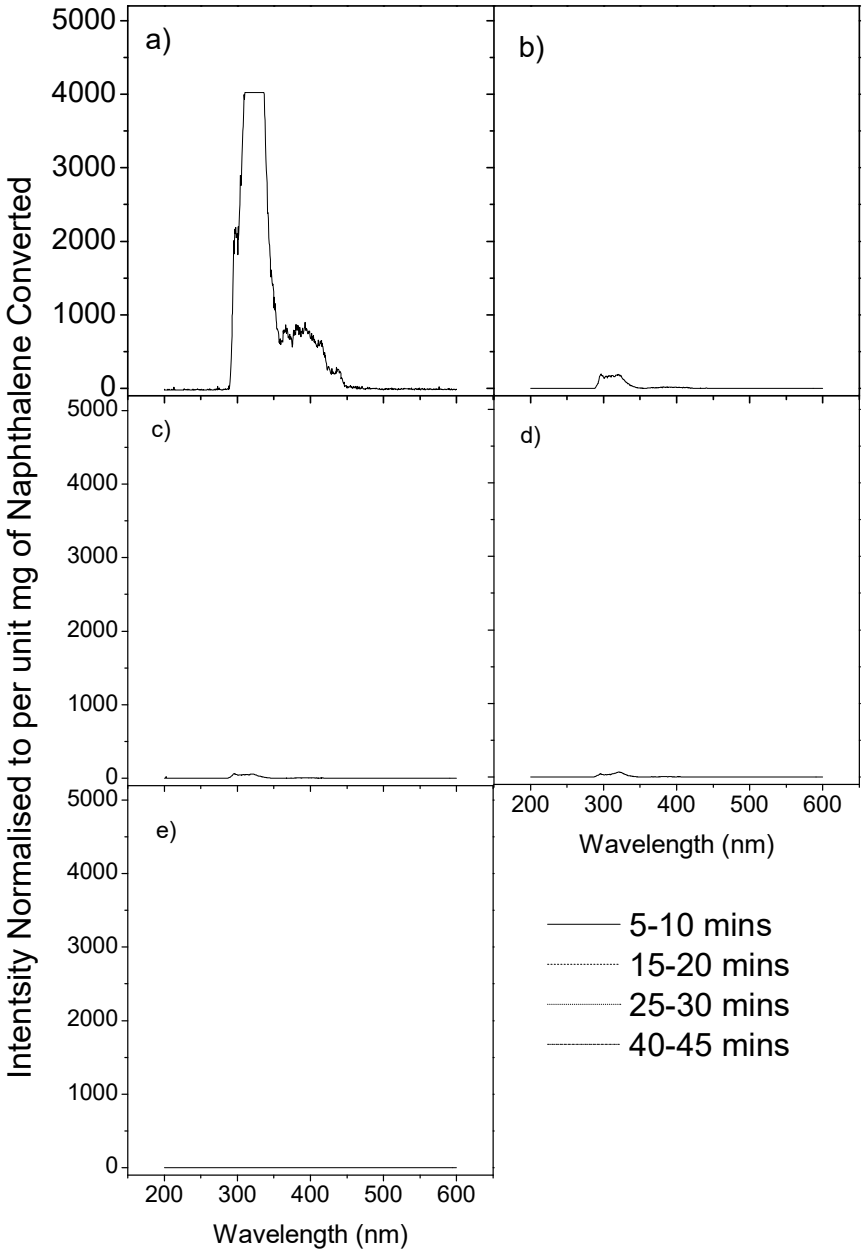

Figure 4-5: Normalised UV-Intensity of Gases Captured in Methanol/Chloroform Trap when Naphthalene is passed over different Biochar Catalysts a) No Catalyst b) Raw Biochar c) K-Form Biochar d) Mg-Form Biochar e) Fe(III)-Form Biochar. Intensity normalised to per mg of naphthalene converted over the 5 minute capture period.

4.5 Further Discussions on Possible Mechanisms for Naphthalene Destruction

The data presented in previous sections enable us to identify the dominant mechanism responsible for the naphthalene conversion during pyrolysis over the biochars. There are two mechanisms for naphthalene destruction proposed in open literature. First, naphthalene can be converted into larger ringed PAHs via polymerisation, as shown in Reaction 4.1 [294]. Reaction 4.1 only shows two naphthalene molecules bonding to form a 4-ringed polyaromatic hydrocarbon (PAH), however, there is a potential for the reaction to proceed further and larger PAHs be formed. As shown in Figure 4-5 and discussed in the previous section, reaction 4.1 is not the dominant mechanism

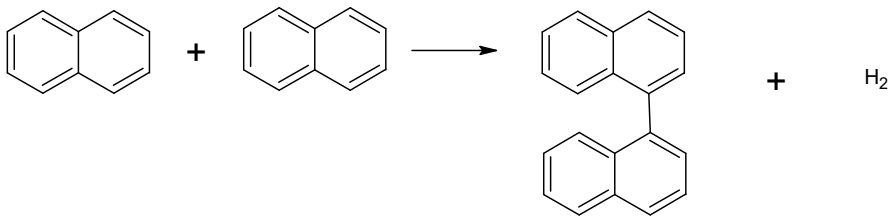

4.1

The first stage in the second mechanism reported in the literature is the decomposition of the naphthalene into smaller, straight chained hydrocarbons, as shown in equation 4.2 [151, 262]. Through the analysis of the solvent traps via GC-MS, there was no evidence of these smaller hydrocarbons in the gas stream. Hence, the naphthalene will all decompose via part two of the mechanism, as shown in equation 4.3 [151, 262], into carbon and hydrogen. By looking at the carbon content of the biochars before and after reforming, as shown in Table 4-2, and taking into account the total mass changes, it was found that carbon was deposited on the biochar for all catalysts tested. Hence, this confirms that naphthalene is decomposed via reaction 4.3, however, this mechanism does not explain the increased formation of carbon monoxide that was observed during naphthalene pyrolysis.

$$C_mH_n \text{ (aromatics)} \rightarrow C_mH_x \text{ (coke)} + (n-x)/2H_2 \qquad 4.2$$

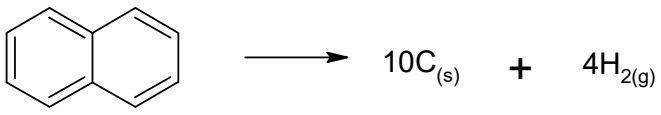

4.3

It is proposed that the carbon monoxide is formed through a reaction of naphthalene with the oxygen in the biochar catalyst. As can be seen in Table 4-2, the oxygen content of all biochar catalysts is less when exposed to naphthalene compared to those thermally treated in the absence of naphthalene. However, when comparing the total oxygen and hydrogen lost to that added to the syngas as seen in Figure 4-6 and Figure 4-7 respectively, there is a significant amount of gas that is unaccounted for in the measurements of carbon monoxide and hydrogen. When comparing the amount of hydrogen unaccounted for to the oxygen, as seen in Figure 4-8, the molar ratio is approximately 2:1 for all biochars. This suggests that there is a formation of water in the pyrolysis of naphthalene over a biochar catalyst.

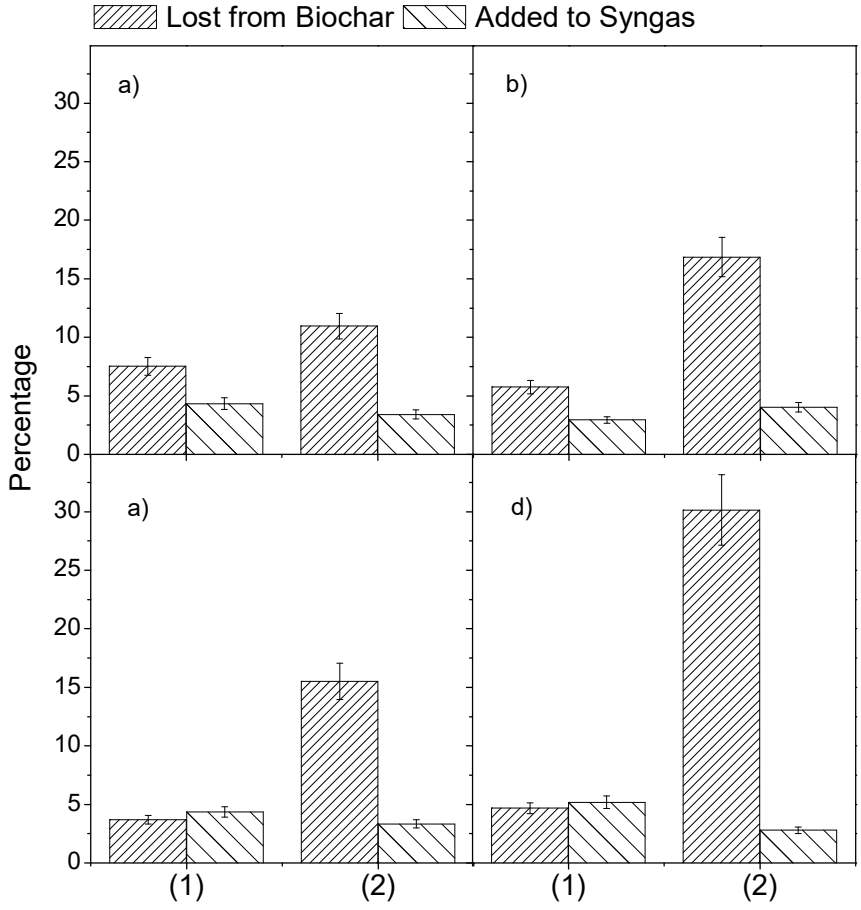

Figure 4-6: Percentage of total oxygen lost from a) Raw Biochar, b) K-Form Biochar, c) Mg-Form Biochar, d) Fe(III)-Form Biochar after 47 minutes at 900 °C based on total oxygen in biochar exposed to 900 °C for 0 minutes (1) in the absence of naphthalene and (2) in the presence of naphthalene

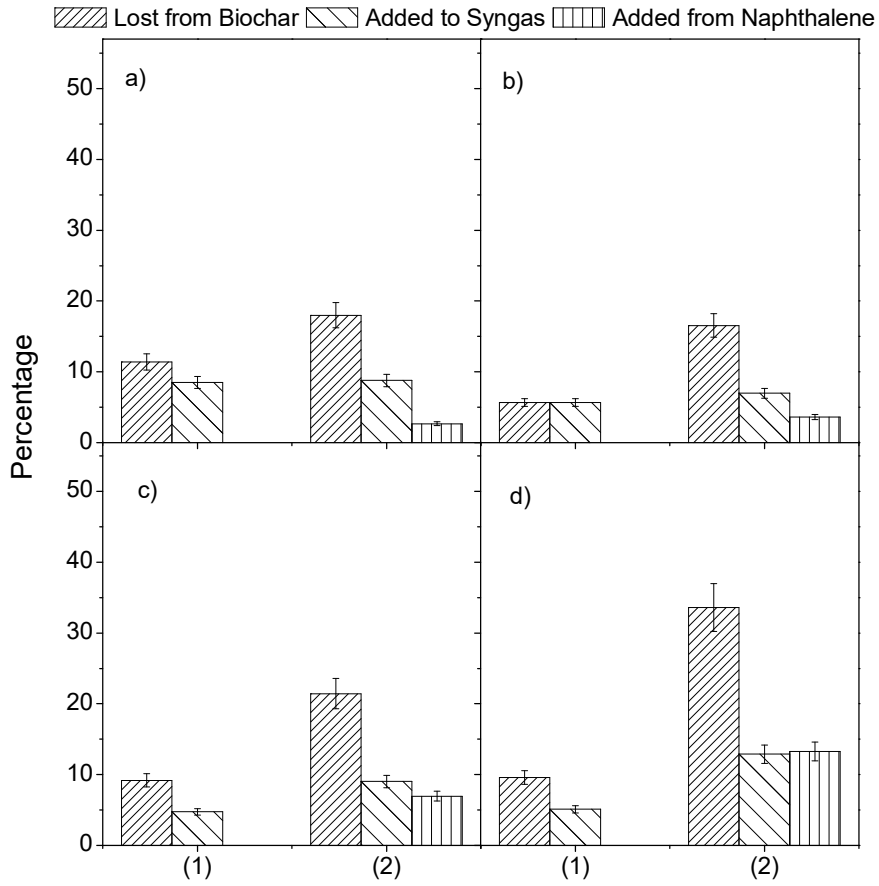

Figure 4-7: Percentage of total hydrogen lost from a) Raw Biochar, b) K-Form Biochar, c) Mg-Form Biochar, d) Fe(III)-Form Biochar after 47 minutes at 900 °C based on total hydrogen in biochar exposed to 900 °C for 0 minutes (1) in the absence of naphthalene and (2) in the presence of naphthalene

As there is suspected water formed during the process, there may be a gasification of the carbon in biochar, as seen in equation 4.4. The gasification reaction may explain the initial spike in hydrogen and carbon monoxide concentrations for all biochar catalysts tested with naphthalene, as seen in Figure 4-2 and Figure 4-3 respectively. However, when comparing the increase in hydrogen and carbon monoxide for biochar catalyst with and without naphthalene, the molar ratio is not equal to 1:1, with the amount of carbon monoxide formed being greater. This indicates the large initial spike of formation of carbon monoxide is through the reaction of naphthalene with the oxygen in biochar. For K-Form Biochar and Mg-Form Biochar, there is was measurable carbon dioxide formed in the first 6 minutes of naphthalene pyrolysis, not observed in the other biochars. This is formed through the water-gas shift reaction seen in equation 4.5.

$$C + H_2O \rightarrow CO + H_2 \qquad 4.4$$

$$CO + H_2O \rightarrow CO_2 + H_2 \quad (4.5)$$

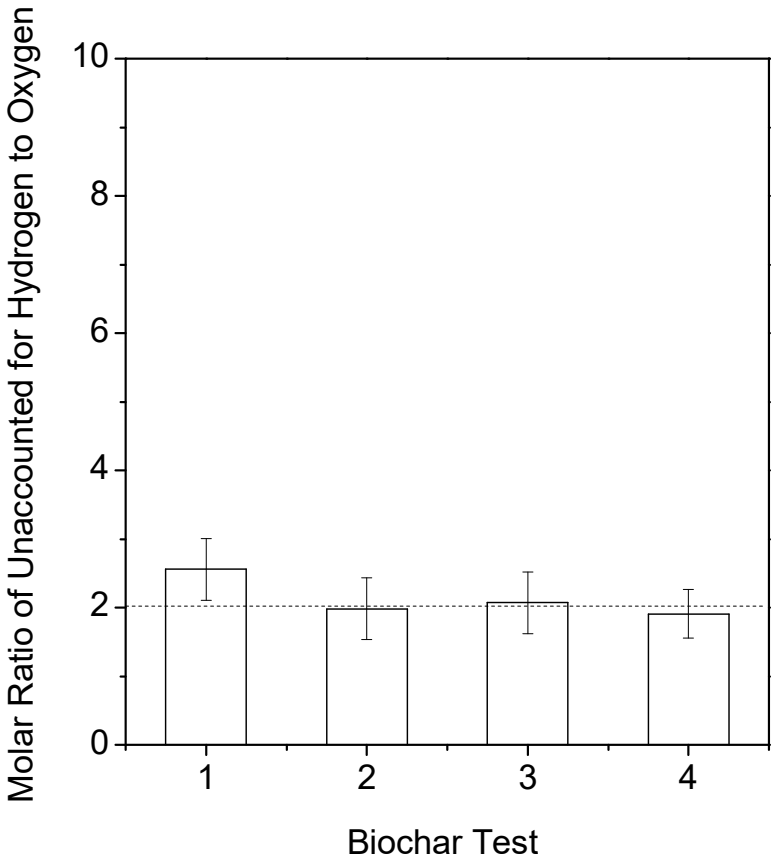

Figure 4-8: Molar ratio of hydrogen and oxygen unaccounted for when completing a mass balance comparing the amount lost from the biochar to the amount captured in the gas during the pyrolysis of naphthalene over (1) Raw biochar (2) K-Form biochar (3) Mg-Form biochar and (4) Fe(III)-Form biochar

As a result of all of these observations, a new mechanism is proposed for the pyrolysis of naphthalene over a biochar supported catalyst. It is proposed that the naphthalene interacts with the biochar to form CO, H_2, and H_2O. However, by comparing the carbon monoxide formation rate (Figure 4-3) and the naphthalene conversion (Figure 4-1), it can be concluded that the interaction of naphthalene with the oxygen in biochar is not necessarily the driving force in the pyrolysis mechanism. For all biochars, after the initial spike in CO concentration, the rate of carbon monoxide released from the biochar is less in the presence of naphthalene than that released in thermal cracking without naphthalene after approximately 10 minutes. This suggests that the oxygen available to react with the naphthalene are rapidly consumed. However, the naphthalene is still being converted for all catalysts after the reaction with oxygen slows down. The conversion of naphthalene then follows the mechanism outlined in

equation 4.3. It can also be seen from Table 4-2 that the loaded metal concentration in the biochar catalysts exposed to naphthalene is less than those that underwent pyrolysis in the absence of naphthalene. This is associated with the reaction of naphthalene with oxygen. These surface groups, such as carboxylate, are often negatively charged allowing somewhere for the positively charged metal to bond. If these groups provide the oxygen to react with naphthalene, these metallic species are no longer bonded to the biochar and are lost in the gas stream. The remaining metallic species on the biochar remain in their pure metallic form or remain bonded to chlorine.

4.6 Conclusion

Naphthalene conversion over biochar was observed under pyrolysis conditions. The raw biochar and biochars loaded with additional K and Mg can remove up to 18, 37, and 51% of naphthalene respectively. Biochar loaded with Fe (III) can effectively remove all of the naphthalene for periods up to 20 minutes. During the pyrolysis of naphthalene over biochar based catalysts, there is a spike in the carbon monoxide observed in the syngas. Carbon was measured being deposited on the biochar showing that naphthalene is also decomposed into carbon and hydrogen. There was no evidence of polymerisation of naphthalene into larger PAHs. When completing a mass balance on the amount of hydrogen and oxygen lost from the biochar and the amount captured in the gas during pyrolysis of naphthalene, an imbalance was observed. The molar ratio of missing hydrogen to oxygen was approximately 2:1 in all cases inferring water is formed in the process.

CHAPTER 5 STEAM REFORMING OF NAPHTHALENE OVER A SIMULATED MOVING BED OF K-LOADED BIOCHAR

5.1 Introduction

Biomass gasification is an attractive technical route for producing syngas that is feedstock for energy production and the synthesis of specialty chemicals. A well-known issue is that the syngas may contain notorious tar that can potentially lead to detrimental operating problems of downstream equipment [21, 295-297]. The maximum allowable limits are 100 mg/m^3 for gas engines, 5 mg/m^3 for gas turbines and 1 mg/m^3 for Fischer-Tropsch Synthesis [22, 31, 295]. One of the main components in the tar within syngas is naphthalene [21, 256, 298, 299], which is a refractory tar compound and notoriously hard to remove from the syngas [21, 262] hence is often used as a model compound in various studies [253, 256, 300-302].

Non-catalytic steam reforming of tar in syngas is normally slow and not able to reduce the tar concentration to be below the acceptable limit [151]. Consequently, a catalyst is required for tar elimination. Biochar-based catalysts are attractive options for catalytic cleaning of syngas for several reasons. For example, biochar itself undergoes gasification reactions that increase the calorific value of the syngas [115, 303]. It can also be easily produced from biomass that is the feedstock of the process. As a carbon-based catalyst, there are also no issues associated with the disposal of spent catalysts because of various attractive utilisation options including as a fuel for energy recovery [40, 80] and/or as nutrients-laden biochar returned to land for soil amendment [47, 145, 304], carbon bio-sequestration [54, 124], and nutrients recycling [42, 135, 136].

Fixed bed reformers are simple to construct and are commonly used either as a primary reformer, where the catalyst is incorporated within the gasification process, or as a secondary reformer for syngas cleaning in further downstream [31, 296, 305, 306]. The limitations with fixed-bed reforming are issues associated with catalyst replacement in batch operations [226, 266] and the difficulties in maintaining the temperature profile along the bed [307]. One solution is the use of a moving bed, as

those reported previously [23, 265]. However, little work has been conducted in regards to the use of a moving bed of biochar in the removal of a model compound from a gas stream. Therefore, this chapter is designed to carry out experimental investigation into naphthalene reforming over a simulated moving bed of K-loaded biochar catalyst for syngas cleaning and spent biochar production. Focus is placed on biochar gasification, naphthalene removal over the moving bed of biochar, steam consumption and utilisation efficiency, catalytic activities of biochar and the properties of the spent biochar.

5.2 Naphthalene Conversion and Moving Bed Stabilisation

Figure 5-1 shows the naphthalene concentration in the outlet gas and subsequent conversion as the amount of biochar in the moving bed and corresponding bed depth increases. Without any biochar in the reactor, there is an approximately 20 % conversion of the naphthalene reducing the concentration from 4500 mg/m^3 to 3600 mg/m^3. This is due to thermal cracking of naphthalene within the stainless steel reactor, in particular over the stainless steel mesh in the baskets. After the addition of 3.8 mm of K-form biochar (the smallest bed depth tested), the naphthalene concentration in the syngas is reduced to approximately 2200 mg/m^3. The concentration then continues to decrease with increasing bed depth. The critical naphthalene concentration for the syngas to be used in a gas engine is 100 mg/m^3. This concentration is reached at a bed depth of 33 mm. At the largest bed depth tested, 38 mm, the naphthalene concentration was reduced to an average 15 mg/m^3. The corresponding space time of naphthalene at this bed depth is 0.775 seconds. It is to be noted that there is no data on the void fraction of biochar; hence the space time is calculated from the initial flow rate of gas and assuming an empty bed.

Variations in the naphthalene inlet concentration may occur; therefore it must be ensured that the concentration at the exit will always be below 100 mg/m^3. The naphthalene concentrations in the gas after exiting the reactor is shown in Figure 5-3 panel b). Due to the experimental restrictions, the biochar could not be added and removed from the reactor via a continuous fashion. As a result, the moving bed analysis was repeated four times once all 10 baskets were added to the reactor (corresponding to a biochar bed depth of 38 mm) with the biochar in the bottom basket removed each time and fresh biochar placed on top. Each time the steam reforming

was conducted, it was noted as an iteration. As can be seen there is a slight variation in the naphthalene exit concentration with the maximum concentration being 10 mg/m^3 and the minimum 30 mg/m^3 with the average being concentration is 15 mg/m^3. Despite the variation, the concentration remains well below 100 mg/m^3 on each occasion.

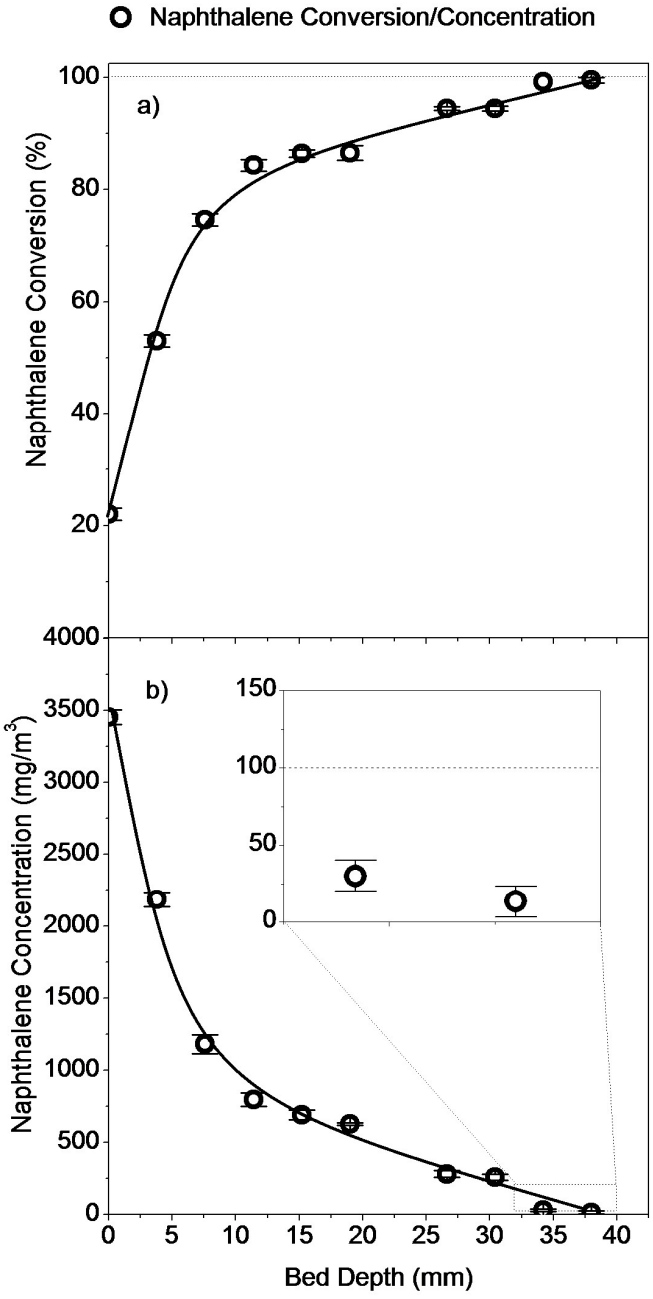

Figure 5-1: Conversion (a) and concentration (b) of naphthalene at the reactor outlet during naphthalene reforming over a moving bed of biochar, as a function of biochar bed depth. Horizontal line indicate the desired concentrations for a gas engine (100 ppmv)

During the steam reforming process it is important to study the carbon conversion in the biochar catalyst. The gasification of the catalyst increases the calorific value of the outlet gas through the formation of hydrogen and carbon dioxide; however, it must be ensured that the biochar catalyst is not completely consumed before it exits the moving bed. The nature of the carbon conversion can provide insights in regards to the reaction process. A positive carbon conversion suggests that the naphthalene is converted via steam reforming and there is sufficient steam. A negative conversion indicates the deposition of coke on the catalyst from naphthalene [151, 262], eventually leading to the fouling and subsequent deactivation of the catalyst. Figure 5-2 outlines the percentage of carbon gasified from the biochar catalyst based on the mass changes in the baskets with increasing bed depth. At the smallest bed depth of 3.8 mm, approximately 4.8 % of the carbon available in the biochar catalyst had gasified. The carbon conversion in the catalyst then increases until a bed depth of approximately 22.5 mm. At this point, approximately 26% of the carbon in the catalyst had been gasified. Past this point, the biochar bed had been stabilised and there is no further mass change due to gasification. The overall loss in carbon in the biochar indicated there was sufficient steam to reform the naphthalene but not too much to consume all of the catalyst.

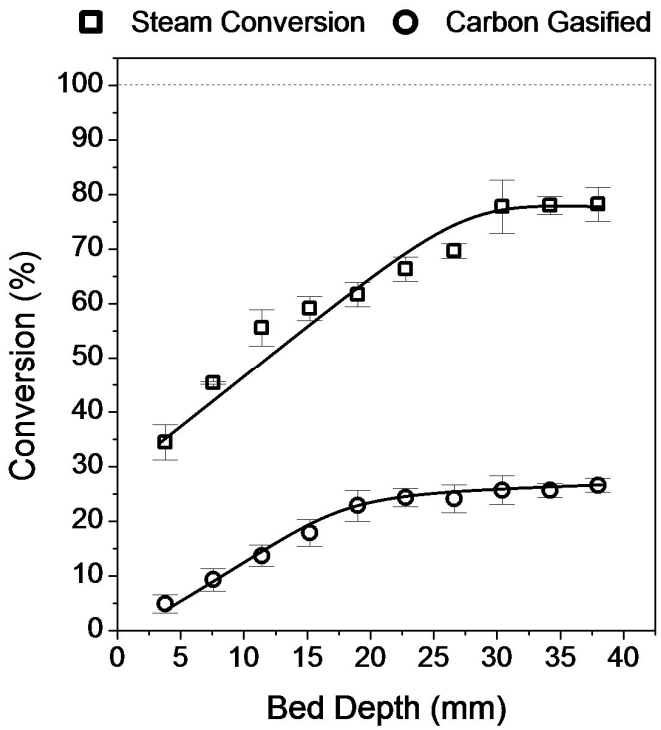

Figure 5-2: Conversion of steam and amount of carbon gasified from biochar during the steam reforming of naphthalene over a moving bed of biochar along the bed.

Figure 5-2 also shows the amount of steam consumed in this process. The steam conversion is calculated by comparing the steam added to the reactor with the composition of the outlet gas. Past a bed depth of approximately 30 mm the steam conversion remains constant. At this point, approximately 78% of the steam had been converted with 76-80% conversion seen at the maximum bed depth. This conversion is known as the steam utilisation efficiency. A high steam utilisation efficiency is important as steam is an undesirable component in the syngas due to it providing no calorific value and can condense when the gas is cooled, promoting corrosion. It was seen that the carbon conversion in the biochar remained constant after 22 mm, the difference in stabilisation points indicates between these two points, the steam is selectively reacting with naphthalene. Despite the stabilisation of steam conversion the naphthalene is still being converted past this point, as seen in Figure 5-1. This indicates that, even though the steam gasification of the carbon in biochar had ceased, it remains active in the steam reforming of naphthalene.

5.3 Outlet Gas Quality

Figure 5-3 panel a) shows the rates of gas formation during the steam reforming of naphthalene once the bed depth had reached a maximum. The total formation rate of gases is ranges from approximately 0.9 to 0.95 mmol per minute per gram of biochar in the moving bed on a dry ash free basis. The variation in formation rate is within the specified error bars. The syngas composition is similar from each of the experiments with the volume fraction of H_2, CO, and CO_2 being 58, 32, and 10 % respectively excluding the argon carrier gas. This indicates that the gasification of the biochar had stabilised at this point. Methane is also formed, however the methane formation rate is relatively small compared to the other gases therefore it cannot be seen clearly in Figure 5-3. It is formed at a rate of approximately 0.004 mmol per minute per gram of biochar (daf basis). Under these experimental conditions, this corresponds to approximately 700 ppm of methane in the outlet gas. This is promising as the presence of methane is undesirable in syngas, in particular if it is to be used in Fischer-Tropsch synthesis. Methane fouls the catalysts that are used in FT synthesis, hence its presence in syngas should be minimised.

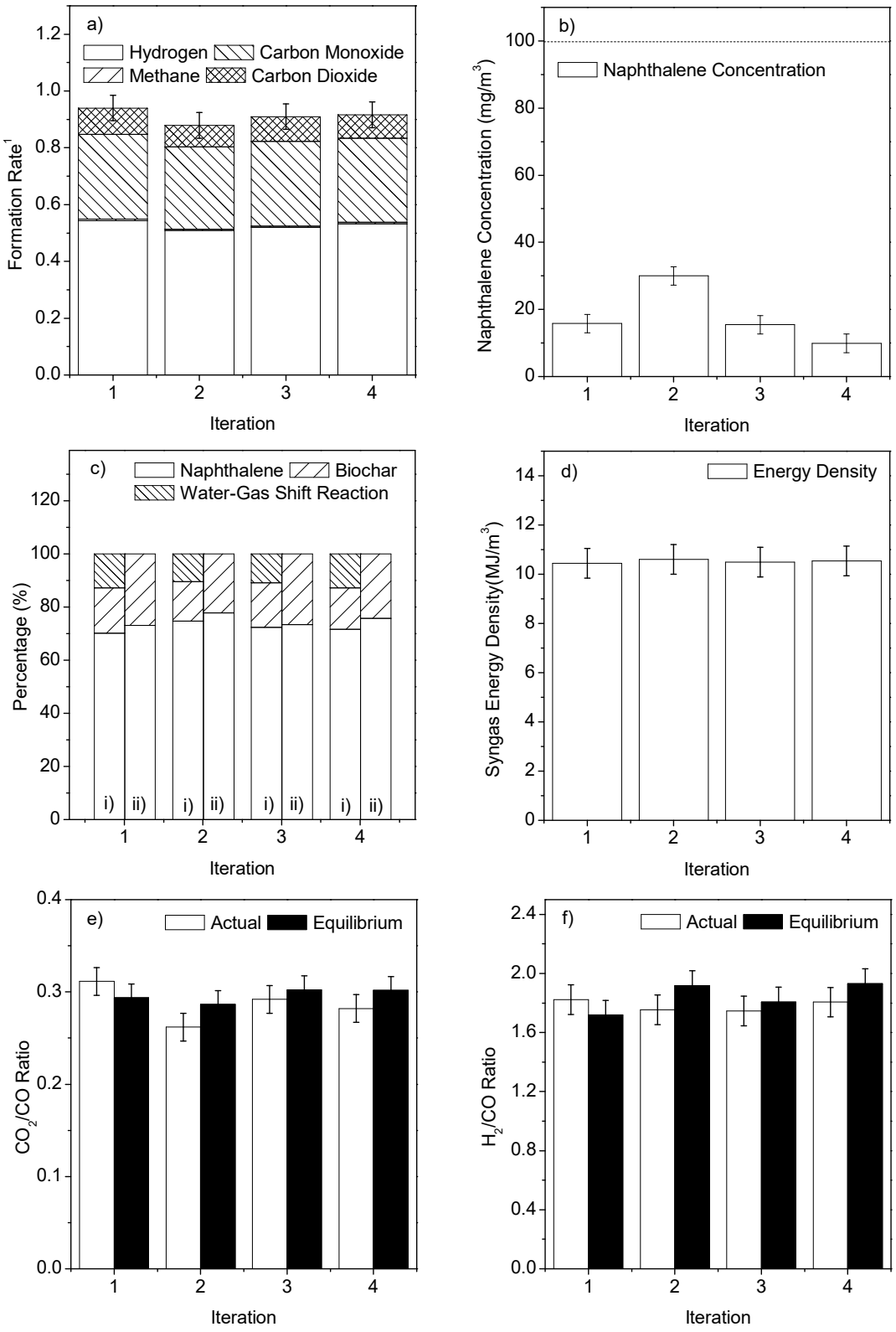

Figure 5-3: Composition and quality of gas after exiting biochar moving bed a) Formation rate of non-condensable gases [1]mmol of gas per minute per gram of biochar (daf basis) b) Naphthalene concentration in outlet for each experiment c) Percentage of i) hydrogen and ii) carbon monoxide attributed to steam reforming of naphthalene, water gas shift reaction, and gasification of biochar d) Lower heating value of syngas e) CO_2/CO molar ratio for each iteration f) H_2/CO molar ratio for each iteration

The formation of H_2, CO, and CO_2 can be attributed to three reactions; the steam reforming of naphthalene, the steam gasification of biochar, and the water gas shift (WGS) reaction, as seen in equation 5.1. Chapter 4 showed that the naphthalene reacts with the oxygen in the biochar to form CO; however, this reaction is assumed to be insignificant when compared to steam reforming. Figure 5-3 shows what percentage of hydrogen and carbon dioxide is contributed by the naphthalene steam reforming, the steam gasification of biochar, and the WGS reaction. For both hydrogen and carbon monoxide, the major contribution comes from the naphthalene steam reforming reaction. For the carbon monoxide, approximately 75% (by volume) of this is contributed from the steam gasification of naphthalene and the remaining 25% from the steam gasification. Hydrogen is also formed via the WGS reaction, hence this is considered. 73%, 11%, and 16% of the hydrogen is contributed via the steam reforming of naphthalene, WGS reaction, and steam gasification of biochar respectively.

$$CO + H_2O \rightarrow CO_2 + H_2 \qquad 5.1$$

It is possible to gain more insight on the extent of each of the reactions by studying the CO_2/CO and H_2/CO ratios. As the WGS reaction is the only reaction where CO_2 is formed, the extent of the WGS reaction can be confirmed through the CO_2/CO ratio. The CO_2/CO ratio for each iteration is shown in Figure 5-3 panel e). For each of the iterations, the ratio is approximately 0.3. This means that, at these conditions, the reactants are favoured as the ratio is less than one. For the H_2/CO ratio, a comparison can be made between the actual ratio and theoretical ratio each individual reaction. Through the cracking of naphthalene and subsequent deposition of carbon on the biochar, the theoretical H_2/CO ratio in the syngas would be infinite assuming there is no reaction between the naphthalene and oxygen in the biochar. Addition of sufficient steam to only gasify the carbon deposited increases the ratio to 1.4. If the steam selectively reacts with the biochar and there is no steam reforming of naphthalene the maximum ratio of H_2/CO would be 1.01 taking into account the hydrogen present in the biochar, the composition of which is shown in Table 5-1. Based on this analysis and conclusions made previously, the actual H_2/CO ratio should be between 1.01 and 1.4 as the naphthalene is converted via steam reforming. From the results shown in Figure 5-3, as the majority of the gases can be contributed to the naphthalene, it is to

be assumed that the H_2/CO ratio will be closer to 1.4. The actual H_2/CO ratio from each iteration is shown in Figure 5-3. The average ratio from each ratio is approximately 1.8, however, when removing the H_2 formed and CO consumed in the WGS reaction, the new H_2/CO ratio becomes approximately 1.25. This lies within the ratio of 1.01 and 1.4, confirming that there is both the steam reforming of naphthalene and gasification of biochar.

As discussed in a previous study,[115] the actual versus the equilibrium ratios of CO_2/CO and H_2/CO can provide information on the primary product of the reaction. Both the steam reforming of naphthalene and steam gasification of biochar can proceed directly to the formation of carbon dioxide opposed to carbon monoxide. Lower ratios than equilibrium indicate CO is the primary product whereas if the ratio is higher than the equilibrium, CO_2 is the primary product and the above reactions are prominent. The equilibrium ratios can be calculated by using equations 5.2 and 5.3 based on the WGS reaction. At the experimental temperature (830 °C), the equilibrium constant is 0.96.

$$\left(\frac{p_{CO_2}}{p_{CO}}\right)_{eq} = K_{eq}\left(\frac{p_{H_2O}}{p_{H_2}}\right)_{actual} \quad 5.2$$

$$\left(\frac{p_{H_2}}{p_{CO}}\right)_{eq} = K_{eq}\left(\frac{p_{H_2O}}{p_{CO_2}}\right)_{actual} \quad 5.3$$

Figure 5-3 panel e) and f) shows the actual CO_2/CO and H_2/CO ratios against the equilibrium values. As can be seen, the WGS reaction has reached equilibrium as the actual ratios are similar to the equilibrium values. The rate of biochar gasification slows down well before the gas exits the biochar bed, hence there is sufficient time for the water gas shift reaction to reach equilibrium. As the water gas shift reaction has reached equilibrium, this is the maximum steam conversion that can be achieved in this reactor system. Any further conversion of the steam will shift the equilibrium back to the left. As the actual values are close to the equilibrium value it shows that the catalyst has no effect on the equilibrium of the WS reaction.

Two important components in the outlet gas are carbon monoxide and hydrogen as they provide the calorific value of the syngas. Figure 5-3 shows energy density of the syngas. The energy density is calculated based on the molar formation rate of

hydrogen, methane, and carbon monoxide when all 10 baskets are in place in the moving bed. It is assumed that there is no argon in the syngas. The energy density in the syngas varies from 10.4-10.6 MJ/m^3 with an average of 10.5 MJ/m^3. Typical densities of syngas resulting from biochar gasification vary from 4-17 MJ/m^3.[308] Higher energy densities than the ones shown in Figure 5-3 are a result of an increase in the extent of biochar gasification Based on the amount of biochar in the moving bed, the energy output of this process in terms of the LHV ranges between 215 to 225 J/min/g of biochar (daf basis).

5.4 Biochar Composition at Exit of Reactor

One advantage of the moving bed reactor is the ability to remove the biochar of the reactor at a constant rate either because the catalyst has been spent or that the naphthalene concentration has decreased below the desired value. The collected biochar catalyst can be recycled back to the soil in order to not only enhance the soil properties but create a carbon negative process. The properties of biochar before it was loaded with KCl (Raw Biochar), after it reached 830 °C reactor but before it was exposed to naphthalene (Biochar-based Catalyst), and the biochar collected from the bottom of the bed from the four iterations (Biochar Product 1-4) are given in Table 5-1. As can be seen, there is a slight variation in the outlet biochar properties. This is a result of the variation in the biomass properties and heterogeneous nature of the biochar structure opposed to variations in the experimental set-up.

Table 5-1: Elemental composition of biochar before undergoing steam reforming and after exiting the moving bed

Sample	Moisture (wt%, ad[a])	Proximate Analysis (wt%, db[b])			Elemental Analysis (wt % daf basis[c])					Inorganic Concentrations (wt%, db[b])				
		Ash	VM[d]	FC[e]	C	H	N	O[f]	S	Cl	Na	K	Mg	Ca
Raw Biochar	4.1	2.3	7.9	89.7	89.433	1.294	0.421	8.846	0.01	0.09	0.02	0.257	0.132	0.681
Biochar-based Catalyst	5.54	8.10	8.3	89.2	87.147	1.182	0.365	10.50	0.01	2.40	0.02	2.65	0.06	0.15
Biochar Product 1	3.88	8.53	9.74	76.10	89.172	1.171	0.200	8.653	0.01	2.41	0.02	1.92	0.13	0.44
Biochar Product 2	2.77	8.73	11.77	79.46	91.202	1.378	0.198	6.508	0.01	2.11	0.03	1.96	0.10	0.40
Biochar Product 3	2.80	5.91	11.01	78.84	89.246	1.143	0.148	8.833	0.01	1.92	0.02	1.77	0.12	0.46
Biochar Product 4	3.27	5.85	11.40	77.46	91.417	1.042	0.147	6.700	0.01	2.10	0.06	1.99	0.08	0.41

[a]Air dried basis. [b]Dry basis. [c]dry and ash-free basis. [d]Volatile matter. [e]Fixed carbon [f]By difference

Table 5-2: Critical biochar properties before addition to the reactor and after steam reforming

Sample	wt% Carbon Loss	wt% Potassium Retained	Surface Area (m^2/g)	Pore Volume (cm^3/g)	H/C Ratio	O/C Ratio
Raw Biochar	-	-	39.41	0.0117	0.0862	0.0742
Biochar-based Catalyst	0.71	47.3	20.64	0.00766	0.0808	0.0904
Biochar Product 1	28.49	25.1	629.80	0.313	0.0782	0.0727
Biochar Product 2	28.79	22.7	680.47	0.400	0.0900	0.0535
Biochar Product 3	26.31	21.2	777.90	0.423	0.0763	0.0742
Biochar Product 4	25.94	22.4	729.70	0.402	0.0679	0.0550

As it is the intention to recycle the spent biochar it is crucial to ensure that the biochar is stable before adding it back to the soil. If it is not stable, it will break down and the potential benefits of the biochar to the soil will be lost and the carbon will not be bio-sequestered. The critical properties to determine the stability of the biochar are the H/C and O/C ratios as well as the reactivity of the biochar. The lower the H/C and O/C ratios, the more stable the biochar is in the soil. The Van Krevelen Diagram for all of the biochars tested is shown in Figure 5-4. As can be seen, the H/C-O/C ratio increases upon the initial gasification of the biochar compared with the biochar upon heating to 830 °C. These ratios then decrease after the gasification of biochar has stopped. As the biochar exits the reactor, the H/C and O/C ratios are at the lowest, providing the biochar with the greatest stability. In order for the biochar to be stable in the soil for 1000 years, the O/C ratio needs to be less than 0.2.[309] As can be seen, the O/C ratio for all of the biochars removed from the moving bed is much lower than the limit specified. Hence they will be suitable to be added back to the soil.

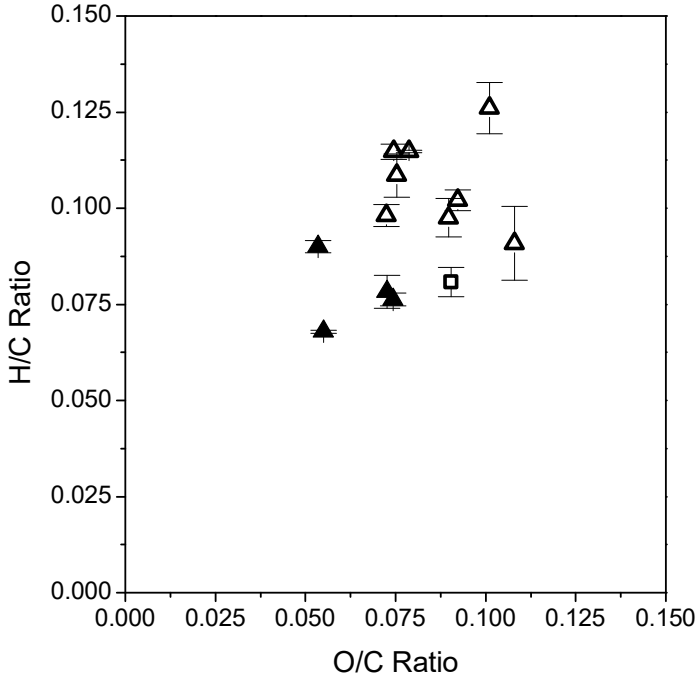

Figure 5-4: Van Krevelen Diagram for all biochars tested. □ Biochar-based catalysts Δ Biochar collected within the moving bed ▲Biochar product

Along with the H/C and O/C ratios, the reactivity of the biochar also indicates how stable it is with the lower the reactivity of the biochar, the more stable the biochar in

the soil. Figure 5-5 shows the reactivity of the biochar before and after steam reforming as a function of conversion in air at 425 °C. As can be seen, the reactivity for all of the biochars collected at the exit of the moving bed are lower than the biochar that was heated to 830 °C with no steam reforming. This confirms the conclusions made by studying at the O/C and H/C results.

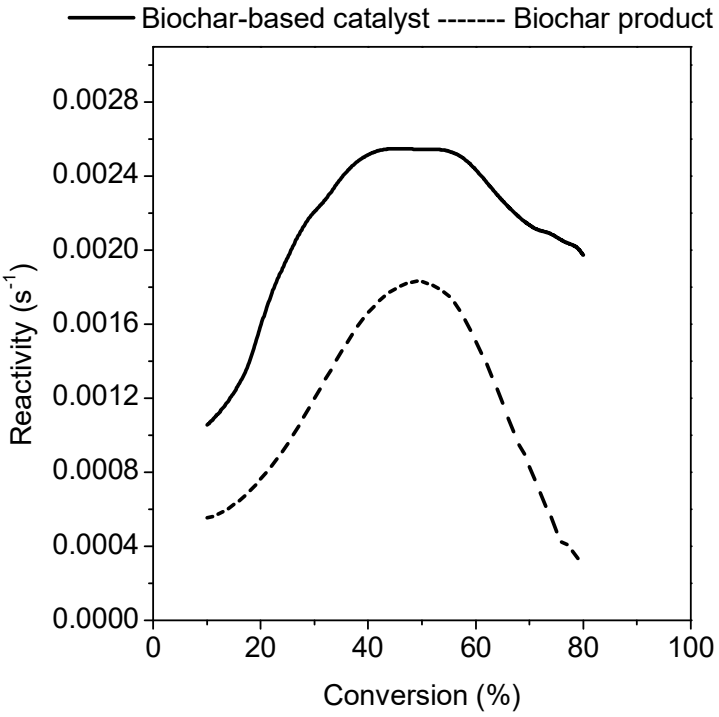

Figure 5-5: Specific reactivity of the biochar-based catalyst and the biochar product as a function of conversion tested in air at 425 °C

Potassium loaded onto the biochar as well as the other metals inherently contained within the biochar can be potentially leached into the soil. These metals, in particular potassium, are beneficial in the growth of the replanted biomass. Hence, it is crucial that these valuable metals are retained in the biochar during the steam reforming process. Table 5-2 shows the percentage of metals retained in the biochar catalyst. Upon heating to 830 °C, approximately 47% of the potassium has been retained on the biochar. There are then further losses of potassium during the steam reforming process until there is approximately 22 % of potassium is retained on the biochar. The reasons for the significant losses in potassium from the biochar are associated with how it is bonded onto the surface. There are three ways in which potassium is present on the biochar. The first is through the bonding of the potassium of with the oxygen containing surface groups. It was shown in the Chapter 4 that naphthalene reacts with

the oxygen in the biochar and releasing the potassium. The second way potassium is bonded is through its metallic form [310]. This form of potassium will be lost during the gasification of the biochar, however, as the potassium to chlorine ratio, as shown Table 5-1, is approximately 1:1, it is unlikely the potassium is bonded to the biochar catalyst in this manner. Finally, the potassium remains on the surface as potassium chloride as it was originally loaded. As the interaction between the potassium chloride and biochar is weak, it can be easily lost as the gas stream moves over the catalyst and as it is gasified.

Another important property of the biochar when returning the biochar to the soil is the surface area. There are many benefits of a biochar with a high surface area with the main benefit being the water holding capacity. Generally, the higher the surface area, the higher the water holding capacity of the biochar [46, 47, 145-148]. Figure 5-6 shows the surface area and pore volume of the biochar as it moves down the moving bed. As can be seen, there is an increase from approximately 20 m^2/g to 400 m^2/g after the initial gasification. There is then an increase until the final basket reaches an average of 700 m^2/g. The pore volume increases with a similar trend. The final basket ranges from 630 to 777 m^2/g. Despite there being a significant difference in the surface area from the final basket, there is still a substantial increase in surface area from the initial biochar.

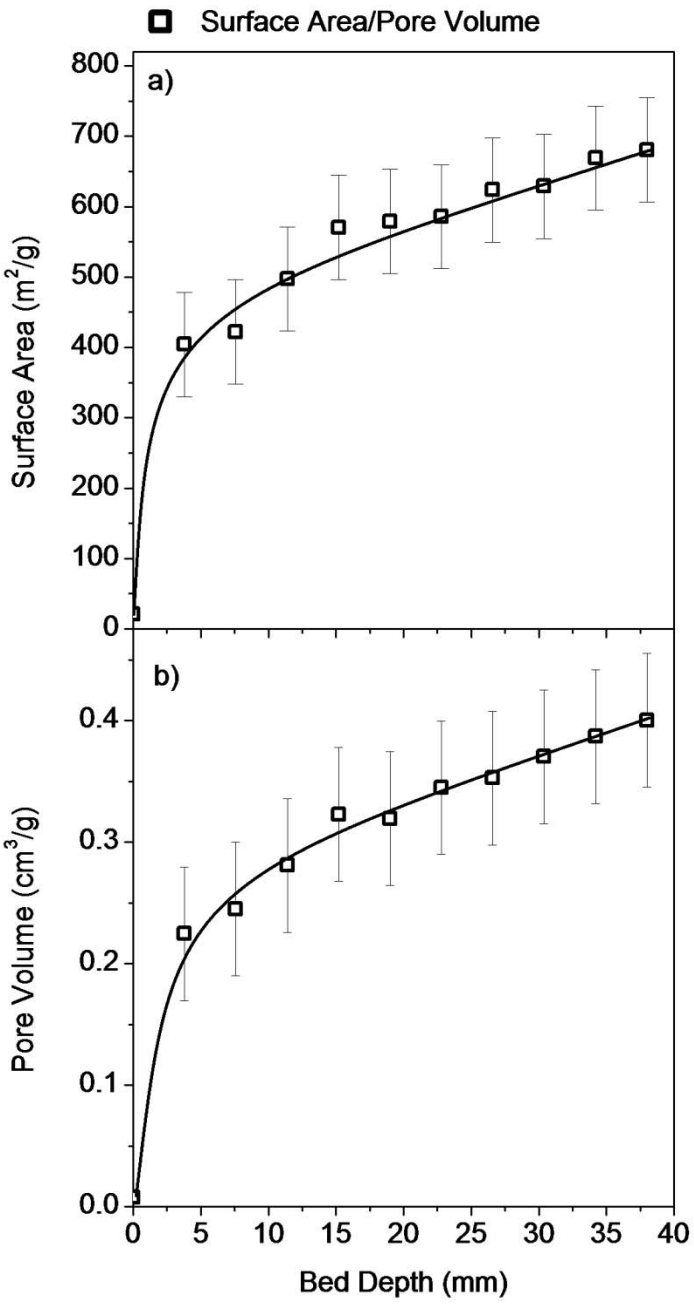

Figure 5-6: Surface area (a) and pore volume (b) of biochars after the steam reforming of naphthalene at increasing bed depth

5.5 Conclusions

It has been shown that a moving bed of K-Form biochar can be an effective catalyst in the steam reforming of naphthalene contained in a syngas. Under the conditions used in this study, the naphthalene concentration in the syngas can be reduced to 100 mg/m3

with a bed depth 34 mm with a final concentration of approximately 15 mg/m^3 with 38 mm of biochar. Apart from argon, the main components of the gas exiting the moving bed are hydrogen, carbon monoxide, and carbon dioxide as well as a small amount of methane. These gases are predominately a result of the steam reforming of naphthalene with the remainder from the steam gasification of the biochar catalyst. The steam utilisation efficiency for this process ranged between 78-80%. Upon exiting the moving bed, the biochar can be added back to the soil. The O/C ratio and reactivity showed that the biochar exiting the bed is more stable in the soil than the biochar added into the reactor. The steam reforming also increases the surface area of the biochar from 20 m^2/g to 700 m^2/g, enhancing the water holding capacity of the biochar.

CHAPTER 6 TWO-STAGE FAST PYROLYSIS OF BIOMASS AND STEAM REFORMING OF TAR OVER A MOVING BED OF BIOCHAR CATALYST: PROOF OF CONCEPT AND ECONOMIC ANALYSIS

6.1 Introduction

The production of electricity via renewable sources in Australia is increasing, however, there is still a strong reliance on fossil fuels with only 14-17% of electricity produced via renewable sources in Australia [1, 2]. Electricity production by wood based biomass is a fledgling industry in Australia contributing to 8.6% of the renewable production [1]. To boost this number, there is a potential to use Mallee Eucalyptus that is planted and harvested in the South-West of Western Australia as an energy source [8, 9]. One issue with the production of a syngas from biomass is the tar content of the final syngas [21, 31]. It has been shown in Chapter 5 that a clean syngas can be achieved by passing a naphthalene containing syngas over a moving bed of biochar catalyst. However, this process used a model compound to represent tar therefore it is unclear how this process will behave using a tar produced from biomass.

A downfall of biomass being an economically feasible renewable energy source are costs associated with growing and transporting the biomass, costs that are non-existent in other renewable energy sources such as wind or solar. Due to the dispersed population in Western Australia, significant costs are associated with transporting the biomass [94] and it may be more cost effective to look at alternatives at utilising the biomass energy such as creating a bioslurry [95]. There are also significant capital costs in constructing biomass energy conversion plants. A 2004 Australian study specified a capital investment of $AU5.3M was required for the construction of a 1 MW biomass plant and $AU12.46M and $AU47.44M for 5 and 30 MW respectively [87]. This results in the electricity production price varying from 20.0 to 10.7 AU¢ per kWh for a 1 and 30 MW biomass plant respectively. Several international economic studies have also been completed [89-91, 93, 311] with capital investments varying from $US46.1M for a 550 dry ton per day plant [92] to $US287M for 2000 dry tons per day of biomass [312]. An economic analysis needs to be completed to determine

if electricity can be generated from the two-stage pyrolysis and steam reforming of biomass at a lower cost than that purchased from Western Australia's primary electricity supplier, Synergy.

One incentive for the use of a biomass based energy source in Australia is the Carbon Credits (Carbon Farming Initiative) Act 2011 [313]. In this carbon scheme, credits are awarded to farmers who offset carbon. These credits can then be on-sold to consumers that require carbon credits to operate processes that emit greenhouse gases. Through the sequestration of carbon by adding the spent biochar catalyst into the soil, a carbon negative process can be created from the two-stage pyrolysis/reforming. It must be determined what variations in the carbon credit price have on the overall economic feasibility of this two-stage process.

As there is a potential for biomass to be used as an energy source in Western Australia, the aim of this study is to prove that it is both technologically and economically viable and provide the first full economic analysis of building and operating a biomass energy production plant in this area of Western Australia. The first stage of this chapter is to prove that a moving bed of a biochar catalyst can effectively clean a syngas of a tar produced from the pyrolysis of biomass. The results from this laboratory based study will then be scaled up into an industrial scale in order to provide electricity from biomass. Finally, an economic analysis will be completed on this process to ensure that it is profitable and resilient to change.

6.2 Cleaning of Tar-containing Gas

6.2.1 Tar Properties in the Absence of Biochar

Before the investigation into what effect the biochar catalyst has on the reforming of tar, it first must be established how much tar is in the gas stream before it reaches the biochar bed. This study is completed through the fast pyrolysis of biomass at 500 °C followed by the steam gasification of the volatiles at 830 °C in the absence of a moving bed of biochar. Based on the gas flow rate of 2 L/min and a biomass addition rate of 0.2 g/min, the concentration of tar at the exit of the moving bed reactor was measured at 3500 mg/m^3.

Through analysing the captured tar via GC-MS, it was found that the main components in the tar are benzene, toluene, and naphthalene. There is also a measurable amount of acenaphthylene, phenanthrene, and pyrene in the tar. The structures of these compounds are given in Figure 6-1. The common feature of all these components is the presence of an aromatic ring structure. There was no evidence of smaller, straight chain hydrocarbons or oxygen containing compounds in the captured tar.

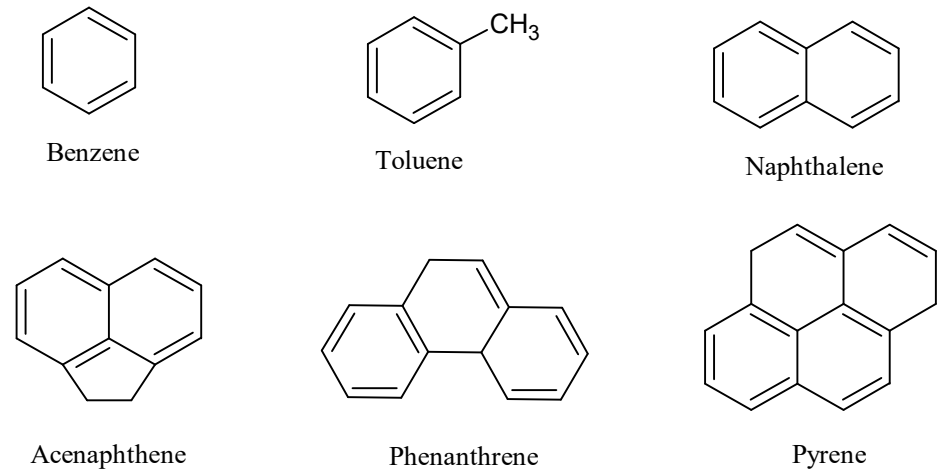

Figure 6-1: Structures of the major aromatic compounds in tar produced from the pyrolysis of biomass and subsequent steam gasification of syngas

The GC-MS analysis of the tar captured in the solvent traps showed aromatic compounds with up to four rings present. There is the possibly that larger aromatic compounds may be present that cannot be detected by the GC-MS. These larger aromatic structures can be detected by analysing the tar solution via UV-Fluorescence. The UV-Fluorescence output of the tar captured from 0.1, 0.2, and 0.3 g/min of biomass addition is shown in Figure 6-2. The intensity of the peaks have been normalised to per gram of biomass added. As can be seen, there are distinct peaks indicating the presence of several different polyaromatic hydrocarbons (PAH's). The peaks between a wavelength of 280 and 360 nm indicate PAH's of 2-3 rings. The three peaks between 280-360 nm confirm the presence of naphthalene (2 rings), acenaphthene (2.5 rings), and phenanthrene (3 rings). The presence of PAH's larger than what can be detected on the GC-MS are confirmed through the presence of peaks above 360 nm. The peak at approximately 380 nm can be attributed to pyrene (4 rings), where the peaks up to 480 nm are from PAH's of 5-6 rings not seen on the GC-MS analysis.

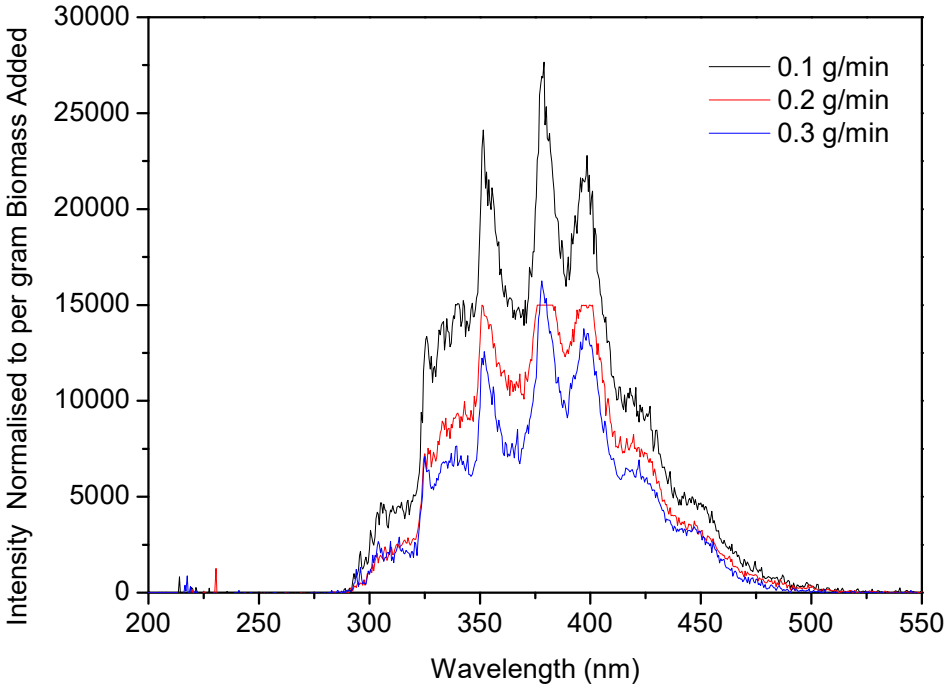

Figure 6-2: UV Fluorecence analysis of tar solutions after the fast pyrolysis of different biomass addition rates followed by the subsequent gasification of the syngas with no biochar catalyst with the intensity normalised to per gram of biomass added

6.2.2 Reforming of Tar over a Moving Bed of Biochar

Figure 6-3 shows the tar concentration in the syngas after the being passed over a moving bed of biochar catalyst at different bed depths. There is a significant conversion of tar with a bed depth of 5.4 mm with approximately 58 wt% being reformed at this point. The amount of tar continues to decrease in the moving bed of biochar until it reaches a concentration of 100 mg/m^3 at the maximum bed depth of 54 mm. This corresponds to a reaction space time of 0.478 seconds. This tar concentration is the same what is acceptable in a gas engine[23], however, some there will be some fluctuations in this as the biomass being fed is not of a consistent composition.

A semi-quantitative analysis can be completed on the conversion of each of the individual components of the tar. This can be done by comparing the peak area of each individual compound from the GC-MS analysis at increasing bed depths with the peak area when there is no biochar catalyst. The percentage converted of each compound

versus bed depth is given in Figure 6-3 panel a). The two largest species present in the tar that can be measured on the GC-MS, acenaphthene and pyrene, are reformed by the moving bed of biochar with a conversion of 100 wt%. The pyrene is fully reformed after a bed depth of 21.6 mm and the acenaphthene after 37.8 mm. The next largest compound, phenanthrene, is reformed to 99.0 wt%. The naphthalene and toluene are reformed to an extent of 95 wt%, whilst there is only an 80 wt% reforming of benzene. There was no evidence of smaller hydrocarbons or oxygen containing compounds being formed during steam reforming.

The semi-quantitative analysis indicates the major components of the tar at the exit of the moving bed are benzene, toluene, and naphthalene. However, compounds such as benzene and toluene can often be handled by gas engines with naphthalene being the major compound of concern. Figure 6-3 shows the naphthalene concentration in the gas. The naphthalene concentration in the syngas starts at approximately 1000 mg/m^3, corresponding to approximately 30% of the tar. After a bed depth of 5.4 mm, 23.4% of the naphthalene is reformed. At the same reaction time in Chapter 5 looking at naphthalene as a model compound, 25% of the naphthalene is reformed. As the other compounds are reformed at a faster rate, the percentage of naphthalene within the tar increases with increasing bed depth. The naphthalene concentration drops below the limit of 100 mg/m^3 at a bed depth of 37.8 mm corresponding to a space time of 0.335 s. The final naphthalene concentration at a bed depth of 54 mm is approximately 44 mg/m^3. This is much lower than the 100 mg/m^3 limit required for gas engines.

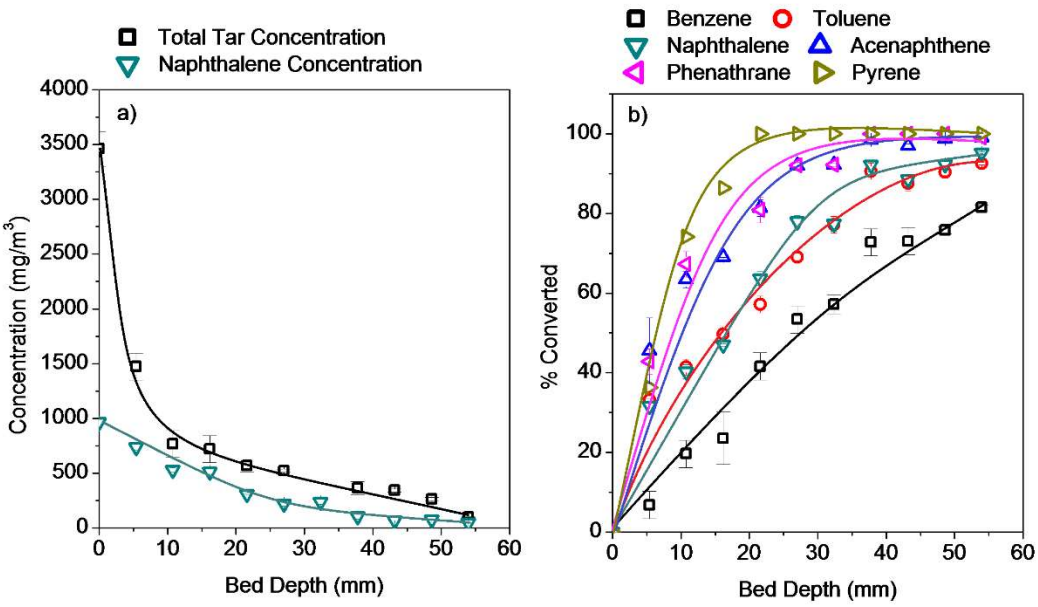

Figure 6-3: a) Total tar concentration and naphthalene concentration in the syngas at specified bed depths in the moving bed of biochar b) Conversion of individual components of tar at different bed depths

It was confirmed that during the cracking of aromatic tar compounds, they do not form smaller, straight chain hydrocarbons. However, there is a potential for the rings to polymerise and form larger ringed aromatic compounds. The UV-Fluorescence analysis of the captured tar solutions are shown in Figure 6-4. The intensity has been normalised to per mg of tar captured. The UV-Fluorescence peak shape for a bed depth of 5.4 mm is similar to the peak shape when no biochar is present as seen in Figure 6-2. As the bed depth increases, the peak heights of all of the PAH's decrease. At the largest bed depth of 54 mm, the normalised peaks of 3-6 ringed PAH's are significantly lower than at the smallest bed depth. This confirms that they are reformed over the biochar bed. At a bed depth 54 mm, there is a large peak at 280 nm, which corresponds to naphthalene. The normalised intensity of this peak increases with increasing bed depth, hence showing that a great fraction of the tar consists of naphthalene at 54 mm than at the smallest bed depth. This confirms the results obtained using GC-MS.

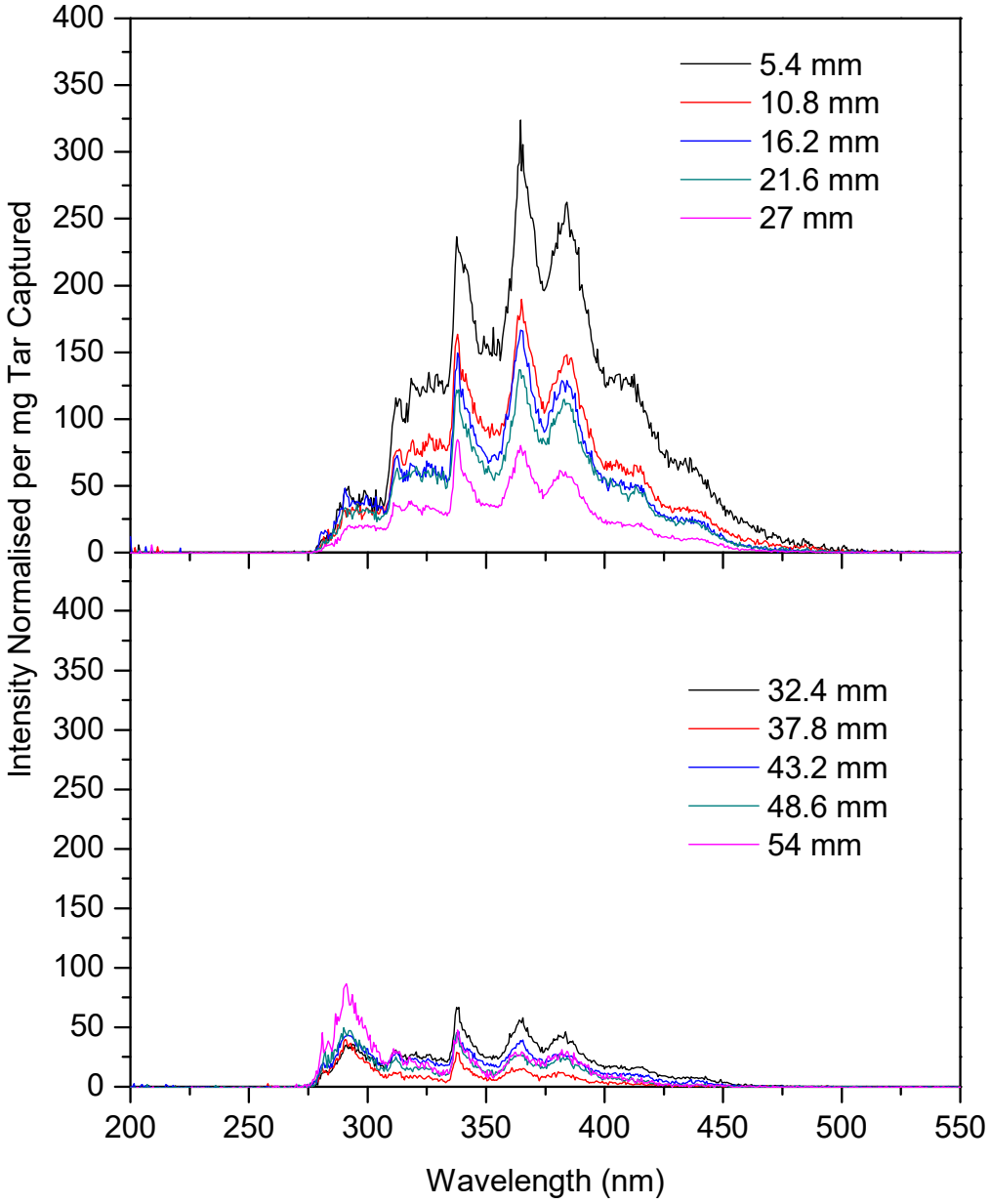

Figure 6-4: UV Fluorecence analysis of tar solutions after the fast pyrolysis of biomass followed by the subsequent gasification of the syngas at different biochar bed depths with the intensity normalised per mg of tar captured in the solvent traps

6.3 Optimum Process Design to Ensure Clean Syngas

Figure 6-5 outlines the block diagram for the two-stage pyrolysis/steam reforming of biomass for energy production. There are many benefits in using this reactor configuration over traditional biomass gasification reactors. A two-stage reactor implementing a moving bed of catalyst is operated in a continuous fashion opposed to traditional fixed-bed operations, which are batch operations. The continuous operation of the reactor ensures that biochar can be removed at a constant rate, where in traditional moving bed gasifiers, all of the biochar is gasified therefore losing the potential for bio-sequestration. This reactor configuration also has significant variability in the operation mode. If energy is not immediately required, a bioslurry can be produced for energy production later on. If there is a spike in required energy, more steam can be added to further gasify the biochar.

The results obtained in the laboratory tests, outlined in section 6.2, were scaled up to achieve an industrial scale process, as shown in Figure 6-5. A previous study compared the logistical costs of biomass transport vs. bioslurry transport. [95] It was found that small bioenergy plants of approximately 200 tonnes per day that use a biomass feed are more economical that production plants using a bioslurry feed. As this reaction set-up uses a biomass feed the production rate will be set as 200 dry tonnes per day. The biomass is added to the pyrolysis vessel in a continuous manner in a fast pyrolysis configuration. An auger reactor can be used in this process they allow the bio-oil to be easily collected and the feed rate to be varied. Under a fast pyrolysis configuration, the typical solid residence time is 0.5-10 seconds [314].

An inert carrier gas is required in this process, typically argon or nitrogen. Typical biomass gasification vessels have an inert gas concentration of 30-90 vol% in the final syngas [31]. Argon was used in the experiment but was at a much higher flow rate than required to ensure the safety of operation. In this process, the outlet gas from the gas engine can be recycled to act as the carrier gas. For composition of the outlet gas given in Figure 6-5 it was assumed that there was no carrier gas involved in the process as it has no bearing on the total calorific value of the outlet gas and the amount of carrier gas required varies depending on the process.

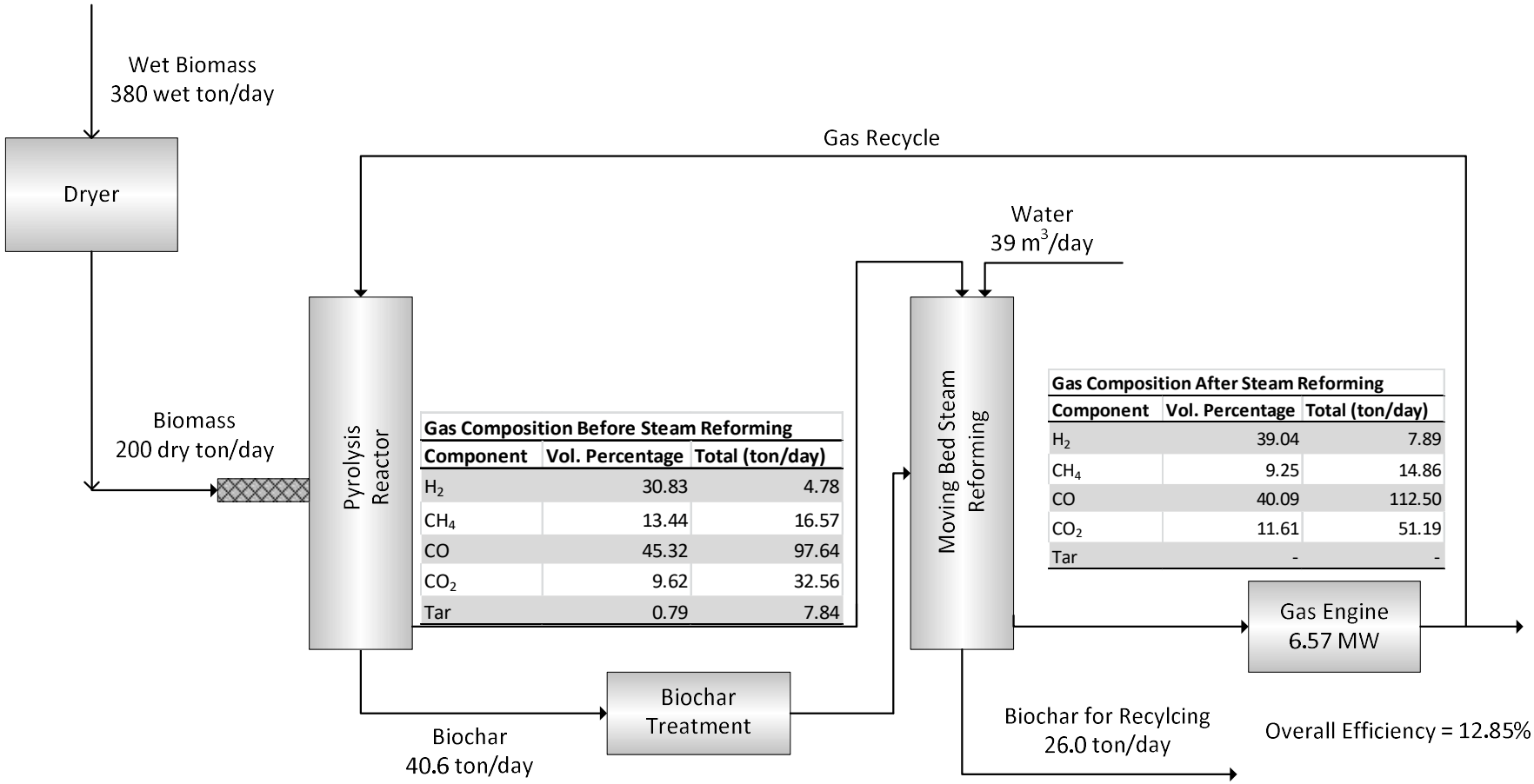

Gas Composition Before Steam Reforming		
Component	Vol. Percentage	Total (ton/day)
H_2	30.83	4.78
CH_4	13.44	16.57
CO	45.32	97.64
CO_2	9.62	32.56
Tar	0.79	7.84

Gas Composition After Steam Reforming		
Component	Vol. Percentage	Total (ton/day)
H_2	39.04	7.89
CH_4	9.25	14.86
CO	40.09	112.50
CO_2	11.61	51.19
Tar	-	-

Figure 6-5: Block flow diagram of two stage pyrolysis/steam reforming reactor set-up including syngas composition before the gas reaches the moving bed and after it exits the moving bed of biochar

At a pyrolysis temperature of 500 °C, it was seen that the yield of biochar was 20.3 wt% when compared to the amount of biomass fed into the reactor. Based on 200 dry tons per day of biomass fed, 40.6 tonnes of biochar on a dry basis is produced per day. The remainder of the biomass is converted into volatiles consisting of tar and non-condensable gases, which is carried to the steam reforming vessel. At this stage, the biochar is then removed from the pyrolysis vessel in a continuous manner and sent for treatment with KCl before it is added to the reforming vessel. The addition of KCl increases the catalytic ability of the catalyst. Other additives can be used to increase the catalytic ability of the biochar.

Before the volatiles reach the moving bed of biochar for cleaning, there is a thermal cracking of the tar due to the increase in temperature from 500 °C to 830 °C. It was found in the pilot scale plant that the addition of steam had no further effect on the cracking of tar when no catalyst was present. Figure 6-5 shows the syngas composition before it reaches the moving bed. As can be seen, the main components of the syngas are carbon monoxide and hydrogen with methane and carbon dioxide also present. The concentration of tar remaining in the gas is much higher than the acceptable limit for a gas engine. Hence thermal cracking at 830 °C is insufficient and there needs to be further reforming.

Figure 6-5 shows the syngas composition after the gas has exited the moving bed. These values were calculated based on the assumption that all of the biochar produced in the pyrolysis process is added to the moving bed reactor at the same rate it was produced. The results obtained from the pilot-scale experiments were adjusted to reflect this. As can be seen there is a significant amount of hydrogen produced in the reforming section with the hydrogen production increasing from 4.78 to 7.89 ton per day. There is also an increase in carbon monoxide and carbon dioxide production. The formation of these species in the reforming reaction is due to the steam reforming of the tar, the steam gasification of the biochar, and the water-gas shift reaction outlined in Equations 6.1, 6.2, and 6.3 respectively. It can also be seen there is a small decrease in methane content. This is promising as the presence of methane should be avoided if the syngas is to be used in Fischer-Tropsch synthesis.

$$C_{\mathrm{m}}H_{\mathrm{n}} + \mathrm{m}\, H_2O \rightarrow \mathrm{m}\, CO + (\mathrm{m} + \mathrm{n}/2)H_2 \qquad 6.1$$

$$C + H_2O \rightarrow CO + 2H_2 \quad 6.2$$

$$CO + H_2O \rightarrow CO_2 + 2H_2 \quad 6.3$$

A negative repercussion of using the biochar as a catalyst in steam reforming is the loss of carbon available for bio-sequestration through the steam gasification of biochar. If all of the biochar produced after pyrolysis is added back into the soil, approximately 32% of the carbon from the biomass is sequestered. In the experimental study, it was observed that 29% of the carbon was gasified in the biochar during the steam reforming reaction. As a result, 26.0 ton per day of biochar is available for sequestration. This results in 23.5% of the carbon from the biomass being sequestered after steam reforming.

A steam utilisation efficiency of 74% was observed in the experimental work. Hence, to complete the steam reforming of the tar and gasification of biochar observed in the experimental work, 39 tons per day of steam is required.

In the pilot scale experiment, to reduce the tar concentration in the syngas to 100 mg/m^3, a space time of 0.478 seconds was required in the biochar bed for the gas. However, the initial tar concentration was only 3700 mg/m^3 due to the increased inert gas flow rate. For the 200 ton per day biomass plant with no carrier gas, the tar concentration will be approximately 41 600 mg/m^3 before the gas reaches the bed. As the tar is a complex mixture of components it is difficult to generate the reaction kinetics for the cracking of tar. Based on the result in Figure 6-3 it is assumed that the reaction kinetics are second order. To reduce the tar concentration to 100 mg/m^3, the space time required in the moving bed is 10.46 seconds. Based on the gas flow rate, the total volume of the moving bed of biochar needs to be 29.03 m^3. This corresponds to 6.55 ton of biochar (daf basis) being in the reactor at any time. As a result, the biochar will be in the moving bed for an average period of 3.87 hours.

From the outlet gas composition shown in Figure 6-5, the LHV of the syngas is 1.96 GJ/min. This corresponds to an energy density in the gas of 11.52 MJ/m^3. When removing the energy required to heat the system, the net energy produced from the process is 1.57 GJ/min. Energy is required to heat the raw materials to the reaction temperatures, vaporize the water to steam, counteract the heat losses from the endothermic steam gasification, and maintain the required reactor temperature. The

reactors can be insulated to minimise the heat losses. To maintain the reactor temperature, a burner can be added to combust a fraction of the syngas.

The final stage in the process is the gas engine. A gas engine efficiency of 25% will be used in this study. Hence the total power available from this plant is 6.57 MW. Based on this output, the biomass plant can provide enough electricity to power approximately 9 600 homes [315].

The overall efficiency of this process when compared to the amount of energy available in the biomass feed was 12.85%. The major losses in efficiency were a result of the low gas engine efficiency, the formation of carbon dioxide, and the energy required to maintain the reaction temperature.

6.4 Economic Analysis of Commercial Two-Stage Pyrolysis/Reforming Process

It has been proven technically that a two-stage pyrolysis/reforming set-up can efficiently produce electricity. Now it must be determined whether it is economically viable when compared to the electrical sale price. Table 6-1 shows the upstream costs of biomass production. Four major costs are associated with taking the biomass from the farm to the production plant; the growth of biomass on the farm, the harvesting of the biomass, the on-farm transport of the mallee, and the transport of the biomass from the farm to the production plant. The costing of growing mallee eucalyptus, harvesting and on-farm transport were taken from a 2009 study by Yu et.al. [94] looking into the biomass supply chain in Western Australia. As can be seen, the largest cost came from transporting the biomass on the farm followed by the growth of the biomass. The on farm transport costs incorporate the costs to move the biomass from the harvester to the road haulage truck. Hence, the on-farm biomass is dependent on the farm size. The average farm size in the south west is 7x7 km and will be used in this study to calculate the on-farm haulage [94]. To calculate the off-farm biomass transport cost the biomass from the farm, the method was adopted from a study by Wu et.al. [95] The cost of transporting biomass was assumed to be $0.2 per ton green biomass per km. The average transport distance for a biomass plant of 200 ton per day in the south-west of Western Australia is 27.4 km, as calculated from equation 3.5.

Table 6-1: Costs of Upstream Biomass Treatment

Biomass Treatment	Cost ($AU/ton green biomass)	Total Cost ($AU/yr)	Reference
Biomass Growth	13.10	1 569 037	[94]
Harvesting of Biomass	6.71	803 399	[94]
On-farm Biomass Transport	13.98	1 674 507	[94]
Off-farm Biomass Transport	0.2[1]	672 227	[95, 283]
Total		1 719 170	

[1]$ per ton green biomass per km transported

Table 6-2 outlines the capital costs for the construction of the 200 ton per day two-stage pyrolysis/reforming production plant. As can be seen, the major capital cost comes from the auger pyrolysis vessel. The grinder to reduce the particle size of the biomass and boiler to maintain the temperature of the vessel is incorporated within the capital cost of the auger. There is also a large capital cost associated with the moving bed reactor and subsequent boiler to maintain the temperature of the reformer. As there is limited information on the capital cost of moving bed reformers it was assumed that the capital cost is the same as a fluid-bed gasifier. The installation of all of this equipment was assumed to be 45% of the cost of the purchased equipment. Other capital costs to consider are the connection of the plant to the electricity grid, installation of auxiliary equipment, site works, and design of the plant. Contingency was calculated of 10% of all of the capital costs described in Table 6-2 and the working capital was 15% of all capital costs including the contingency. The culmination of all of these costs results in a total capital investment for this biomass plant of approximately $AU36.5M.

Table 6-2: Capital Costing of Constructing Two-Stage Pyrolysis/Reforming of Biomass to Produce Electricity

Cost Estimate	Cost ($AU)	Reference
Dryer	742 563	[93]
Auger Pyrolysis Vessel	6 866 094	[95]
Moving Bed Reformer	3 475 847	[87]
Boiler	3 045 845	[87]
Gas Engine	2 512 918	[87]
Total	16 643 268	
Installation[1]	7 489 471	[282]
Auxiliary Equipment	1 815 563	[87]
Grid Connection	788 336	[87]
Civils and Infrastructure	310 557	[87]
Design and Project Management	1 779 729	[87]
Contingency[2]	2 882 692	[282]
Working Capital[3]	4 756 442	[282]
Total	36 466 058	

[1]Installation calculated as 45% of the total cost of equipment purchase. [2]Contigency calculated as 10% of installed equipment. [3]Working capital calculated as 15% of total capital cost

Table 6-3 outlines the operational costs of running the plant per year. The operational labour was calculated from data retrieved from the study by Stucley et.al. [87] and guidelines outlined in Perry's Chemical Engineering Handbook [282]. The costs for maintenance and consumables were adopted from the study from Stucley et.al. [87] The process water was required for the steam in the moving bed reactor, whilst there are costs associated with transporting the biochar back to the farm for sequestration. As a result the total operating cost is AU$1.25M per year.

Table 6-3: Operational Costs of Running Two-Stage Pyrolysis/Reforming of Biomass to Produce Electricity

	Units	Cost/unit ($AU)	Total Cost ($AU/yr)	Reference
Operational Labour				
Clerk	0.2	50000	10 000	[87]
Plant Manager	1	100000	100 000	[87]
Plant Engineer	1	80000	80 000	[87]
Tradesman	1	60000	60 000	[87]
Plant Operator	2	60000	120 000	[87]
Boiler Attendant	2	60000	120 000	[87]
Total			490 000	
Maintenance			489 623	[87]
Consumables			158 797	[87]
Process Water			12 032	[316]
Biochar Transport			96 297	[95]
Total			4 246 749	

The summary of all of the costs associated with this biomass energy production plant is provided in Table 6-4. The costs for Biomass Growth/Harvesting/Transport, capital cost, and operating cost were outlined Table 6-1, Table 6-2, and Table 6-3 respectively. From the carbon credit scheme, $AU 658k per year in revenue can be generated. It was assumed that all of the carbon credits awarded via sequestering the biochar at the exit of the reactor could be on-sold for $AU 23 per ton CO_2 equivalent [313]. Based on the upstream costs, operating costs, and revenue, the production cost of electricity from this process is 10.201 AU¢ per kWh assuming that the plant is operated for 330 days per year 24 hours per day.

Table 6-4: Summary of Costs of Two-Stage Pyrolysis/Reforming Process

	Cost
Biomass Growth/Harvesting/Transport ($AU/year)	4 719 170
Capital Cost ($AU)	36 466 058
Operating Cost ($AU/year)	1 246 749
Carbon Credits ($AU/year)	-657 800
Production Cost (c/kWh)	10.201

This production cost can be compared to the historical pricing of purchasing electricity in Western Australia, as seen in Figure 6-6. Synergy quotes the average cost of purchasing electricity from the grid at 26.4740 AU¢ per kWh [317] for private purchase for the home and for a commercial business as 31.8798 AU¢ per kWh with the minimum cost being 16.2966 AU¢ per kWh for large businesses with a high voltage demand [318]. These costs were then adjusted to the historical electricity price calculated from the cost index obtained from the Australian Bureau of Statistics [319]. The production cost was adjusted to each year using the chemical engineering cost index [281, 282]. As can be seen, the electricity purchase price increased significantly from 2008 to 2013 before remaining relatively constant until 2017. Past 2017, the purchase of electricity is expected to increase dramatically [320]. Despite the variation in electricity purchase cost, the cost of production of electricity via two-stage biomass pyrolysis/reforming consistently remains below the purchase cost. Based on the minimum cost of electricity, the capital cost, and the production cost it would take approximately 11.5 years for the plant to become profitable, which corresponds to 3.16 biomass growth cycles. At the private sale price, the breakeven time is reduced to 0.861 growth cycles.

Figure 6-6 outlines the sensitivity analysis that several factors have on the electricity production cost from biomass. All of these production costs have been compared to the minimum electricity purchase price of 16.2966 AU¢ per kWh. The first such sensitivity analysis was on the plant capacity, as shown in panel b) in Figure 6-6. It was assumed that the minimum plant size was 50 dry tonnes per day whilst the maximum is 1000 tonnes per day, any larger than this and it is more economically viable to produce a bioslurry to reduce transportation costs [95]. The maximum production cost was seen at 50 dry tons per day with 12.566 AU¢ per kWh, however, this is still lower than the minimum purchase price. This plant results in a breakeven time of 32.7 years or 10.24 growth cycles. The production cost decreases until it reaches a minimum of 9.953 AU¢ per kWh at 400 dry tons per day. The production cost then increases to 10.364 AU¢ per kWh at 1000 tonnes per day. The breakeven time decreases with plant capacity with the minimum achieved at 1000 tons per day of 1.403 growth cycles.

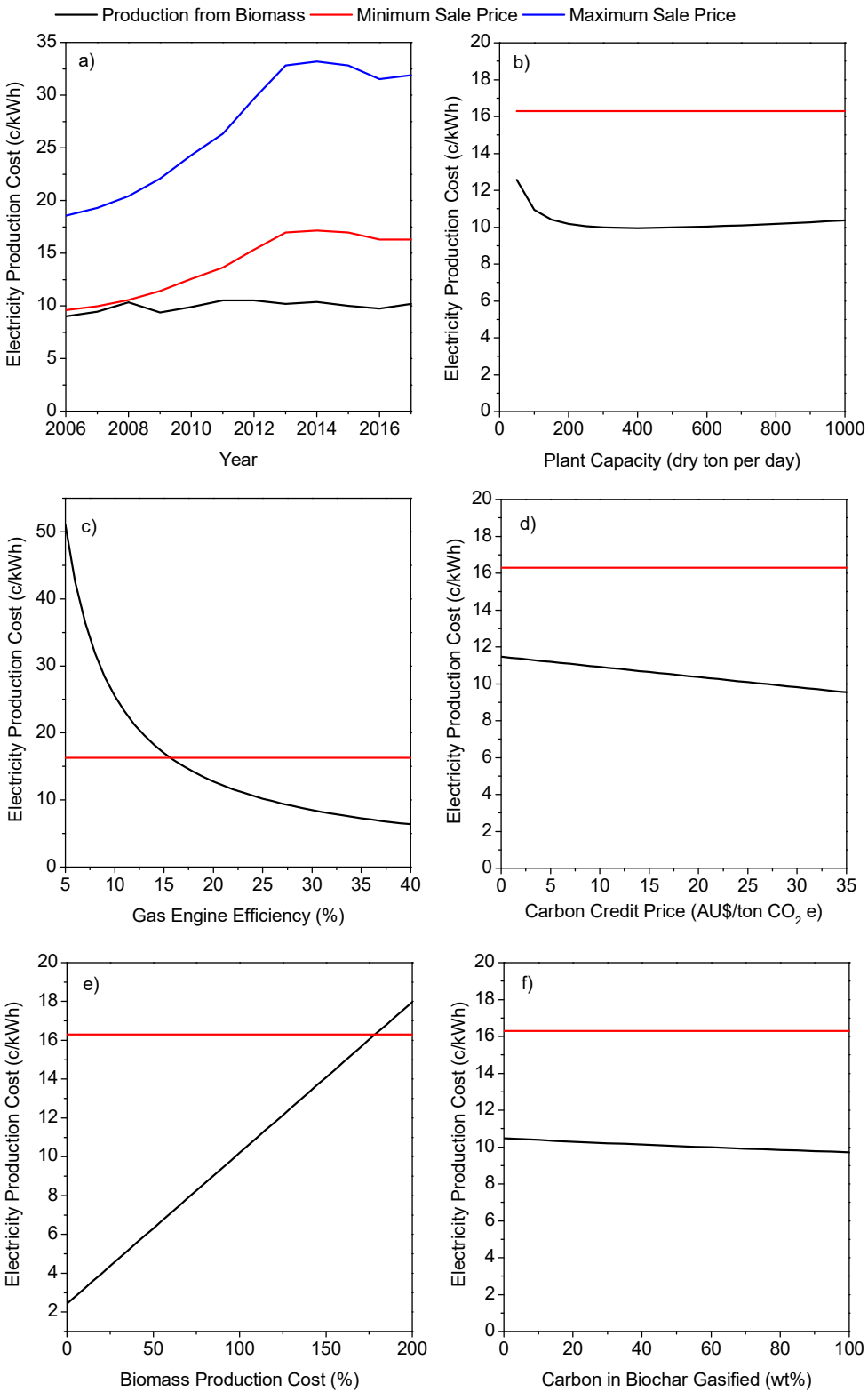

Figure 6-6: Sensitivity analysis of biomass electricity production cost analysis a) Historical pricing of electricity compered to production cost of electricity from biomass b) Electricity production cost with varying plant capacity given in dry tons of biomass feed per day c) Electricity production cost with increasing gas engine efficiency d) Electricity production cost with varying carbon credit price given in AU$ per ton of CO2 equivalent sequestered e) Electricity production cost with varying biomass production cost given as a percentage of the base case. F) Electricity production cost with increasing carbon in biochar gasified.

Panel c) in Figure 6-6 shows the sensitivity analysis for gas engine efficiency. As expected, the production cost decreases with gas engine efficiency. At a minimum gas engine efficiency of 5%, the production cost increases to 51.03 AU¢ per kWh. The production cost drops below the minimum grid purchase price at a gas engine efficiency of 16%. Increasing the gas engine efficiency to 40% decreases the production cost to 6.379 AU¢ per kWh.

There is a possibility that the carbon credit price can be varied depending on the current political climate and could be abolished altogether. The variation in the carbon credit price is shown in Panel d) in Figure 6-6. As can be seen, the production cost is resilient to changes in the carbon credit price. At a maximum credit price of $AU35 per ton CO_2 equivalent, the production cost is 9.542 AU¢ per kWh. If the carbon credit scheme is eliminated, the production cost increases to 11.465 AU¢ per kWh. This is still below the 16.2966 AU¢ per kWh minimum sale price. Hence, the plant can still turn a profit if this scheme is discontinued.

As seen in Table 6-1 and Table 6-4, there is a significant cost associated with the growth, harvesting, and on farm transport of biomass. Panel e) shows the sensitivity analysis of these biomass production costs. It is given as a percentage where 100% represents the biomass production cost as calculated in Table 6-1. When removing these production costs, the production cost reduces to 2.424 AU¢ per kWh. The production costs need to increase to 178% of the original calculated costs in order for the production cost to increase above the 16.2966 AU¢ per kWh sale price.

The final sensitivity analysis to consider is the amount of biochar gasified in the moving bed reformer, as shown in Panel f) in Figure 6-6. This reactor configuration has the potential to vary the amount of biochar gasified to suit the needs of the plant. Based on the experimental work, it was seen that the 29% of the carbon in the biochar was converted, resulting in the 6.57 MW output. However, as the gasification of carbon produces carbon monoxide and hydrogen, the conversion of carbon in the biochar can be increased to maximise the energy output from the plant. However, by increasing the gasification, more steam is required as well as there being a loss in income from the carbon credits scheme as a result of the sequestration of less carbon. By increasing the carbon conversion to 100 % in the biochar, the plant output can be increased to 7.66 MW whilst maintaining the 200 dry ton per day of biomass capacity.

These calculations were completed by assuming that the ratio of each gas produced from gasification in the syngas remains consistent. By gasifying 100% of the carbon, the production cost is reduced to 9.719 AU¢ per kWh compared with 10.201 AU¢ per kWh at 29% carbon conversion and 10.479 AU¢ per kWh when there is no gasification of the biochar. There is a decrease in production cost when all of the carbon is gasified, however, this does not take into account the intangible benefits of minimising the gasification such as the benefits the introduction of the biochar has to the soil growth properties as well as the benefits to the environment by creating a carbon negative process through the sequestration of the carbon.

6.5 Conclusion

It was shown in this study that a moving bed of biochar can be used to clean a syngas containing tar produced from the fast pyrolysis of biomass. By heating biomass to 500 °C followed by the heating of the gas to 830 °C creates a syngas containing approximately 3500 mg/m^3 of tar with the remainder of the gas being the non-condensable gases hydrogen, methane, carbon monoxide, carbon dioxide and argon. The main constituents of the tar were benzene, toluene, naphthalene, acenaphthylene, phenanthrene, and pyrene. After passing through a moving bed of biochar with a bed depth of 54 mm corresponding to a space time of 0.478 s, the tar concentration was reduced to 100 mg/m^3. The acenaphthylene, phenanthrene, and pyrene were all completely reformed leaving benzene, toluene, and naphthalene in the syngas. Benzene and toluene are not damaging to gas engines therefore can be ignored, leaving a naphthalene concentration of 44 mg/m^3. Along with the pyrolysis of biomass and reforming of tar, the steam gasification of the biochar catalyst also contributed to the calorific value of the syngas through the formation of carbon monoxide and hydrogen.

Upon scaling up to a 200 dry ton per day biomass energy conversion plant, the output was calculated to be 6.57 MW assuming 25% gas engine efficiency. The total efficiency of the process was 12.85% based on the energy available in the biomass feed. A total of 26 ton per day of spent biochar catalyst was produced per day resulting in 23.4% of the carbon from the biomass being sequestered. The total capital investment of a 200 dry ton per day biomass plant is $AU36.5M. Based on the costs of growing, harvesting, and transporting the biomass ($AU 4.72M per year) and plant operating costs ($AU 1.25M per year), the cost of producing power from biomass is

10.201 c/kWh, well below the minimum sale price of 16.2966 AU¢ per kWh. By increasing the amount of biochar gasified in the moving bed to 100 %, the electricity production cost can be decreased to 9.719 AU¢ per kWh, however, this reduction in cost is at the expense of creating a carbon negative process.

CHAPTER 7 ENVIRONMENTAL BENEFITS OF SEQUESTERING BIOCHAR COLLECTED FROM A MOVING BED REACTOR

7.1 Introduction

After the moving bed reforming process, as described in Chapter 5 and Chapter 6, spent biochar catalyst is collected. Through minimising the amount of biochar that is converted via steam gasification and introducing the biochar into the soil where the biomass is grown, a significant portion of the carbon can be sequestered and hence create a carbon negative process. Typically, the biochar is added to the soil at concentrations ranging from 5-50 tonnes per hectare [120, 121]. For the full potential of the carbon sequestration to be realised, it must be ensured that the biochar is stable in the soil, quantified through the O/C and H/C elemental ratios. An O/C ratio in the biochar of 0.2 corresponds to a half-life of 1000 years, more than enough time to see out the lifetime of the biomass production [122, 123]. Raw biomass typically has on O/C ratio of more than 1 [122] with some biochars having an O/C ratio as low as 0.1 [124]. Despite the stability of the biochar in the soil, some carbon can leach into the soil mainly in the form of aromatic hydrocarbons [97, 136]. The leaching of these compounds should be avoided as they can potentially restrict the growth of biomass and be hazardous to human health [321].

Not only does the introduction of the biochar into the soil sequester the carbon, there are numerous benefits the biochar has on the regrowth of biomass. The first of which is the leaching of nutrients from the biochar via the water washing from rain water [42-46]. Biomass, particularly Mallee Eucalyptus, contains a significantly large amount of metallic species and it has been shown that up to 90% of these metals are retained in the biochar during pyrolysis [115]. Potassium, nitrogen, and phosphorus, which can be leached from biochar, are particularly beneficial to plant growth [120, 121, 129-132] whilst calcium, magnesium, chlorine, and sodium are also known to enhance soil fertility [133, 134]. There are many factors that affect the leaching characteristics. A study by Kong et. al. [275] showed that biochars prepared via fast pyrolysis have increased rates of magnesium and calcium leaching but decreased sodium and

potassium leaching compared to slow pyrolysis biochar. Through the partial gasification (5-10% conversion) of these biochars, the amount of nutrients that can be leached and the leaching rate are both increased [136]. As the biochars collected from the exit of the moving bed has undergone partial gasification, it is expected that the nutrients leaching of these biochars is enhanced.

Biochar is known to be able to hold a significant amount of water [146] with factors such as surface area, pore size, and surface structure effecting the water holding capacity (WHC) [47, 146-148, 322]. Soils in the south west of Western Australia are often sandy with low WHC and any rain water is immediately drained away. Hence, biochars with high surface areas will be beneficial to the soils where the biomass is planted. Finally, after the removal of inorganic compounds from the biochar through leaching, there are numerous surface groups available on the biochar such as oxalate and oxonium. These groups have the potential to bond with fertilisers added to the soil, such as potassium and phosphorous, and hold them in the soil opposed to being washed away [121, 139-141]. The ability of the biochar to hold these nutrients is called the anion exchange capacity (AEC) and cation exchange capacity (CEC) [129, 130].

The aim of this chapter is to quantify the benefits of adding biochar into the soil where the biomass is regrown. The leaching characteristics, WHC, and exchange capacities of biochars collected from the moving bed experiments conducted in Chapters 5 and 6 will be quantified and compared to biochars prepared via pyrolysis. Particular focus will be placed on whether the steam reforming process enhances the agronomical benefits of the biochar. This will be the first study to combine all of these tests in order to realise the positive potential of recycling spent biochar catalysts.

7.2 Biochar Properties

Table 7-1 and Table 7-2 outline the proximate analysis and ultimate analysis respectively of all the biochars to be tested in this study. As can be seen from the proximate analysis the biochar prepared from slow pyrolysis at 500 °C (500P) has the highest volatile content. Subsequently heating the biochar to 900 °C (900P) reduces the amount of volatiles in the biochar whilst maintaining the fixed carbon in the biochar. This is confirmed in the ultimate analysis with the decrease in hydrogen and

oxygen content. Acid washing the biochar decreases the ash content with minimal changes in the volatiles and fixed carbon.

Table 7-1: Proximate analysis of biochar samples. Moisture content is given after the sample has been air dried. Ash, volatiles, and fixed carbon given as wt% on a dry basis (d.b).

Sample	Moisture (wt%)	Ash (wt%, d.b.)	Volatiles (wt%, d.b.)	Fixed Carbon (wt%, d.b.)
500P	5.63	1.83	28.05	63.76
900P	4.10	2.27	10.19	87.20
900AW	5.10	1.61	9.97	84.48
830SG	2.29	5.82	14.49	76.67
830SRN	3.18	7.26	10.98	77.97
830SRT	1.90	7.99	13.06	73.49

Table 7-2: Ultimate analysis of biochar samples. All values given as wt% on a dry ash free (daf) basis.

Sample	Carbon	Hydrogen	Nitrogen	Oxygen[1]	Sulphur
500P	86.5	3.48	0.30	9.71	0.01
900P	91.1	1.30	0.32	7.30	0.01
900AW	91.2	0.90	0.29	7.22	0.01
830SG	89.8	1.26	0.14	8.37	0.01
830SRN	90.3	1.18	0.17	7.67	0.03
830SRT	89.2	1.02	0.26	9.46	0.02

[1]Oxygen content is calculated by difference. 70% of the chlorine remains in the ash. Hence, 30% of the chlorine content was included in the oxygen calculations

During the steam gasification/reforming process, there is little change in the volatile material in the biochar due to the reforming temperature (830 °C) being lower than what the biochar was prepared at (900 °C). The increased ash content is due to the potassium chloride loaded onto the biochar before the steam gasification/steam reforming process. The carbon percentage decreases due to the steam gasification of the carbon in the biochar. The carbon content of the biochar subject to steam gasification is less than that collected from steam reforming of naphthalene as the steam selectively reacts with the naphthalene opposed to the biochar. Increase gasification occurs in the 830SRT biochar when compared to the other biochars due to a higher steam to biochar ratio used in the moving bed experiment. The decrease in carbon content subsequently increases the oxygen concentration. The O/C ratios of the biochars range from 0.0842 for 500P biochar and 0.0637 for 830SRN biochar, well

below the threshold of 0.2 for the biochar to be considered stable when added to soil [122, 123].

Table 7-3 outlines the content of all of the inorganic species in the biochar. For the majority of the species, it appears that the content increases during the heating of the biochar from 500 °C to 900 °C. However, when taking into account the total mass loss during the heating process, there is a small loss of each of these species. As expected, the concentration of each of the metallic species decreases during the acid washing process. However, the acid washing does not completely remove all of the metallic species. There is also still a large amount of residual chlorine remaining on the biochar after the acid washing process. Even with extensive water washing, not all of the chlorine could be removed.

Table 7-3: Inorganic contents of biochar samples. All values given as wt% on a d.b.

Sample	Na	K	Mg	Ca	Cl	P	Si	Fe	Al
500P	0.089	0.195	0.100	0.385	0.005	0.133	0.011	0.002	0.038
900P	0.098	0.247	0.117	0.457	0.003	0.114	0.109	0.003	0.023
900AW	0.071	0.104	0.099	0.273	1.205	0.094	0.009	0.001	0.024
830SG	0.014	2.103	0.185	0.494	1.540	0.365	0.923	0.899	0.028
830SRN	0.033	1.910	0.108	0.428	2.135	0.291	1.697	0.837	0.185
830SRT	0.018	0.403	0.224	0.362	0.200	0.186	0.075	1.270	0.063

The chlorine and potassium concentrations are high in the steam reforming/gasification biochars due to the loading of potassium chloride before the moving bed reactions. Losses in potassium and chlorine are observed in the moving bed; therefore these concentrations are lower than what was loaded onto the raw biochar. The potassium and chlorine concentrations are lower in steam reforming of tar as the amount of potassium chloride loaded on the biochar originally was lower than in steam gasification and steam reforming of naphthalene.

There is a measurable increase in iron and silicon contents in the biochar during steam gasification/reforming. The increase in iron content can be contributed to the reactor being constructed of stainless steel therefore some of the iron is transferred from the reactor to the biochar. The increase in silicon content can be attributed to the grease

required to seal the reactor. Silicon deposition on biochar was not observed in the steam reforming of tar as the reactor was modified to eliminate the need for the grease.

7.3 Leaching of Inorganic Species Contained in Biochar

Figure 7-1 and Figure 7-2 show the amount of sodium, potassium, magnesium, calcium, and chlorine lost during each stage of the steam gasification/reforming process. Figure 7-1 provides the percentages lost based on what was originally in the biomass and Figure 7-2 is based on the inorganic content of the biochar before it was fed into the moving bed reactor. Four biochars were collected at different points in the moving bed from each experiment. Samples were collected corresponding to a gasification/reforming time of 7, 28, 49, and 70 minutes for the 830SG and 830SRN biochars and 10, 40, 70, and 100 minutes for 830SRT biochars.

As can be seen from Figure 7-1 there is a large variation in where each of the inorganic species are lost. Only 11% of the sodium lost during the pyrolysis of biochar at 500 °C. There appears to be minimal loss of chlorine and potassium during this step in the process as the percentages in the graph include what is loaded onto the biochar later in the process. Approximately 41% and 31% of the magnesium and calcium are lost from the biomass during pyrolysis to 500 °C. Subsequently heating the biomass to 900 °C does not result in significant further losses of the inorganic species. The maximum losses occur with sodium where only approximately 6% is lost during this stage.

Acid washing has a mixed effect on the removal of metallic species from the biochar. After acid washing approximately 60.3%, 47.4%, and 38.6% of the sodium, magnesium, and calcium respectively are retained in the biochar. This corresponds to 22.7%, 8.9%, and 26.8% of the sodium, magnesium, and calcium respectively being removed from the biochar through acid washing when compared to what was in the biomass.

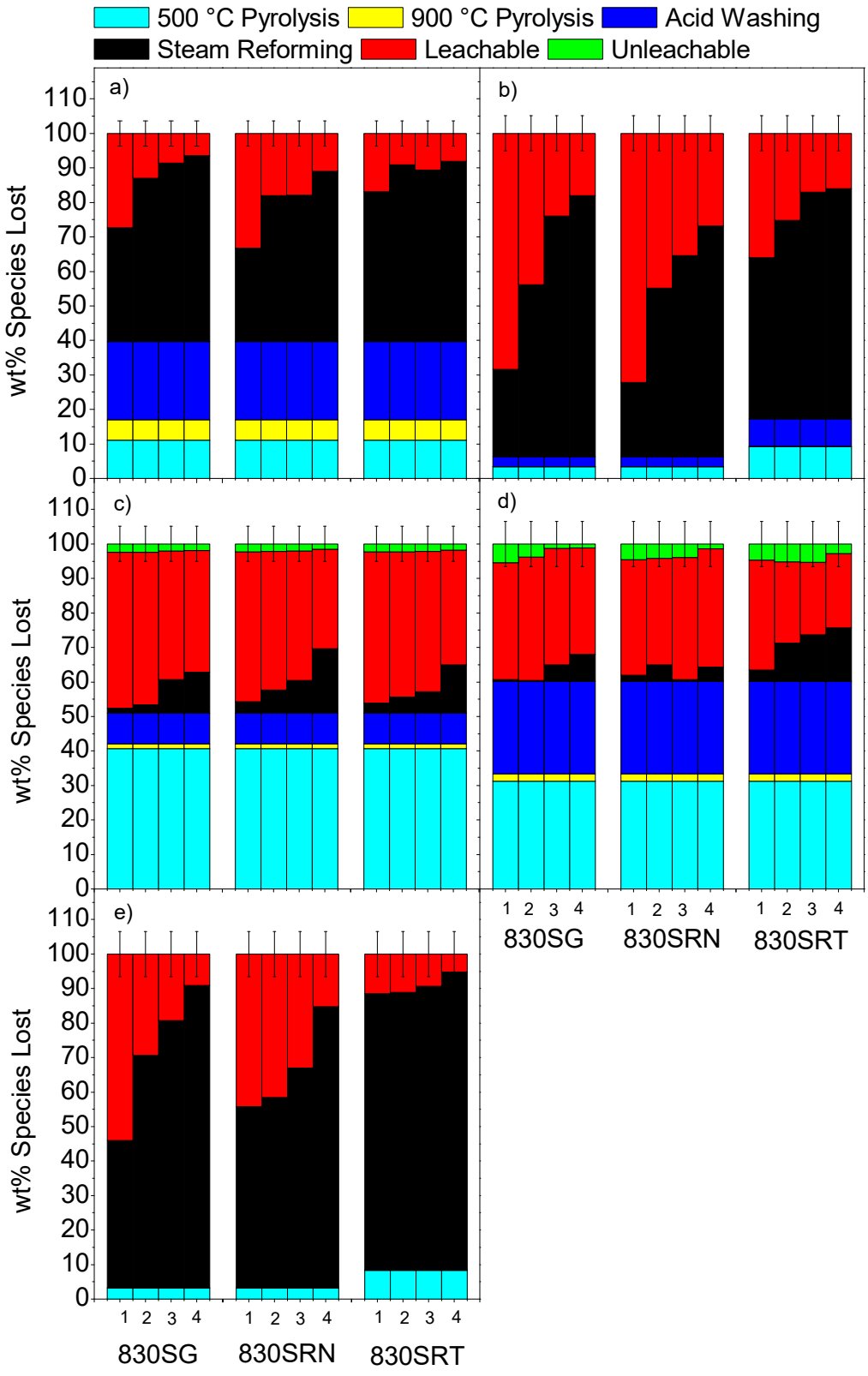

Figure 7-1: The amount of a) sodium b) potassium c) magnesium d) calcium and e) chlorine lost during pyrolysis to 500 °C, pyrolysis to 900 °C, acid washing, moving bed steam gasification/reforming, the percentage water leached, and the percentage of unleachable material based on the content in the fresh biomass at a steam gasification/reforming time of 1) 7 minutes 2) 28 minutes 3) 49 minutes and 4) 70 minutes for 830SG and 80SRN biochars and 1) 10 minutes 2) 40 minutes 3) 70 minutes and 4) 100 minutes for 830SRT

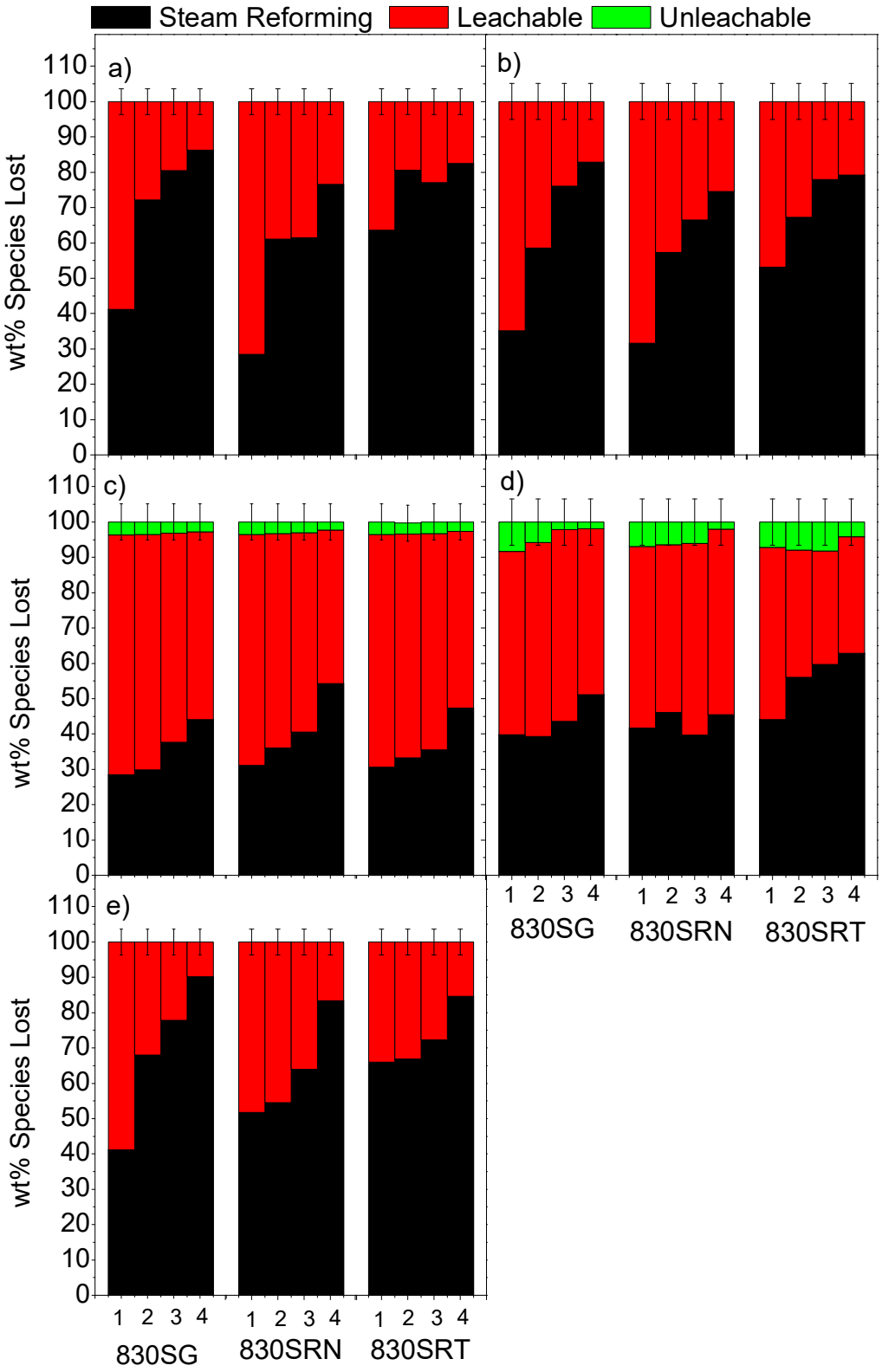

Figure 7-2: The amount of a) sodium b) potassium c) magnesium d) calcium and e) chlorine lost during the moving bed steam gasification/reforming, the percentage water leached, and the percentage of unleachable material based on the content in the biochar fed into the moving bed reaction at a steam gasification/reforming time of 1) 7 minutes 2) 28 minutes 3) 49 minutes and 4) 70 minutes for 830SG and 80SRN biochars and 1) 10 minutes 2) 40 minutes 3) 70 minutes and 4) 100 minutes for 830SRT

There are significant variations in the behaviour of each of the inorganic species during the steam gasification/reforming experiments. The loss of the divalent compounds magnesium and calcium are the lowest of the five compounds. The loss of magnesium during the moving bed experiments range from 1.4-3.9% for the shortest gasification/reforming time and 11.8-18.6% at the exit of the moving bed when compared to the content in biomass and 28.4-31.1% and 44.1-54.3% respectively when compared to the content in biochar. Similar results are seen in calcium with 39.7-44.1% lost after the shortest gasification time and 45.5-62.8% lost at the exit of the reactor when compared to the content of the biochar fed into the reactor. These relatively small losses are because of the stronger bonds formed with these divalent compounds when compared to monovalent compounds. It can be seen that for all five species, the amount of the species lost increases with increasing gasification/reforming time.

The losses observed in the monovalent compounds are much higher than seen with the divalent compounds. Losses of sodium during the steam gasification/reforming process are up to 49.4-53.9% based on biomass and 76.5-82.2% based on the content in the raw biochar. The raw biochar has a sodium content of only 0.052% therefore the loss of sodium during steam gasification/reforming is insignificant in terms of nutrient properties of the biochar. There are also significant losses in potassium and chlorine. It was seen that 74.6-82.9 % and 83.3-90.2% when compared to the content in the fresh biochar of potassium and chlorine respectively are lost during the moving bed reforming process. The increases losses in the monovalent species are greater than the divalent species as the bond strength with the biochar is weaker. As with the divalent species, the monovalent species lost increases with gasification/reforming time.

After the steam gasification/reforming in the moving bed, the remaining species in the biochar are available to be water leached, however, it may not be possible to leach all of these species completely. For the monovalent compounds, potassium, chlorine, and sodium, it was found that 100% of the inorganic species could be leached for all of the biochars. There is a small amount of magnesium and calcium that cannot be leached and remain in the biochar. It was seen that the amount of unleachable magnesium decreases from 3.5-3.6 to 2.3-2.9 % when compared to the content in biochar with

increased gasification/reforming time. A similar trend is seen in calcium with a decrease in unleachable metal from 6.7-8.4 to 1.9-4.2 % when compared to the content in biochar. The decrease in unleachable metal content is due to the increased surface area of the biochar, as seen in Figure 7-6.

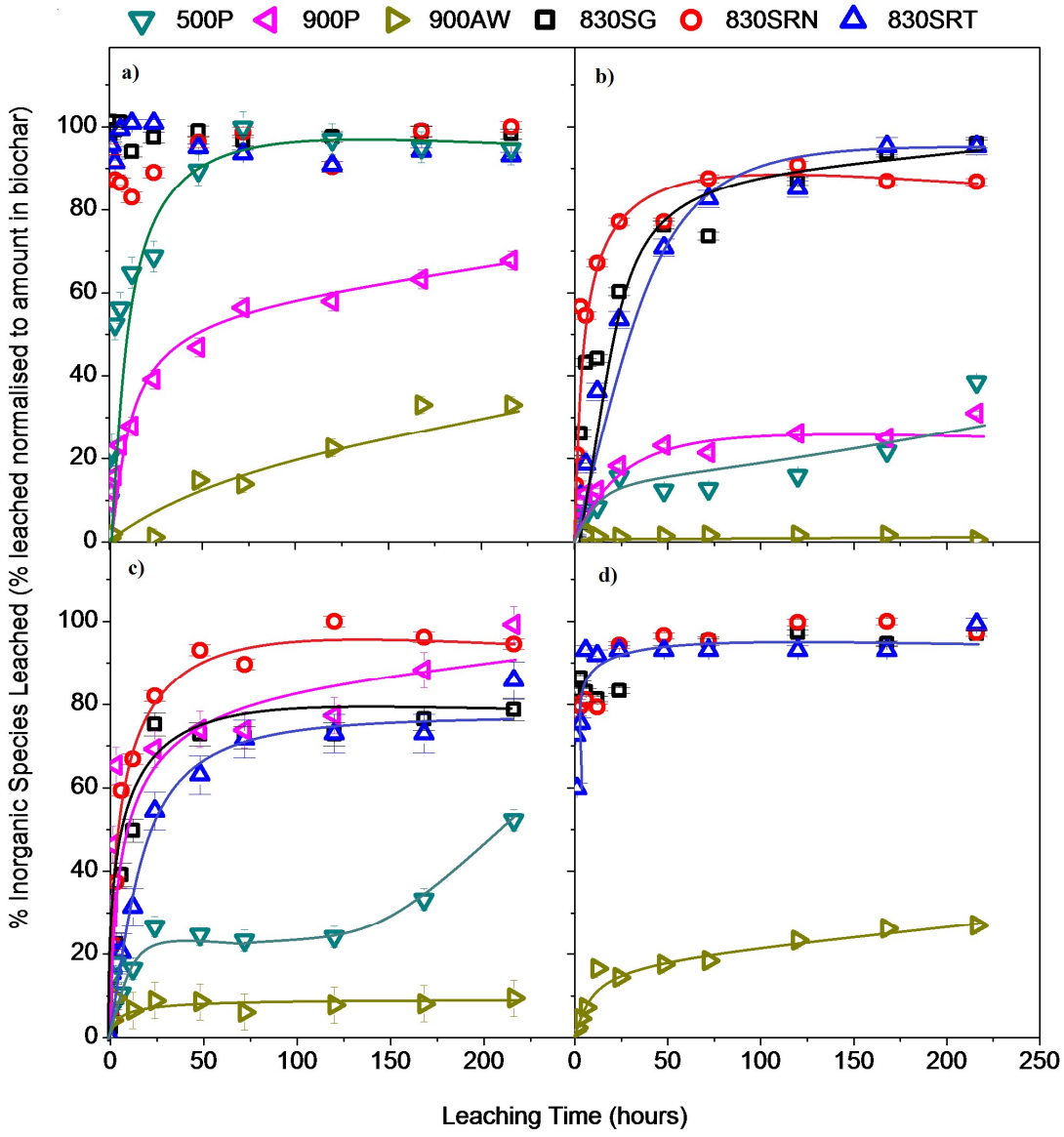

Figure 7-3: Leaching rate of a) potassium b) magnesium c) calcium and d) chlorine from biochar collected from the final basket in steam gasification/reforming experiments

Expanding on the leaching results shown in Figure 7-1 and Figure 7-2, it can be determined how the species of note leach from the biochar over time. Figure 7-3 outlines the leaching over time of potassium, magnesium, calcium, and chlorine for

500P, 900P, 900AW, 830SG, 830SRN, and 830SRT biochars. Due to the low concentration in some of the biochars, the sodium leaching over time could not be accurately measured. As can be seen, the potassium and chlorine are completely leached almost immediately from the biochars subject to steam gasification/reforming. Between 93 and 98 % of the potassium is leached in the first 15 minutes. As the potassium and chloride were loaded onto the biochar as KCl salt, it is suspected that they remain on the surface in the highly water soluble salt form. The remainder of the potassium and chlorine is bonded to the surface groups of the biochar, however, as they are both monovalent ions, the bonding is weak and they are easily leached. For biochars subject to pyrolysis, the leaching of potassium is much slower when compared to those from steam gasification/reforming. Biochar subject to 500 °C pyrolysis sees 100% of the potassium being leached from the biochar. Increasing the pyrolysis temperature to 900 °C and subsequently acid washing the biochar decreased the amount of leachable potassium to 64 and 30% respectively. The heating of the biochar to 900 °C and acid washing reduces the loosely bonded potassium available for leaching therefore leaving unleachable potassium.

As can be seen in Table 7-3, the amount of chlorine in the pyrolysis biochars is very low and could not be measured accurately during leaching. Despite extensive water washing, there is still significant amount of chlorine present on the biochar after acid washing. In Figure 7-3, it can be seen that only approximately 33% of the chlorine can be leached from the acid washed biochar even after leaching for 11 days. This indicates that further water washing will not be able eliminate all of the chlorine added on the biochar from acid washing.

The leaching of magnesium and calcium is much slower than potassium and chlorine in biochars that have undergone steam gasification/reforming. The bond strength of divalent species with biochar is much higher when compared to monovalent species. The maximum leaching of magnesium and calcium is achieved at a leaching time of 216 hours, leaving the unleachable material present in the biochar shown in Figure 7-1 and Figure 7-2. When looking at the biochars subject to pyrolysis, the leaching rate and amount of leachable magnesium is less for all three biochars. The amount of magnesium leached is similar for 500 °C and 900 °C pyrolysis with 38 and 33% leached respectively. The calcium leaching reaches 52% in 500 °C pyrolysis biochar

whilst 100 % can be leached from the 900 °C pyrolysis biochar. Less than 10 % of the magnesium and calcium can be leached from the acid washed biochar. This can mainly be attributed to the reduced surface area in the acid washed biochar. Acid washing collapses the pores in the biochar (as shown in Figure 7-6) and hence restricts access to the leachable species.

Table 7-4 outlines the leaching kinetics of the biochars tested. Based on the r^2 values, it can be seen that the pseudo-second order provides a good fit for all of the data. The initial leaching rate (h) is an important factor as when biochar is added to the soil the biochar is not necessarily soaking in water, therefore it is important that the species are leached rapidly. As can be seen, the initial leaching rate for potassium and magnesium decrease and the rate for calcium increases from subsequently heating the biochar from 500 to 900 °C. The chlorine concentration in the 500P and 900P biochars was too low to accurately measure the leaching kinetics. Acid washing the biochar significantly decreases the initial leaching rate of all metallic species. This is a result of the acid washing process removing the majority of the water soluble metallic species from the biochar. The steam gasification/reforming process increases the leaching rate of all of the inorganic species. The potassium and chlorine initial leaching rate is significantly high due to the majority of these species existing as the highly soluble salt on the surface of the biochar. Magnesium and calcium leaching rates are increased due to the increase in surface area, as seen in Figure 7-6, allowing access to the water soluble species.

Table 7-4: Kinetic parameters calculated from the water leaching of each of the six biochars tested (k is the overall leaching rate and h is the initial leaching rate both given in L $mg^{-1}day^{-1}$)

Sample	K			Mg			Ca			Cl		
	k	h	r^2	k	h	r^2	k	h	r^2	k	h	r^2
500P	7.65	8.46	1.00	65.28	0.35	0.98	21.77	4.47	0.99	-	-	-
900P	2.29	1.81	1.00	9.03	0.30	0.98	1.14	6.24	0.98	-	-	-
900AW	1.37	0.048	0.94	1078	0.066	0.99	47.51	0.62	0.98	0.68	2.00	0.98
830SG	8.63	833.3	1.00	1.80	1.43	0.99	1.94	6.98	0.98	6.233	128.2	0.98
830SRN	1.22	169.5	1.00	5.97	4.40	1.00	1.45	19.96	0.98	223	11111	1.00
830SRT	846	3333	1.00	1.38	1.22	0.99	2.25	3.00	0.99	11.48	6.98	1.00

Despite the losses in metallic species during the steam gasification/reforming, the moving bed process is beneficial to the leaching of inorganic species. When compared to the biochar prepared to pyrolysis, the rate and total amount of metallic species that are valuable to the fertility of the soil are greater in the biochar collected from the outlet of the moving bed.

7.4 Leaching of Organic Compounds

A major benefit of using biochar as a catalyst followed by its reintroduction into the soil is the sequestration of carbon. The carbon is sequestered as it is stored in the soil opposed to being converted to CO_2 if it was to be used in energy production. However, if this carbon is leached into the soil, it is once again reabsorbed by the regrowing biomass and the sequestration nullified. Figure 7-4 panel a) shows the amount of carbon leached from the biochar with increased gasification/reforming time. As can be seen, the amount of carbon leached is consistently at approximately 0.5 % of the carbon present in each biochar catalyst. There is no distinguishable trend with the amount of carbon leached and the steam reforming time.

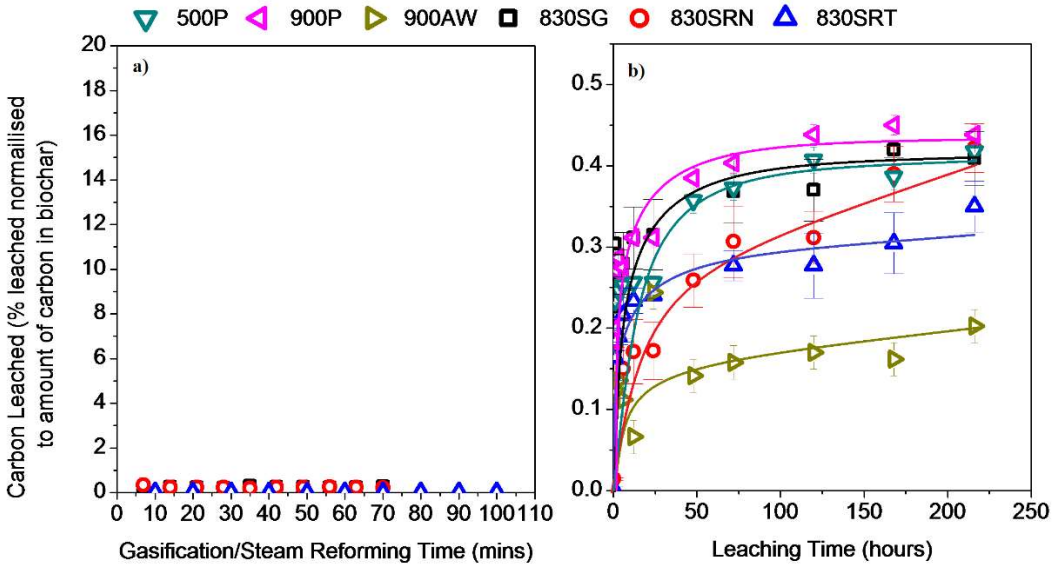

Figure 7-4: a) Total amount of carbon leached from biochars from steam gasification/reforming as a % of total carbon in biochar b) Leaching kinetics of carbon from the biochar in the final basket of steam reforming/gasification

Figure 7-4 also shows the amount of carbon leached over leaching time. As can be seen, the amount of carbon increases slowly over leaching time. The slow leaching of carbon is significant as, opposed to the inorganic species, the leaching of carbon should be minimised. After a leaching period of approximately 220 hours, the amount of carbon leached remains constant. The maximum amount of carbon leached for the majority of the biochars tested range between 0.36 and 0.45 wt% of the carbon on the biochar. The anomaly is the acid washed biochar, where only 0.2 wt% of the carbon is leached due to some of the leachable carbon being removed in the acid washing process.

As these catalysts had been used to reform naphthalene and tar from the syngas and there was evidence of carbon leaching, it is a possibility that these compounds remain on the biochar and are responsible for the water leachable carbon. There is also known to be polyaromatic hydrocarbons (PAH) present on the surface of the biochar as seen in the volatiles measured in the biochars as shown in Table 7-1. As some of these compounds can be hazardous to both the environment and human health, it is important that they are not leached into the soil [321]. Figure 7-5 shows the UV-Fluorescence spectrum of the water leaching solution from all of the biochars tested. As can be seen there are no observable peaks. This means that the carbon leached in the water does not consist of hazardous aromatic rings.

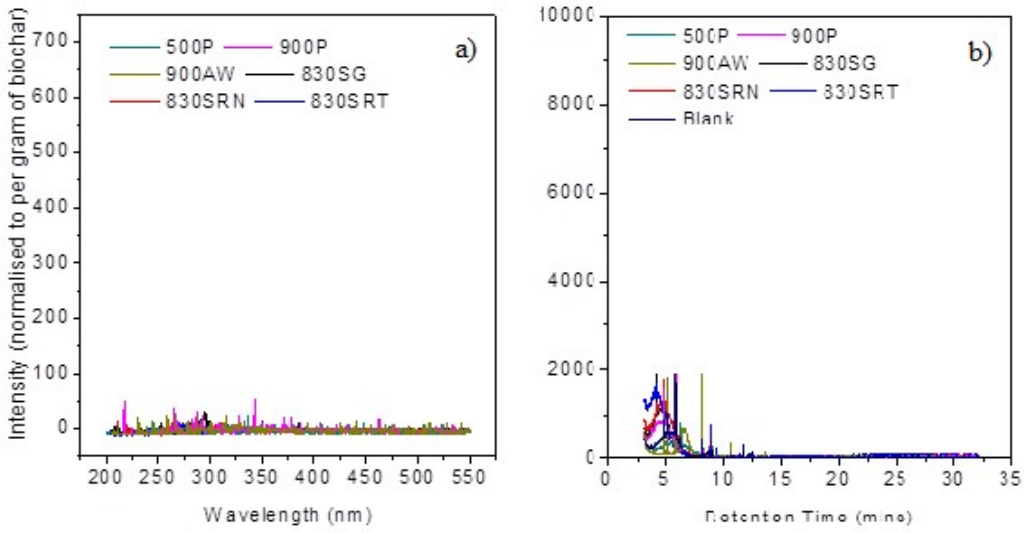

Figure 7-5: a) UV-Fluorescence spectrum of water leaching solutions from biochars collected at the exit of the moving bed reactor normalised to per gram of biochar leached in 1 L of water b) GC-MS spectrum of methanol-chloroform solutions after leaching of biochars from the outlet of the moving bed reactor and fresh biochar

Even though there was no evidence pf aromatics from UV Fluorescence, these compounds could exist in a non-water soluble form. Figure 7-5 shows the GC-MS analysis of biochars leached in methanol/chloroform. By leaching the biochar in an organic solvent and analysing using a GC-MS allows for greater accuracy of the individual organic components present on biochar. As can be seen from the graph, there are no obvious peaks from the organic leaching of all biochars. The small peaks that are observable can be attributed in impurities in the solvent. This confirms the results obtained from the UV-Fluorecence stating that there are minimal leachable organic species on all of the biochars tested. This means that the biochars collected from the moving bed reactor are all potentially safe to be recycled back to the soil as they pose no health hazards associated with the leaching of organic compounds.

7.5 Water Holding Capacity

It is well known that biochars have a high WHC due to the presence of hydrophilic surface groups. Hence adding biochar into the soil will improve water retention. The soil in the south west, the location where the biochar is to be recycled and where the mallee biomass is grown, mainly consists of sand. This soil is known to have a low WHC and testing a silica sand yielded a water holding capacity of only 0.25 g of water held per gram of sand. Figure 7-6 shows the water holding capacity, surface area and

pore volume of all of the biochars tested. When increasing the pyrolysis temperature from 500 °C to 900 °C there is an increase in surface area from 40.7 to 154.2 m^2/g and a small increase in pore volume from 0.150 to 0.168 cm^3/g. Despite the increase in surface area and pore volume, there is a decrease in the WHC from 4.10 to 1.07 g water/g of biochar. The decrease in WHC is as a result of the loss of the oxygen containing hydrophilic surface groups through an increase in pyrolysis temperature. This is seen in a decrease in oxygen content as shown in Table 7-2. Acid washing the 900 °C biochar decreases the surface area and pore volume to 4.2 m^2/g and 0.003 cm^3/g as a result of the acid collapsing the pores. Despite this, the WHC capacity increases to 2.91 g water/g of biochar with no evidence in the increase in oxygen content. During acid washing, the surface groups are protonated increasing their ability to form hydrogen bonding with water, therefore increasing the WHC of the biochar.

After exiting the moving bed, the biochar has been partially gasified, increasing the surface area to a range of 511.7 to 680.5 m^2/g and increasing the pore volume to a range of 0.247 to 0.400 cm^3/g depending on the reaction process. This results in increasing the WHC to 4.62 to 5.80 g water per g biochar. Despite the increase in WHC on per gram of biochar basis, this is not reflected when looking at per gram of biomass fed into the reactor. The 500P biochar has a WHC of 0.918 g water per gram of biomass used. The resultant mass losses from the increase in pyrolysis temperature and the steam gasification of the biochar, the WHC of the biochars collected from the moving bed reactor ranges from 0.640 to 0.741 g water per gram of biomass initially used. Hence, if all of the biochar is to be added to the soil, there will be more total water held if the biochar is removed after 500 °C compared to the biochar collected after the moving bed reforming process.

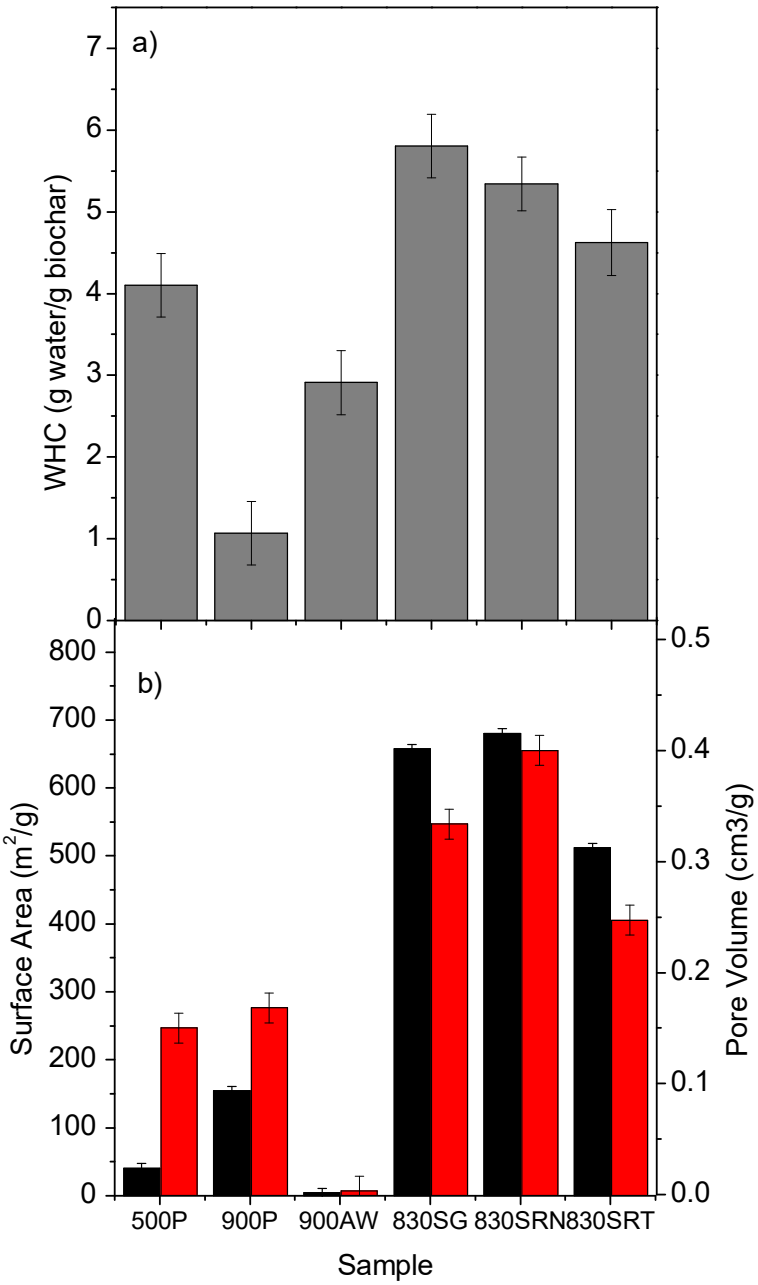

Figure 7-6: a) Water Holding Capacity and b) Surface Area/Pore Volume for i) Steam Gasification Biochar ii) Steam Reforming of Naphthalene Biochar and iii) Steam Reforming of Tar Biochar for different Steam Gasification/Reforming Times

Table 7-5: Literature review of the water holding capacities of biochars used as a soil amendment

Ref	Biomass	Reactor	Heating Rate	Temp	Surface Area (m^2/g)	Water Holding Capacity (g water/g biochar)
[47]	Red Oak	Fluidised Bed	Fast	500 °C	-	0.23
[322]	Switchgrass	Fixed Bed Microwave	Slow	400 °C	46.93	0.35
[323]	Hardwood and Hickory	Fixed Bed	Slow	-	153	0.36
[324]	Poultry Litter	Fixed Bed	20 °C/min	450 °C	34	1.1
[325]	Maize	Retort	Fast	750 °C	217	0.32
[326]	Pine	Retort	Slow	400 °C	0.19	2.47
[146]	Poplar	Fixed Bed	Slow	550 °C	210.57	3.98
[327]	Switchgrass	Fixed Bed	Slow	500 °C	62.2	0.51
[328]	Prune Residues	Fixed Bed	Slow	500 °C	141	0.85
[329]	Straw	Various	Various	Various	150-350	0.20-0.56
[330]	Douglas-fir chips	Retort	Slow	620 °C	280	0.80
This Study	Mallee Eucalyptus - Wood	Fixed Bed	Slow 10 °C/min	500-900°C	4.24-154.2	1.07-4.01
This Study	Mallee Eucalyptus - Wood	Moving Bed Steam Reforming	Fast	Slow	511.7-680.5	4.60-5.80

There have been extensive studies on the WHC of biochars prepared from pyrolysis; however, this is the first study to look at the WHC of biochars that have been prepared via partial gasification. Table 7-5 outlines the literature summary for the WHC of biochars used as a soil amendment. As can be seen, there is a significant variability in the WHC of biochar with the maximum being 3.98 g of water per gram of biochar. It appears that increasing WHC is directly proportional to surface area. When comparing the literature to the results obtained in this study, it can be seen that the biochars collected after moving bed reforming is much higher than all of the biochars collected after pyrolysis.

7.6 Exchangeable Bases/Exchange Capacities

As discussed previously, the metallic species can be bonded to the negatively charged surface groups on the biochar. The metallic species bonded in this way are known as the exchangeable bases and are tested by chemically exchanging one species with another. As this is a chemical bond, they are held much stronger on the biochar compared to the species adsorbed on the surface in a salt form. These exchangeable bases also need to be on the surface and accessible to allow the exchange to occur. In the biochar tested here, these cationic species are sodium, potassium, magnesium, and calcium. Figure 7-7 shows the exchangeable bases on each of the biochars tested. The amount of exchangeable bases in the pyrolysis biochars are relatively low. This is because the amount of the metallic species in the biomass feed is low, and as a result, the concentration is low in the biochar samples. The acid washing of biochar reduces the exchangeable bases from 0.241 cmol per kilogram of biochar to 0.016 cmol per kilogram of biochar. The reduction in exchangeable bases is a result of the acid removing these metallic species from the surface of the biochar and the closing of the pores, therefore not allowing access to the bases to be exchanged. The steam gasification/reforming process significantly increased the number of exchangeable bases. The exchangeable bases after steam gasification is 6.84 cmol per kilogram of biochar, steam reforming of naphthalene is 5.55 cmol per kilogram of biochar, and steam reforming of tar is 5.68 cmol per kilogram of biochar. In all cases, these exchangeable bases are predominately calcium. The increase is as a result of the increased surface area allowing access for the calcium to be exchanged. There is also some potassium within the exchangeable bases as a result of the potassium from loaded salt bonding with the biochar surface groups. However, the majority of the potassium on the final biochar product exists in the form of potassium chloride salt, which is initially removed in the exchange process.

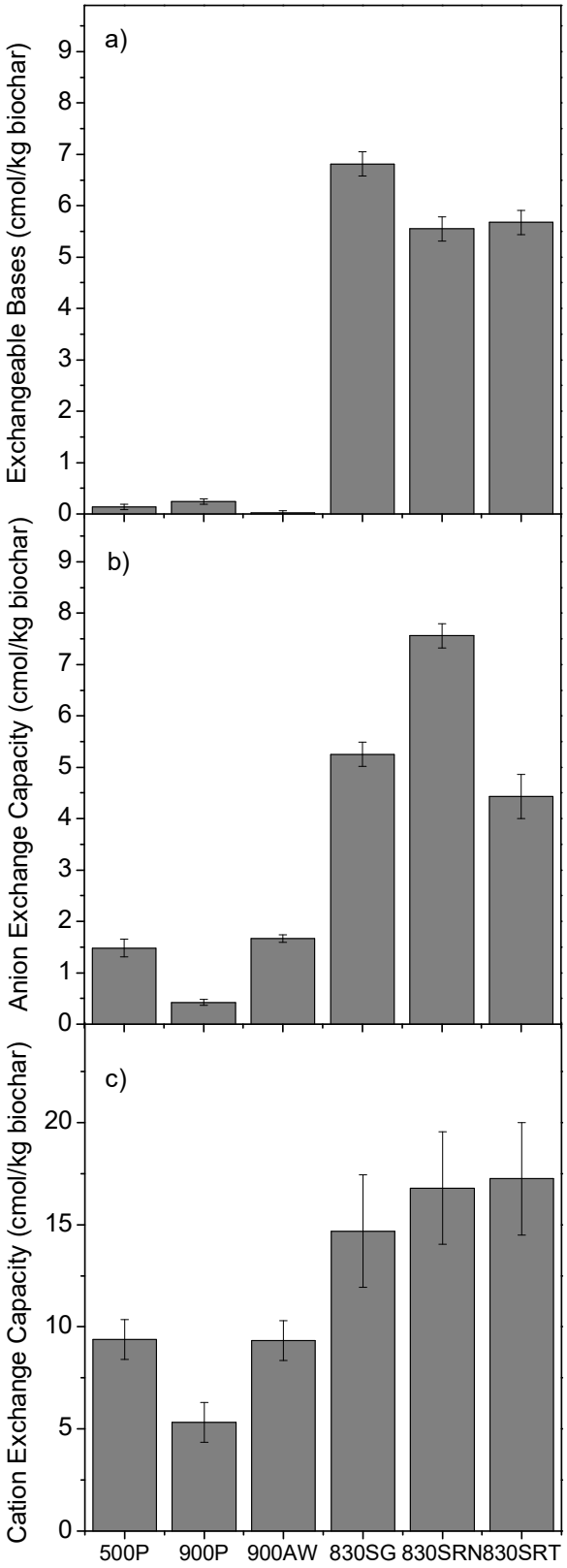

Figure 7-7: a) Exchangeable Bases b) Anion Exchange Capacity and c) Cation Exchange Capacity for i) Steam Gasification Biochar ii) Steam Reforming of Naphthalene Biochar and iii) Steam Reforming of Tar Biochar for different Steam Gasification/Reforming Times

After the leaching of the metallic species from the biochar, there are active surface groups remaining on the biochar. These include negatively charged oxalate groups and positively charged oxonium groups. Fertiliser is often added to the soil to increase the fertility of the soil. This fertiliser is often washed away immediately from the soil due to the low water holding capacity as discussed in the previous section. The surface groups on the biochar can bond with the valuable positively charged species such as potassium and negatively charged species such as phosphorus and nitrogen. The ability for the biochar to hold these positively and negatively charged species are known as the cation exchange capacity (CEC) and anion exchange capacity (AEC) respectively. Sandy soils in the south west of Western Australia often have low exchange capacities. The AEC for the silica sand was tested at 0.00658 cmol per kg of sand and the CEC tested for silica sand was 0.957 cmol per kg of sand.

Figure 7-7 shows the AEC and CEC of the tested biochars. As can be seen there is a large upgrade in the AEC going from the pyrolysis biochars to the biochars collected from the moving bed. The AEC for the acid washed biochar was 1.66 cmol per kg of biochar whereas the AEC after the steam reforming of naphthalene was 5.68 cmol per kg of biochar. An increase in CEC was also observed during the steam reforming/gasification. The CEC for acid washed biochar was 9.32 cmol per kg of biochar, which was upgraded to 17.3 cmol per kg of biochar after the steam reforming of tar. The CEC is much higher than the exchangeable bases indicating that not all of the surface groups are occupied by metallic species as the biochar exits the bed.

Typically biochar is added to the soil at 5-50 tonnes per hectare. With these high AEC and CEC, the biochar has the potential to hold a significant amount of fertiliser in the soil. Even taking into account the conversion of carbon from the steam gasification/reforming process, the AEC and CEC is upgraded. Hence, the process of steam gasification/reforming is beneficial to the exchange properties of the biochar.

7.7 Conclusion

Biochar is a valuable commodity in regards to enhancing soil properties when sequestered after being used as a catalyst to clean syngas. The process of steam gasification/reforming using a biochar catalyst in a moving bed configuration

enhances the leaching properties of the biochar. All of the available potassium, chlorine, and sodium can be leached from the biochar and approximately 94 and 96% respectively of magnesium and calcium can be leached. The rate at which these species are leached also increases with steam gasification/reforming when compared to pyrolysis biochar. Despite the increase in inorganic compound leaching, only 0.5 % of the carbon from biochar is water leached and there is no discernible difference in biochar collected from the moving bed to pyrolysis biochar. This indicates that the biochar is very stable within the soil and its carbon bio-sequestration potential optimised. It was found that this leached carbon does not consist of hazardous aromatic hydrocarbons and there is no deposition as a result of the steam reforming of naphthalene or tar. On a per gram basis, the WHC of biochar is upgraded from 4.10 grams of water per gram of biochar after pyrolysis at 500 °C to 5.80 grams of water per gram of biochar after steam reforming of naphthalene. However, when taking into account the amount of biochar gasified in the process, the total amount of water that can be held by the biochar remains similar when taking into account the total yield from the process. Finally, the exchange capacities are drastically increased due to steam gasification/reforming. The exchangeable bases increase from 0.241 to 5.55 cmol per kilogram, the AEC increases from 1.48 to 7.56 cmol per kg, and the CEC increases from 9.37 to 16.79 cmol per kilogram when comparing biochar collected after pyrolysis to biochar exiting the moving bed. This means that biochar is valuable in retaining fertilisers in the soil.

CHAPTER 8 CONCLUSIONS AND RECOMMENDATIONS

8.1 Introduction

This chapter summarises the key research findings from this PhD study. This study has developed a novel method of cleaning a tar-containing syngas produced from the pyrolysis and subsequent gasification of biomass using a biochar-based catalyst whilst allowing the biochar to be collected at a continuous rate once it is spent as a catalyst. Firstly, it was found that there is a reaction between naphthalene and oxygen in the biochar producing carbon monoxide when there is no steam present in the system. Secondly, through the addition of steam into the process, a moving bed of biochar-based catalyst can reduce the naphthalene concentration in syngas from approximately 3600 to 15 mg/m^3. A moving bed of biochar allows the process to be continuous and has the benefit of the biochar catalyst being activated in the upper portion of the bed and then collected in a continuous manner from the bottom of the bed when necessary. Thirdly, the moving bed configuration is also effective in cleaning a tar-containing syngas produced from the continuous fast pyrolysis of biomass. Finally, the biochar collected from the moving bed can have many benefits in association with the regrowth of biomass when added to the soil, including leaching of valuable nutrients into the soil and increasing the water holding capacity of the soil. In addition, this section will highlight recommendations based on the findings of this work for future research to be completed on this area.

8.2 Conclusions

8.2.1 Pyrolysis of Naphthalene over Metal Loaded Biochars at 900 °C

- Thermal cracking of naphthalene at 900 °C when no catalyst is present in the reactor vessel is negligible

- Fe(III) loaded biochar provides the highest activity of all of the catalysts tested in relation to naphthalene pyrolysis with 100% conversion of naphthalene observed.

- The conversion of naphthalene varied when other catalysts were used with Mg-loaded biochar converting 51% of the naphthalene, K-loaded biochar 37%, and raw biochar 18%.

- There was a measurable decrease in activity for naphthalene pyrolysis over time in all catalysts tested.

- A spike in carbon monoxide in the outlet gas was observed during naphthalene pyrolysis over the biochar based catalysts when compared to the gas collected during thermal cracking of the biochar indicating that naphthalene reacts with the oxygen on the surface of biochar.

- An imbalance was observed in the amount of oxygen and hydrogen collected in the gas compared to the amount lost in the biochar. A molar ratio of approximately 2:1 of missing hydrogen to oxygen was observed indicating that water is formed in the process.

- There was measurable deposition of carbon on the naphthalene during the pyrolysis of naphthalene indicating that it is also decomposed into carbon and hydrogen.

- There was no evidence of the naphthalene being polymerised into larger polyaromatic hydrocarbons during pyrolysis over biochar catalysts.

8.2.2 Reforming of Naphthalene over a Bed of Biochar Catalysts under Steam Gasification Conditions: Fixed Bed vs. Moving Bed

- A moving bed of K-loaded biochar can reduce the naphthalene concentration in syngas from 3600 mg/m^3 to 15 mg/m^3 under steam reforming conditions. The bed depth used was 38 mm with a total space time of 0.775s.

- In this process approximately 1 mmol/min per gram of biochar of syngas is produced consisting of hydrogen, carbon monoxide, and carbon dioxide with minimal methane produced.

- The formation of the gases is mainly results from the steam reforming of naphthalene with the remainder from the steam gasification of biochar and the water gas shift reaction

- There was no evidence of the catalyst shifting the equilibrium in the water gas shift reaction.

- A steam utilisation efficiency of 78-80% was observed in the process.

- The biochar was collected from the bottom of the moving bed was found to be more stable if it was to be added to the soil when compared to the biochar catalyst fed into the reactor due to lower O/C ratio and lower reactivity.

- Steam gasification of biochar in the moving bed increased the surface area of the biochar from 20 m^2/g at the inlet of the reactor to 700 m^2/g at the outlet.

8.2.3 Reforming of Tar Produced from the Fast Pyrolysis of Biomass Followed by the Gasification of the Syngas

- Fast pyrolysis of woody biomass at 500 °C and an addition rate of 0.2 g/min in 2 L/min of argon followed by the subsequent steam gasification at 830 °C with no catalyst present results in a tar concentration of 3500 mg/m^3 with the major components of the tar being benzene, toluene, naphthalene, acenaphthylene, phenanthrene, and pyrene.

- Steam reforming over a moving bed of biochar with a bed depth of 54 mm and a corresponding space time of 0.478 s reduced the tar concentration to 100 mg/m3.

- It was found that the acenaphthylene, phenanthrene, and pyrene were completely reformed with the remaining tar consisting of benzene, toluene, and naphthalene.

- The concentration of naphthalene in the exit syngas was 44 mg/m^3.

- Results achieved in the laboratory were then scaled up into a 200 dry ton per day of biomass operation resulting in an electricity output of 6.57 MW and total efficiency of 12.85% based on the energy available in the biomass feed.

- 26 tons per day of biochar is collected from the outlet of the moving bed in this process and when added back to the soil results in the sequestration of 23.4% of the carbon in the biomass.

- The total capital investment of the 200 ton per day biomass plant was $AU 36.5M with a production cost of 10.201 ¢/kWh.

- A sensitivity analysis showed that the production cost was most sensitive to the gas engine efficiency and the cost to get the biomass from the farm to the plant and least sensitive to the amount of carbon gasified from the biochar and the credit received from carbon sequestration.

8.2.4 Soil Amendment Properties of Biochar Catalyst after Steam Reforming of Naphthalene and Tar

- Biochar collected from the outlet of the moving bed experiments outlined in Chapters 5 and 6 have numerous benefits to the growth of the biomass used to produce the biochar.

- The moving bed steam reforming process increased both the extent and rate the inorganic species can be leached from the biochar using water compared to biochar prepared via pyrolysis.

- All of the potassium, chlorine, and sodium can be leached into water from the biochars collected from the exit of the moving bed where approximately 94% of the magnesium and 96% of the calcium can be leached.

- Water leaching of carbon can be problematic and it was discovered that only 0.5% of the carbon is leached from the biochar and this leached carbon does not consist of hazardous aromatic hydrocarbons.

- The water holding capacity of biochar collected after 500 °C pyrolysis was measured at 4.10 grams of water per gram of biochar, which increased to 5.80 grams of water per gram of biochar after steam reforming.

- The moving bed process also results in the increase of the anion and cation exchange capacities of the biochar with an increase from 1.48 to 7.56 cmol per kg in anion exchange capacity and 9.37 to 16.79 cmol per kg in cation exchange capacity when compared to biochar produced via pyrolysis.

8.3 Recommendations

Based on the conclusions made in this study, the following recommendations for future work can be made:

1. It was observed that the naphthalene reacted with the oxygen in the biochar, however, it was unclear what the exact form that this oxygen takes in the biochar. Further studies can be completed on analysing the surface properties of the biochar after being exposed to naphthalene in the absence of steam for different periods of time with focus on the oxygen containing surface groups. This will determine whether the oxygen exclusively comes from the surface groups or from other sources. Isotope study may also considered to examine the possible oxygen exchange during the reaction;

2. Extensive losses in metallic species from the biochar, especially those loaded onto the biochar, were observed in all experiments. These losses should be minimised as it is costly to load the biochar with these compounds and their presence in syngas can be hazardous to downstream equipment. Tests can be conducted to determine whether these loses can be minimised and if there is a minimum concentration of metal that can be loaded in order to ensure that the biochar is still active in the steam reforming of naphthalene/tar;

3. Only wood based catalysts were used in these experiments. Bark and leaf biochar based catalysts can also be produced and may have profoundly different catalytic abilities. In reality, the biomass feed will be a mixture of wood, bark, and leaf therefore it must be determined whether catalysts produced from each component of the tree and a combination there of can clean syngas under steam reforming conditions;

4. The concept of a two stage pyrolysis of biomass followed by the steam reforming of the tar-containing syngas over a simulated moving bed of biochar was proven to be effective on a laboratory scale. Before this process can be commercialised, a larger scale pilot plant using an actual moving bed of biochar catalyst with a capacity to handle up to one ton of biomass feed needs to be constructed and operated for scaling up study;

5. Nitrogen and sulphur are also present in biomass and can be potentially beneficial in the regrowth of biomass. The release of these species may also be undesired during the two-stage gasification process, from environmental point of view. Therefore, the quantification of the losses of these components along with the water leaching of these components needs to be investigated.

REFERENCES

[1] K. Thorton, Clean Energy Australia Report 2016, in, Clean Energy Council, 2016.
[2] A. Ball, S. Ahmad, C. McCluskey, P. Pham, I. Ahn, L. Dawson, T. Nguyen, D. Nowakowski, Australian Energy Statistics 2016, in, Australian Government, Department of Industry, Innovation and Science, 2016.
[3] Climate at a Glance: Global Time Series, in, NOAA National Centers for Environmental Information, http://www.ncdc.noaa.gov/cag/, 2017.
[4] C. Stucley, S. Schuck, R. Sims, J. Bland, B. Marino, M. Borowitzka, A. Abadi, J. Bartle, R. Giles, Q. Thomas, Bioenergy in Australia, Status and Opportunities, in, 2012.
[5] H. Wu, Y. Yu, K. Yip, Bioslurry as a Fuel. 1. Viability of a Bioslurry-Based Bioenergy Supply Chain for Mallee Biomass in Western Australia, Energy & Fuels, 24 (2010) 5652-5659.
[6] J.R. Bartle, A. Abadi, Toward Sustainable Production of Second Generation Bioenergy Feedstocks†, Energy & Fuels, 24 (2010) 2-9.
[7] P. Gilbert, C. Ryu, V. Sharifi, J. Swithenbank, Tar reduction in pyrolysis vapours from biomass over a hot char bed, Bioresour Technol, 100 (2009) 6045-6051.
[8] J. Bartle, G. Olsen, D. Cooper, T. Hobbs, Scale of biomass production from new woody crops for salinity control in dryland agriculture in Australia, International Journal of Global Energy Issues, 27 (2007) 115.
[9] C.J. Clarke, R.J. George, R.W. Bell, T.J. Hatton, Dryland salinity in south-western Australia: its origins, remedies, and future research directions, Australian Journal of Soil Research, 40 (2002) 93-113.
[10] T. Phuphuakrat, N. Nipattummakul, T. Namioka, S. Kerdsuwan, K. Yoshikawa, Characterization of tar content in the syngas produced in a downdraft type fixed bed gasification system from dried sewage sludge, Fuel, 89 (2010) 2278-2284.
[11] D.M. Keown, J.-I. Hayashi, C.-Z. Li, Drastic changes in biomass char structure and reactivity upon contact with steam, Fuel, 87 (2008) 1127-1132.
[12] Y. Huang, X. Yin, C. Wu, C. Wang, J. Xie, Z. Zhou, L. Ma, H. Li, Effects of metal catalysts on CO2 gasification reactivity of biomass char, Biotechnol Adv, 27 (2009) 568-572.
[13] E. Byambajav, Y. Hachiyama, S. Kudo, K. Norinaga, J.-i. Hayashi, Kinetics and Mechanism of CO2 Gasification of Chars from 11 Mongolian Lignites, Energy & Fuels, 30 (2016) 1636-1646.
[14] R.T. Hamilton, D.A. Sams, F. Shadman, Variation of rate during potassium-catalysed CO2 gasification of coal char, Fuel, 63 (1984) 1008-1012.
[15] C.M. Kinoshita, Y. Wang, J. Zhou, Tar formation under different biomass gasification conditions, Journal of Analytical and Applied Pyrolysis, 29 (1994) 169-181.
[16] D.C. Elliott, E.G. Baker, The Effect of Catalysis on Wood-Gasification Tar Composition, Biomass, 9 (1986) 195-203.
[17] Y. Tursun, S. Xu, G. Wang, C. Wang, Y. Xiao, Tar formation during co-gasification of biomass and coal under different gasification condition, Journal of Analytical and Applied Pyrolysis, 111 (2015) 191-199.
[18] Y. Song, Y. Wang, X. Hu, S. Hu, J. Xiang, L. Zhang, S. Zhang, Z. Min, C.-Z. Li, Effects of volatile–char interactions on in situ destruction of nascent tar during the

pyrolysis and gasification of biomass. Part I. Roles of nascent char, Fuel, 122 (2014) 60-66.
[19] Y. Song, Y. Wang, X. Hu, J. Xiang, S. Hu, D. Mourant, T. Li, L. Wu, C.-Z. Li, Effects of volatile–char interactions on in-situ destruction of nascent tar during the pyrolysis and gasification of biomass. Part II. Roles of steam, Fuel, 143 (2015) 555-562.
[20] V. Nemanova, K. Engvall, Tar Variability in the Producer Gas in a Bubbling Fluidized Bed Gasification System, Energy & Fuels, 28 (2014) 7494-7500.
[21] C. Li, K. Suzuki, Tar property, analysis, reforming mechanism and model for biomass gasification—An overview, Renewable and Sustainable Energy Reviews, 13 (2009) 594-604.
[22] S. Anis, Z.A. Zainal, Tar reduction in biomass producer gas via mechanical, catalytic and thermal methods: A review, Renewable and Sustainable Energy Reviews, 15 (2011) 2355-2377.
[23] L. Dong, M. Asadullah, S. Zhang, X.-S. Wang, H. Wu, C.-Z. Li, An advanced biomass gasification technology with integrated catalytic hot gas cleaning, Fuel, 108 (2013) 409-416.
[24] H. Boerrigter, H. den Uil, Green Diesel from Biomass via Fischer-Tropsch Synthesis: New Insights in Gas Cleaning and Process Design, in: Pyrolysis and Gasification of Biomass and Waste, Strasbourg, France, 2002.
[25] H. Schulz, Short history and present trends of Fischer–Tropsch synthesis, Applied Catalysis A, 186 (1999) 3-12.
[26] X. Meng, W. de Jong, N. Fu, A.H.M. Verkooijen, Biomass gasification in a 100 kWth steam-oxygen blown circulating fluidized bed gasifier: Effects of operational conditions on product gas distribution and tar formation, Biomass and Bioenergy, 35 (2011) 2910-2924.
[27] M.K. Karmakar, J. Mandal, S. Haldar, P.K. Chatterjee, Investigation of fuel gas generation in a pilot scale fluidized bed autothermal gasifier using rice husk, Fuel, 111 (2013) 584-591.
[28] S. Kern, C. Pfeifer, H. Hofbauer, Gasification of wood in a dual fluidized bed gasifier: Influence of fuel feeding on process performance, Chemical Engineering Science, 90 (2013) 284-298.
[29] S. Rapagna, K. Gallucci, M. Di Marcello, M. Matt, M. Nacken, S. Heidenreich, P.U. Foscolo, Gas cleaning, gas conditioning and tar abatement by means of a catalytic filter candle in a biomass fluidized-bed gasifier, Bioresour Technol, 101 (2010) 7134-7141.
[30] Y.D. Kim, C.W. Yang, B.J. Kim, K.S. Kim, J.W. Lee, J.H. Moon, W. Yang, T.U. Yu, U.D. Lee, Air-blown gasification of woody biomass in a bubbling fluidized bed gasifier, Applied Energy, 112 (2013) 414-420.
[31] M. Asadullah, Biomass gasification gas cleaning for downstream applications: A comparative critical review, Renewable and Sustainable Energy Reviews, 40 (2014) 118-132.
[32] H. Zhao, D.J. Draelants, G.V. Baron, Performance of a Nickel-Activated Candle Filter for Naphthalene Cracking, Ind. Eng. Chem. Res., 39 (2000) 3195-3210.
[33] D. Sutton, B. Kelleher, J.R.H. Ross, Review of literature on catalysts for biomass catalysts, Fuel Processing Technology, 73 (2001) 155-173.
[34] S. Meyer, B. Glaser, P. Quicker, Technical, Economical, and Climate-Related Aspects of Biochar Production Technologies: A Literature Review, Environmental Science & Technology, 45 (2011) 9473-9483.

[35] K. Qian, A. Kumar, H. Zhang, D. Bellmer, R. Huhnke, Recent advances in utilization of biochar, Renewable and Sustainable Energy Reviews, 42 (2015) 1055-1064.
[36] Y. Shen, Chars as carbonaceous adsorbents/catalysts for tar elimination during biomass pyrolysis or gasification, Renewable and Sustainable Energy Reviews, 43 (2015) 281-295.
[37] Y. Shen, J. Wang, X. Ge, M. Chen, By-products recycling for syngas cleanup in biomass pyrolysis – An overview, Renewable and Sustainable Energy Reviews, 59 (2016) 1246-1268.
[38] H. Abdullah, H. Wu, Biochar as a Fuel: 1. Properties and Grindability of Biochars Produced from the Pyrolysis of Mallee Wood under Slow-Heating Conditions, Energy and Fuels, 23 (2009) 4174-4181.
[39] H. Abdullah, K.A. Mediaswanti, H. Wu, Biochar as a Fuel: 2. Significant Differences in Fuel Quality and Ash Properties of Biochars from Various Biomass Components of Mallee Trees, Energy & Fuels, 24 (2010) 1972-1979.
[40] K. Yip, M. Xu, C.-Z. Li, S.P. Jiang, H. Wu, Biochar as a Fuel: 3. Mechanistic Understanding on Biochar Thermal Annealing at Mild Temperatures and Its Effect on Biochar Reactivity, Energy & Fuels, 25 (2011) 406-414.
[41] X. Gao, H. Wu, Biochar as a Fuel: 4. Emission Behavior and Characteristics of PM1and PM10from the Combustion of Pulverized Biochar in a Drop-Tube Furnace, Energy & Fuels, 25 (2011) 2702-2710.
[42] S.B. Liaw, H. Wu, Leaching Characteristics of Organic and Inorganic Matter from Biomass by Water: Differences between Batch and Semi-continuous Operations, Industrial & Engineering Chemistry Research, 52 (2013) 4280-4289.
[43] B.M. Jenkins, R.R. Bakker, J.B. Wei, On the properties of washed straw, Biomass and Bioenergy, 10 (1996) 177-200.
[44] D.C. Dayton, B.M. Jenkins, S.Q. Turn, R.R. Bakker, R.B. Williams, D. Belle-Oudry, L.M. Hill, Release of Inorganic Constituents from Leached Biomass during Thermal Conversion, Energy & Fuels, 13 (1999) 860-870.
[45] P.A. Jensen, B. Sander, K. Dam-Johansen, Removal of K and Cl by leaching of straw char, Biomass and Bioenergy, 20 (2001) 447-457.
[46] K.O. Davidsson, J.G. Korsgren, J.B.C. Pettersson, U. Jaglid, The effects of fuel washing techniques on alkali release from biomass, Fuel, 81 (2002) 137-142.
[47] A.S. Basso, F.E. Miguez, D.A. Laird, R. Horton, M. Westgate, Assessing potential of biochar for increasing water-holding capacity of sandy soils, GCB Bioenergy, 5 (2013) 132-143.
[48] M. Inyang, B. Gao, P. Pullammanappallil, W. Ding, A.R. Zimmerman, Biochar from anaerobically digested sugarcane bagasse, Bioresour Technol, 101 (2010) 8868-8872.
[49] B. Singh, B.P. Singh, A.L. Cowie, Characterisation and evaluation of biochars for their application as a soil amendment, Australian Journal of Soil Research, 48 (2010) 516-525.
[50] M. Garcia-Perez, X.S. Wang, J. Shen, M.J. Rhodes, F. Tian, W.-J. Lee, H. Wu, C.-Z. Li, Fast Pyrolysis of Oil Mallee Woody Biomass: Effect of Temperature on the Yield and Quality of Pyrolysis Products, Ind. Eng. Chem. Res., 47 (2008) 1846-1854.
[51] J. Shen, X.-S. Wang, M. Garcia-Perez, D. Mourant, M.J. Rhodes, C.-Z. Li, Effects of particle size on the fast pyrolysis of oil mallee woody biomass, Fuel, 88 (2009) 1810-1817.
[52] D. Mohan, C.U. Pittman, P.H. Steele, Pyrolysis of Wood Biomass for Bio-oil: A Critical Review, Energy and Fuels, 20 (2006) 848-889.

[53] H. Abdullah, D. Mourant, C.-Z. Li, H. Wu, Bioslurry as a Fuel. 3. Fuel and Rheological Properties of Bioslurry Prepared from the Bio-oil and Biochar of Mallee Biomass Fast Pyrolysis, Energy Fuels, 24 (2010) 5669-5676.
[54] J. Yoder, S. Galinato, D. Granatstein, M. Garcia-Pérez, Economic tradeoff between biochar and bio-oil production via pyrolysis, Biomass and Bioenergy, 35 (2011) 1851-1862.
[55] M. Garcia-Perez, J. Shen, X.S. Wang, C.-Z. Li, Production and fuel properties of fast pyrolysis oil/bio-diesel blends, Fuel Processing Technology, 91 (2010) 296-305.
[56] R. Stanger, T. Wall, J. Lucas, M. Mahoney, Dynamic Elemental Thermal Analysis (DETA) – A characterisation technique for the production of biochar and bio-oil from biomass resources, Fuel, 108 (2013) 656-667.
[57] R. Stanger, W. Xie, T. Wall, J. Lucas, M. Mahoney, Dynamic Elemental Thermal Analysis: A technique for continuous measurement of carbon, hydrogen, oxygen chemistry of tar species evolved during coal pyrolysis, Fuel, 103 (2013) 764-772.
[58] D. Laird, The Charcoal Vision: A Win-Win-Win Scenario for Simultaneously Producing Bioenergy, Permanently Sequestering Carbon, while Improving Soil and Water Quality, Agronomy Journal, 100 (2008) 178-181.
[59] T.M. Abdel-Fattah, M.E. Mahmoud, S.B. Ahmed, M.D. Huff, J.W. Lee, S. Kumar, Biochar from woody biomass for removing metal contaminants and carbon sequestration, Journal of Industrial and Engineering Chemistry, 22 (2015) 103-109.
[60] J.H. Windeatt, A.B. Ross, P.T. Williams, P.M. Forster, M.A. Nahil, S. Singh, Characteristics of biochars from crop residues: Potential for carbon sequestration and soil amendment, Journal of Environmental Management, 146 (2014) 189-197.
[61] C.E. Brewer, R. Unger, K. Schmidt-Rohr, R.C. Brown, Criteria to Select Biochars for Field Studies based on Biochar Chemical Properties, BioEnergy Research, 4 (2011) 312-323.
[62] W.-Y. Chen, D.L. Mattern, E. Okinedo, J.C. Senter, A.A. Mattei, C.W. Redwine, Photochemical and acoustic interactions of biochar with CO2and H2O: Applications in power generation and CO2capture, AIChE Journal, 60 (2014) 1054-1065.
[63] J. Lehmann, A handful of carbon, Nature, 447 (2007) 143-144.
[64] N. Abdoulmoumine, S. Adhikari, A. Kulkarni, S. Chattanathan, A review on biomass gasification syngas cleanup, Applied Energy, 155 (2015) 294-307.
[65] C. Xu, J. Donald, E. Byambajav, Y. Ohtsuka, Recent advances in catalysts for hot-gas removal of tar and NH3 from biomass gasification, Fuel, 89 (2010) 1784-1795.
[66] Y. Richardson, J. Blin, A. Julbe, A short overview on purification and conditioning of syngas produced by biomass gasification: Catalytic strategies, process intensification and new concepts, Progress in Energy and Combustion Science, 38 (2012) 765-781.
[67] P.J. Woolcock, R.C. Brown, A review of cleaning technologies for biomass-derived syngas, Biomass and Bioenergy, 52 (2013) 54-84.
[68] R. Frazier, E. Jin, A. Kumar, Life Cycle Assessment of Biochar versus Metal Catalysts Used in Syngas Cleaning, Energies, 8 (2015) 621-644.
[69] P. McKendry, Energy production from biomass (part 1): overview of biomass, Bioresource Technology, 83 (2002) 37-46.
[70] P. McKendry, Energy production from biomass (part 2): conversion technologies, Bioresource Technology, 83 (2002) 47-54.
[71] W.G. Hohenstein, L.L. Wright, Biomass energy production in the United States: an overview, Biomass and Bioenergy, 6 (1994) 161-173.

[72] C. Wu, Z. Wang, L. Wang, J. Huang, P.T. Williams, Catalytic Steam Gasification of Biomass for a Sustainable Hydrogen Future: Influence of Catalyst Composition, Waste and Biomass Valorization, 5 (2013) 175-180.
[73] A. Demirbas, Effects of temperature and particle size on bio-char yield from pyrolysis of agricultural residues, Journal of Analytical and Applied Pyrolysis, 72 (2004) 243-248.
[74] E.N. Yargicoglu, B.Y. Sadasivam, K.R. Reddy, K. Spokas, Physical and chemical characterization of waste wood derived biochars, Waste Manag, 36 (2015) 256-268.
[75] C.D. Le, S.T. Kolaczkowski, Steam gasification of a refuse derived char: Reactivity and kinetics, Chemical Engineering Research and Design, 102 (2015) 389-398.
[76] G. Duman, M.A. Uddin, J. Yanik, Hydrogen production from algal biomass via steam gasification, Bioresour Technol, 166 (2014) 24-30.
[77] I.I. Ahmed, A.K. Gupta, Pyrolysis and gasification of food waste: Syngas characteristics and char gasification kinetics, Applied Energy, 87 (2010) 101-108.
[78] A.I. Casoni, M. Bidegain, M.A. Cubitto, N. Curvetto, M.A. Volpe, Pyrolysis of sunflower seed hulls for obtaining bio-oils, Bioresour Technol, 177 (2015) 406-409.
[79] H. Wu, Q. Fu, R. Giles, J. Bartle, Production of Mallee Biomass in Western Australia Energy Balance Analysis, Energy & Fuels, 22 (2008) 190-198.
[80] A.V. Bridgewater, The technical and economic feasibility of biomass gasification for power generation, Fuel, 74 (1994) 631-653.
[81] Z. Min, M. Asadullah, P. Yimsiri, S. Zhang, H. Wu, C.-Z. Li, Catalytic reforming of tar during gasification. Part I. Steam reforming of biomass tar using ilmenite as a catalyst, Fuel, 90 (2011) 1847-1854.
[82] H. Wu, K. Yip, Z. Kong, C.-Z. Li, D. Liu, Y. Yu, X. Gao, Removal and Recycling of Inherent Inorganic Nutrient Species in Mallee Biomass and Derived Biochars by Water Leaching, Industrial & Engineering Chemistry Research, 50 (2011) 12143-12151.
[83] A. Burton, H. Wu, Differences in Bed Agglomeration Behavior during the Fast Pyrolysis of Mallee Bark, Leaf, and Wood in a Fluidized-Bed Reactor at 500 °C, Energy Fuels, 29 (2015) 3753-3759.
[84] S. van Loo, J. Koppejan, Handbook of Biomass Combustion and Co-Firing, Twente University Press, Netherlands, 2002.
[85] D.A. Tillman, Biomass cofiring: the technology, the experience, the combustion consequences, Biomass and Bioenergy, 19 (2000) 365-384.
[86] T. Nussbaumer, Combustion and Co-combustion of Biomass: Fundamentals, Technologies, and Primary Measures for Emission Reduction, Energy & Fuels, 17 (2003) 1510-1521.
[87] C.R. Stucley, S.M. Schuck, R.E.H. Sims, P.L. Larsen, N.D. Turvey, B.E. Marino, Biomass Energy Production in Australia: Status, Costs and Opportunities for Major Technologies, in: A. Government (Ed.), Australian Government, 2004.
[88] P. Luckow, M.A. Wise, J.J. Dooley, S.H. Kim, Large-scale utilization of biomass energy and carbon dioxide capture and storage in the transport and electricity sectors under stringent CO2 concentration limit scenarios, International Journal of Greenhouse Gas Control, 4 (2010) 865-877.
[89] Biomass for Power Generation, in, International Renewable Energy Agency, 2012.
[90] R.M. Swanson, A. Platon, J.A. Satrio, R.C. Brown, Techno-economic analysis of biomass-to-liquids production based on gasification, Fuel, 89 (2010) S11-S19.

[91] S. Jones, P. Meyer, L. Snowden-Swan, A. Padmaperuma, E. Tan, A. Dutta, J. Jacobson, K. Cafferty, Process Design and Economics for the Conversion of Lignocellulosic Biomass to Hydrocarbon Fuels: Fast Pyrolysis and Hydrotreating Bio-oil Pathway, in, U.S. Department of Energy Bioenergy Technologies, 2013.
[92] M. Ringer, V. Putsche, J. Scahill, Large-Scale Pyrolysis Oil Production A Technology Assessment and Economic Analysis, in, National Renewable Energy Laboratory, 2006.
[93] I.A. Vasalos, A.A. Lappas, E.P. Kopalidou, K.G. Kalogiannis, Biomass catalytic pyrolysis: process design and economic analysis, Wiley Interdisciplinary Reviews: Energy and Environment, 5 (2016) 370-383.
[94] Y. Yu, J. Bartle, C.-Z. Li, H. Wu, Mallee Biomass as a Key Bioenergy Source in Western Australia: Importance of Biomass Supply Chain, Energy & Fuels, 23 (2009) 3290-3299.
[95] H. Wu, Y. Yu, K. Yip, Bioslurry as a Fuel. 1. Viability of a Bioslurry-Based Bioenergy Supply Chain for Mallee Biomass in Western Australia, Energy & Fuels, 24 (2010) 5652-5659.
[96] Z. Wang, F. Wang, J. Cao, J. Wang, Pyrolysis of pine wood in a slowly heating fixed-bed reactor: Potassium carbonate versus calcium hydroxide as a catalyst, Fuel Processing Technology, 91 (2010) 942-950.
[97] P. Morf, P. Hasler, T. Nussbaumer, Mechanisms and Kinetics of Homogeneous Secondary Reactions of Tar from Continuous Pyrolysis of Wood Chips, Fuel, 81 (2002) 843-853.
[98] A. Bridgwater, The Technical and Economic Feasibility of Biomass Gasification for Power Generation, Fuel, 74 (1995) 631-653.
[99] A. Veses, B. Puértolas, M.S. Callén, T. García, Catalytic upgrading of biomass derived pyrolysis vapors over metal-loaded ZSM-5 zeolites: Effect of different metal cations on the bio-oil final properties, Microporous and Mesoporous Materials, 209 (2015) 189-196.
[100] A. Bridgwater, Progress in Thermochemical Biomass Conversion, John Wiley and Sons, 2008.
[101] J.L. Zheng, M.Q. Zhu, J.L. Wen, R.C. Sun, Gasification of bio-oil: Effects of equivalence ratio and gasifying agents on product distribution and gasification efficiency, Bioresour Technol, 211 (2016) 164-172.
[102] J. Yao, J. Liu, H. Hofbauer, G. Chen, B. Yan, R. Shan, W. Li, Biomass to hydrogen-rich syngas via steam gasification of bio-oil/biochar slurry over LaCo1−xCuxO3 perovskite-type catalysts, Energy Conversion and Management, 117 (2016) 343-350.
[103] M. Latifi, F. Berruti, C. Briens, Thermal and catalytic gasification of bio-oils in the Jiggle Bed Reactor for syngas production, International Journal of Hydrogen Energy, 40 (2015) 5856-5868.
[104] H. Guo, F. Peng, H. Zhang, L. Xiong, S. Li, C. Wang, B. Wang, X. Chen, Y. Chen, Production of hydrogen rich bio-oil derived syngas from co-gasification of bio-oil and waste engine oil as feedstock for lower alcohols synthesis in two-stage bed reactor, International Journal of Hydrogen Energy, 39 (2014) 9200-9211.
[105] S. Ren, H. Lei, L. Wang, Q. Bu, S. Chen, J. Wu, Hydrocarbon and hydrogen-rich syngas production by biomass catalytic pyrolysis and bio-oil upgrading over biochar catalysts, RSC Advances, 4 (2014) 10731.
[106] J.R. Kastner, J. Miller, D.P. Geller, J. Locklin, L.H. Keith, T. Johnson, Catalytic esterification of fatty acids using solid acid catalysts generated from biochar and activated carbon, Catalysis Today, 190 (2012) 122-132.

[107] A.M. Dehkhoda, A.H. West, N. Ellis, Biochar based solid acid catalyst for biodiesel production, Applied Catalysis A: General, 382 (2010) 197-204.
[108] R. Ormsby, J.R. Kastner, J. Miller, Hemicellulose hydrolysis using solid acid catalysts generated from biochar, Catalysis Today, 190 (2012) 89-97.
[109] Y. Yu, H. Wu, Bioslurry as a Fuel. 2. Life-Cycle Energy and Carbon Footprints of Bioslurry Fuels from Mallee Biomass in Western Australia, Energy & Fuels, 24 (2010) 5660-5668.
[110] H. Abdullah, H. Wu, Bioslurry as a Fuel. 4. Preparation of Bioslurry Fuels from Biochar and the Bio-oil-Rich Fractions after Bio-oil/Biodiesel Extraction, Energy & Fuels, 25 (2011) 1759-1771.
[111] M. Zhang, X. Gao, H. Wu, A Method for the Quantification of Alkali and Alkaline Earth Metallic Species in Bioslurry Fuels, Energy & Fuels, 27 (2013) 6823-6830.
[112] M. Zhang, H. Wu, Bioslurry as a Fuel. 6. Leaching Characteristics of Alkali and Alkaline Earth Metallic Species from Biochar by Bio-oil Model Compounds, Energy & Fuels, 29 (2015) 2535-2541.
[113] M.H. Ghezelchi, M. Garcia-Perez, H. Wu, Bioslurry as a Fuel. 7: Spray Characteristics of Bio-Oil and Bioslurry via Impact and Twin-Fluid Atomizers, Energy & Fuels, 29 (2015) 8058-8065.
[114] J.M. Encinar, J.F. Gonzalez, J.J. Rodriguez, M.J. Ramiro, Catalysed and Uncatalysed Steam Gasification of Eucalyptus Char: Influence of Variables and Kinetic Study, Fuel, 80 (2001) 2025-2036.
[115] K. Yip, F. Tian, J.-i. Hayashi, H. Wu, Effect of Alkali and Alkaline Earth Metallic Species on Biochar Reactivity and Syngas Composition During Syngas Gasification, Energy & Fuels, 24 (2010) 173-181.
[116] E. Cetin, B. Moghtaderi, R. Gupta, T.F. Wall, Influence of pyrolysis conditions on the structure and gasification reactivity of biomass chars, Fuel, 83 (2004) 2139-2150.
[117] S. Kudo, Y. Hachiyama, H.-S. Kim, K. Norinaga, J.-i. Hayashi, Examination of Kinetics of Non-catalytic Steam Gasification of Biomass/Lignite Chars and Its Relationship with the Variation of the Pore Structure, Energy & Fuels, 28 (2014) 5902-5908.
[118] J.J. Manya, Pyrolysis for biochar purposes: a review to establish current knowledge gaps and research needs, Environ Sci Technol, 46 (2012) 7939-7954.
[119] A. Demirbas, Production and Characterization of Bio-Chars from Biomass via Pyrolysis, Energy Sources, Part A: Recovery, Utilization, and Environmental Effects, 28 (2006) 413-422.
[120] K.Y. Chan, L. Van Zwieten, I. Meszaros, A. Downie, S. Joseph, Agronomic values of greenwaste biochar as a soil amendment, Australian Journal of Soil Research, 45 (2007) 629.
[121] J. Lehmann, S. Joseph, Biochar for Environmental Management, Taylor and Francis, London, UNITED STATES, 2012.
[122] K.A. Spokas, Review of the stability of biochar in soils: predictability of O:C molar ratios, Carbon Management, 1 (2014) 289-303.
[123] T. Xie, B.Y. Sadasivam, K.R. Reddy, C. Wang, K.A. Spokas, Review of the Effects of Biochar Amendment on Soil Properites and Carbon Sequestration, Journal of Hazardous, Toxic, and Radiactive Waste, 20 (2016).
[124] V. Hansen, D. Müller-Stöver, J. Ahrenfeldt, J.K. Holm, U.B. Henriksen, H. Hauggaard-Nielsen, Gasification biochar as a valuable by-product for carbon sequestration and soil amendment, Biomass and Bioenergy, 72 (2015) 300-308.

[125] J. Lehmann, J. Gaunt, M. Rondon, Bio-char Sequestration in Terrestrial Ecosystems – A Review, Mitigation and Adaptation Strategies for Global Change, 11 (2006) 395-419.
[126] R. Renner, Rethinking Biochar, Environmental Science and Technology, 41 (2007) 5932-5933.
[127] M.K. Awasthi, M. Wang, H. Chen, Q. Wang, J. Zhao, X. Ren, D.-s. Li, S.K. Awasthi, F. Shen, R. Li, Z. Zhang, Heterogeneity of biochar amendment to improve the carbon and nitrogen sequestration through the greenhouse gases emissions during sewage sludge composting, Bioresource Technology, 224 (2017) 428-438.
[128] S. Nanda, A.K. Dalai, F. Berruti, J.A. Kozinski, Biochar as an Exceptional Bioresource for Energy, Agronomy, Carbon Sequestration, Activated Carbon and Specialty Materials, Waste and Biomass Valorization, 7 (2015) 201-235.
[129] A. Belay, A.S. Claassens, F. Wehner, Effect of direct nitrogen and potassium and residual phosphorus fertilizers on soil chemical properties, microbial components and maize yield under long-term crop rotation, Biology and Fertility of Soils, 35 (2002) 420-427.
[130] S. Goyal, K. Chander, M.C. Mundra, K.K. Kapoor, Influence of inorganic fertilizers and organic amendment on soil organic matter and soil mirobial properties under tropical conditions, Biol Fertil Soils, 29 (1999) 196-200.
[131] S. Marinari, G. Masciandaro, B. Ceccanti, S. Grego, Influence of organic and mineral fertilisers on soil biological and physical properties, Bioresource Technology, 72 (2000) 9-17.
[132] J.W. Gaskin, C. Steiner, K. Harris, K.C. Das, B. Bibens, Effect of low-temperature pyolysis conditions on biochar for agricultural use, American Society of Agricultural and Biological Engineers, 51 (2008) 2061-2069.
[133] L.R. Bulluck III, M. Brosius, G.K. Evanylo, J.B. Ristaino, Organic and synthetic fertility amendments influence soil microbial, physical and chemical properties on organic and conventional farms, Applied Soil Ecology, 19 (2002) 147-160.
[134] J. Major, M. Rondon, D. Molina, S.J. Riha, J. Lehmann, Maize yield and nutrition during 4 years after biochar application to a Colombian savanna oxisol, Plant and Soil, 333 (2010) 117-128.
[135] Z. Kong, S.B. Liaw, X. Gao, Y. Yu, H. Wu, Leaching characteristics of inherent inorganic nutrients in biochars from the slow and fast pyrolysis of mallee biomass, Fuel, 128 (2014) 433-441.
[136] S.B. Liaw, H. Wu, Tuning Biochar Properties via Partial Gasification: Facilitating Inorganic Nutrients Recycling and Altering Organic Matter Leaching, Energy & Fuels, 29 (2015) 4407-4417.
[137] J.M. Novak, W.J. Busscher, D.L. Laird, M. Ahmedna, D.W. Watts, M.A.S. Niandou, Impact of Biochar Amendment on Fertility of a Southeastern Coastal Plain Soil, Soil Science, 174 (2009) 105-112.
[138] Ravindra, A.K. Mittal, R. Van Grieken, Health Risk Assessment of Urban Suspended Particulate Matter with Special Reference to Polycyclic Aromatic Hydrocarbons: A Review, in: Reviews on Environmental Health, 2001, pp. 169.
[139] L. Zhao, X. Cao, W. Zheng, Q. Wang, F. Yang, Endogenous minerals have influences on surface electrochemistry and ion exchange properties of biochar, Chemosphere, 136 (2015) 133-139.
[140] A. Mukherjee, A.R. Zimmerman, W. Harris, Surface chemistry variations among a series of laboratory-produced biochars, Geoderma, 163 (2011) 247-255.
[141] J.W. Lee, A.C. Buchanan, B.R. Evans, M. Kidder, Oxygenation of Biochar for Enhanced Cation Exchange Capacity, (2013) 35-45.

[142] J.H. Yuan, R.K. Xu, H. Zhang, The forms of alkalis in the biochar produced from crop residues at different temperatures, Bioresour Technol, 102 (2011) 3488-3497.
[143] J.W. Lee, M. Kidder, B.R. Evans, S. Paik, A.C. Buchanan, C.T. Garten, R.C. Brown, Characterization of Biochars Produced from Cornstovers for Soil Amendment, Environmental Science and Technology, 44 (2010) 7970-7974.
[144] M. Lawrinenko, D.A. Laird, Anion exchange capacity of biochar, Green Chem., 17 (2015) 4628-4636.
[145] B.A. Mohamed, N. Ellis, C.S. Kim, X. Bi, R. Emam Ael, Engineered biochar from microwave-assisted catalytic pyrolysis of switchgrass for increasing water-holding capacity and fertility of sandy soil, Sci Total Environ, 566-567 (2016) 387-397.
[146] J. Zhang, C. You, Water Holding Capacity and Absorption Properties of Wood Chars, Energy & Fuels, 27 (2013) 2643-2648.
[147] S. Ismadji, Y. Sudaryanto, S.B. Hartono, L.E. Setiawan, A. Ayucitra, Activated carbon from char obtained from vacuum pyrolysis of teak sawdust: pore structure development and characterization, Bioresour Technol, 96 (2005) 1364-1369.
[148] J. Pastor-Villegas, J.M. Meneses Rodríguez, J.F. Pastor-Valle, J. Rouquerol, R. Denoyel, M. García García, Adsorption–desorption of water vapour on chars prepared from commercial wood charcoals, in relation to their chemical composition, surface chemistry and pore structure, Journal of Analytical and Applied Pyrolysis, 88 (2010) 124-133.
[149] P. Basu, Chapter 7 - Gasification Theory, in: Biomass Gasification, Pyrolysis and Torrefaction (Second Edition), Academic Press, Boston, 2013, pp. 199-248.
[150] P. Basu, Chapter 11 - Production of Synthetic Fuels and Chemicals from Biomass, in: Biomass Gasification, Pyrolysis and Torrefaction (Second Edition), Academic Press, Boston, 2013, pp. 375-404.
[151] S. Hosokai, K. Norinaga, T. Kimura, M. Nakano, C.-Z. Li, J.-i. Hayashi, Reforming of Volatiles from the Biomass Pyrolysis over Charcoal in a Sequence of Coke Deposition and Steam Gasification of Coke, Energy & Fuels, 25 (2011) 5387-5393.
[152] K. Engvall, T. Liliedahl, Biomass and black liquor gasification, in: Technologies for Converting Biomass to Useful Energy, CRC Press, 2013, pp. 175-216.
[153] T. Hanaoka, S. Inoue, S. Uno, T. Ogi, T. Minowa, Effect of woody biomass components on air-steam gasification, Biomass and Bioenergy, 28 (2005) 69-76.
[154] P. Ji, W. Feng, B. Chen, Production of ultrapure hydrogen from biomass gasification with air, Chemical Engineering Science, 64 (2009) 582-592.
[155] A. Sharma, A. Matsumura, T. Takanohashi, Effect of CO2 addition on gas composition of synthesis gas from catalytic gasification of low rank coals, Fuel, 152 (2015) 13-18.
[156] G. Wang, J. Zhang, X. Hou, J. Shao, W. Geng, Study on CO(2) gasification properties and kinetics of biomass chars and anthracite char, Bioresour Technol, 177 (2015) 66-73.
[157] K. Umeki, K. Yamamoto, T. Namioka, K. Yoshikawa, High temperature steam-only gasification of woody biomass, Applied Energy, 87 (2010) 791-798.
[158] L. Bai, Karnowo, S. Kudo, K. Norinaga, Y.-g. Wang, J.-i. Hayashi, Kinetics and Mechanism of Steam Gasification of Char from Hydrothermally Treated Woody Biomass, Energy & Fuels, 28 (2014) 7133-7139.

[159] A. Kumar, D.D. Jones, M.A. Hanna, Thermochemical Biomass Gasification: A Review of the Current Status of the Technology, Energies, 2 (2009) 556-581.
[160] J.T. Shaw, Coal combustion and gasification, Chemical Engineering Science, 41 (1986) 3235.
[161] H. Marsh, D.W. Taylor, Carbon gasification in the Boudouard reaction, Fuel, 54 (1975) 218-219.
[162] R.T. Yang, R.Z. Duan, Kinetics and mechanism of gas-carbon reactions: conformation of etch pits, hydrogen inhibition and anisotropy in reactivity, Carbon, 23 (1985) 325-331.
[163] K.J. Huttinger, Mechanism of water vapor gasification at high hydrogen levels, Carbon, 26 (1988) 79-87.
[164] M.G. Lussier, Z. Zhang, D.J. Miller, Characterizing rate inhibtion in steam/hydrogen gasification via analysis of adsorbed hydrogen, Carbon, 36 (1998) 1361-1369.
[165] M. Kajita, T. Kimura, K. Norinaga, C.-Z. Li, J.-i. Hayashi, Catalytic and Noncatalytic Mechanisms in Steam Gasification of Char from the Pyrolysis of Biomass†, Energy & Fuels, 24 (2010) 108-116.
[166] B. Bayarsaikhan, N. Sonoyama, S. Hosokai, T. Shimada, J.-i. Hayashi, C.-Z. Li, T. Chiba, Inhibition of steam gasification of char by volatiles in a fluidized bed under continuous feeding of a brown coal, Fuel, 85 (2006) 340-349.
[167] P. Basu, Chapter 8 - Design of Biomass Gasifiers, in: Biomass Gasification, Pyrolysis and Torrefaction (Second Edition), Academic Press, Boston, 2013, pp. 249-313.
[168] C. Di Blasi, C. Branca, G. D'Errico, Degradation characteristics of straw and washed straw, Thermochimica Acta, 364 (2000) 133-142.
[169] N.R. Amundson, L.E. Arri, Char Gasification in a Countercurrent Reactor, AIChE Journal, 24 (1978) 87-100.
[170] A. Gómez-Barea, P. Ollero, B. Leckner, Optimization of char and tar conversion in fluidized bed biomass gasifiers, Fuel, 103 (2013) 42-52.
[171] Q. Miao, J. Zhu, S. Barghi, C. Wu, X. Yin, Z. Zhou, Model validation of a CFB biomass gasification model, Renewable Energy, 63 (2014) 317-323.
[172] Q. Miao, J. Zhu, S. Barghi, C. Wu, X. Yin, Z. Zhou, Modeling biomass gasification in circulating fluidized beds, Renewable Energy, 50 (2013) 655-661.
[173] M. Asadullah, T. Miyazawa, S.-i. Ito, K. Kunimori, M. Yamada, K. Tomishige, Catalyst development for the gasification of biomass in the dual-bed gasifier, Applied Catalysis A: General, 255 (2003) 169-180.
[174] P. Brandt, E. Larsen, U. Henriksen, High Tar Reduction in a Two-Stage Gasifier, Energy and Fuels, 14 (2000) 816-819.
[175] K. Göransson, U. Söderlind, T. Henschel, P. Engstrand, W. Zhang, Internal tar/CH4 reforming in a biomass dual fluidised bed gasifier, Biomass Conversion and Biorefinery, 5 (2014) 355-366.
[176] J. Gil, J. Corella, M.P. Aznar, M.A. Caballero, Biomass gasification in atmospheric and bubbling fluidized bed: Effect of the type of gasifying agent on the product distribution, Biomass and Bioenergy, 17 (1999) 389-403.
[177] A. Gómez-Barea, B. Leckner, Estimation of gas composition and char conversion in a fluidized bed biomass gasifier, Fuel, 107 (2013) 419-431.
[178] D. Tapasvi, R.S. Kempegowda, K.-Q. Tran, Ø. Skreiberg, M. Grønli, A simulation study on the torrefied biomass gasification, Energy Conversion and Management, 90 (2015) 446-457.

[179] H. Noubli, S. Valin, B. Spindler, M. Hemati, Development of a modelling tool representing biomass gasification step in a dual fluidized bed, The Canadian Journal of Chemical Engineering, 93 (2015) 340-347.
[180] A. Gomez-Barea, B. Leckner, Gasification of Biomass in Fluidised Bed: Review of Modelling, in: 20th International Conference on Fluidized Bed Combustion, 2009.
[181] D. Neogi, C.C. Chang, W.P. Walawender, L.T. Fan, Study of Coal Gasification in an Experimental Fluidized Bed Reactor, AIChE Journal, 32 (1986) 17-28.
[182] G. Chen, H. Spliethoff, J. Andries, M.P. Glazer, L.B. Yang, Biomass Gasification in a Circulating Fluidised Bed- Part I: Preliminary Experiments and Modelling Development, Energy Sources, 26 (2004) 485-498.
[183] J. Billaud, S. Valin, M. Peyrot, S. Salvador, Influence of H2O, CO2 and O2 addition on biomass gasification in entrained flow reactor conditions: Experiments and modelling, Fuel, 166 (2016) 166-178.
[184] H. Wu, X. Li, J.-i. Hayashi, T. Chiba, C.-Z. Li, Effects of volatile–char interactions on the reactivity of chars from NaCl-loaded Loy Yang brown coal, Fuel, 84 (2005) 1221-1228.
[185] D.M. Keown, J.-i. Hayashi, C.-Z. Li, Effects of volatile–char interactions on the volatilisation of alkali and alkaline earth metallic species during the pyrolysis of biomass, Fuel, 87 (2008) 1187-1194.
[186] C. Franco, F. Pinto, I. Gulyurtlu, I. Cabrita, The study of reactions influencing the biomass steam gasification process, Fuel, 82 (2003) 835-842.
[187] M. Mayerhofer, S. Fendt, H. Spliethoff, M. Gaderer, Fluidized bed gasification of biomass – In bed investigation of gas and tar formation, Fuel, 117 (2014) 1248-1255.
[188] A. Orio, J. Corella, I. Narvaez, Characterisation and activity of different dolomites for hot gas cleaning in biomass gasification, in: Proceedings of Conference on Developments in Thermochemical Biomass Conversion, Banff, Canada, 1996, pp. 1144.
[189] J. Delgado, M.P. Aznar, J. Corella, Biomass Gasification with Steam in Fluidized Bed: Effectiveness of CaO, MgO, and CaO−MgO for Hot Raw Gas Cleaning, Industrial & Engineering Chemistry Research, 36 (1997) 1535-1543.
[190] E.G. Baker, L.K. Mudge, Mechanisms of Catalytic Biomass Gasification, Journal of Analytical and Applied Pyrolysis, 6 (1984) 285-297.
[191] A.I. Paksoy, B.S. Caglayan, A.E. Aksoylu, A study on characterization and methane dry reforming performance of Co–Ce/ZrO2 catalyst, Applied Catalysis B: Environmental, 168-169 (2015) 164-174.
[192] H.-S. Kim, S. Kudo, K. Tahara, Y. Hachiyama, H. Yang, K. Norinaga, J.-i. Hayashi, Detailed Kinetic Analysis and Modeling of Steam Gasification of Char from Ca-Loaded Lignite, Energy & Fuels, 27 (2013) 6617-6631.
[193] T. Kitsuka, B. Bayarsaikhan, N. Sonoyama, S. Hosokai, C.-Z. Li, K. Norinaga, J.-i. Hayashi, Behavior of Inherent Metallic Species as a Crucial Factor for Kinetics of Steam Gasification of Char from Coal Pyrolysis, Energy & Fuels, 21 (2007) 387-394.
[194] L.-x. Zhang, S. Kudo, N. Tsubouchi, J.-i. Hayashi, Y. Ohtsuka, K. Norinaga, Catalytic effects of Na and Ca from inexpensive materials on in-situ steam gasification of char from rapid pyrolysis of low rank coal in a drop-tube reactor, Fuel Processing Technology, 113 (2013) 1-7.
[195] D.C. Elliott, R.T. Hallen, J. Sealock Jr., Alkali Catalysis in Biomass Gasification, Journal of Analytical and Applied Pyrolysis, 6 (1984) 299-316.
[196] L.K. Mudge, J. Sealock Jr., S.L. Weber, Catalyzed Steam Gasification of Biomass, Journal of Analytical and Applied Pyrolysis, 1 (1979) 165-175.

[197] M.G. Dastidar, M.K. Sarkar, A Kinetics Study on Catalytic and Non-Catalytic Steam GAsification of Biomass, Fuel Processing Technology, 7 (1983) 261-275.
[198] C. Font Palma, Modelling of tar formation and evolution for biomass gasification: A review, Applied Energy, 111 (2013) 129-141.
[199] J.R. Kastner, S. Mani, A. Juneja, Catalytic decomposition of tar using iron supported biochar, Fuel Processing Technology, 130 (2015) 31-37.
[200] P. McKendry, Energy production from biomass (part 3): gasification technologies, Bioresource Technology, 83 (2002) 55-63.
[201] M.A. Paisley, D. Anson, Biomass Gasification for Gas Turbine Based Power Generation, (1997) V002T005A002.
[202] Basic Considerations, in: Gas Turbine Combustion, CRC Press, 2010, pp. 1-33.
[203] L. Devi, K.J. Ptasinski, F.J.J.G. Janssen, A review of the primary measures for tar elimination in biomass gasification processes, Biomass and Bioenergy, 24 (2003) 125-140.
[204] R. Guan, W. Li, H. Chen, B. Li, The release of nitrogen species during pyrolysis of model chars loaded with different additives, Fuel Processing Technology, 85 (2004) 1025-1037.
[205] M.U. Rahim, X. Gao, H. Wu, A Method for the Quantification of Chlorine in Low-Rank Solid Fuels, Energy & Fuels, 27 (2013) 6992-6999.
[206] J.N. Knudsen, P.A. Jensen, K. Dam-Johansen, Transformation and Release to the Gas Phase of Cl, K, and S during Combustion of Annual Biomass, Energy & Fuels, 18 (2004) 1385-1399.
[207] Z. Min, J.-Y. Lin, P. Yimsiri, M. Asadullah, C.-Z. Li, Catalytic reforming of tar during gasification. Part V. Decomposition of NOx precursors on the char-supported iron catalyst, Fuel, 116 (2014) 19-24.
[208] M.U. Rahim, X. Gao, M. Garcia-Perez, Y. Li, H. Wu, Release of Chlorine during Mallee Bark Pyrolysis, Energy & Fuels, 27 (2013) 310-317.
[209] T. Valmari, T.M. Lind, E.I. Kauppinen, G. Sfiris, K. Nilsson, W. Maenhaut, Field Study on Ash Behavior during Circulating Fluidized-Bed Combustion of Biomass. 1. Ash Formation, Energy & Fuels, 13 (1999) 379-389.
[210] T. Valmari, T.M. Lind, E.I. Kauppinen, G. Sfiris, K. Nilsson, W. Maenhaut, Field Study on Ash Behavior during Circulating Fluidized-Bed Combustion of Biomass. 2. Ash Deposition and Alkali Vapor Condensation, Energy & Fuels, 13 (1999) 390-395.
[211] J.N. Harb, E.E. Smith, Fireside corrosion in pc-fired boilers, Progress in Energy and Combustion Science, 16 (1990) 169-190.
[212] D.M. Quyn, H. Wu, C.-Z. Li, Volatilisation and catalytic effects of alkali and alkaline earth metallic species during the pyrolysis and gasification of Victorian brown coal. Part I. Volatilisation of Na and Cl from a set of NaCl-loaded samples, Fuel, 81 (2002) 143-149.
[213] H. Wu, D.M. Quyn, C.-Z. Li, Volatilisation and catalytic effects of alkali and alkaline earth metallic species during the pyrolysis and gasification of Victorian brown coal. Part III. The importance of the interactions between volatiles and char at high temperature, Fuel, 81 (2002) 1033-1039.
[214] H. Wu, D.M. Quyn, C.-Z. Li, Volatilisation and Catalytic Effects of Alkali and Alkaline Earth Metallic Species during the Pyrolysis and Gasification of Victorian Brown Coals Part III. The Importance of the Interactions between Volatiles and Char at High Temperature, Fuel, 81 (2002) 1033-1039.
[215] D.M. Quyn, H. Wu, J.-i. Hayashi, C.-Z. Li, Volatilisation and Catalytic Effects of Alkali and Alkaline Earth Metallic Species during the Pyrolysis and Gasification of

Victorian Brown Coals Part IV. Catalytic Effects of NaCl and Ion-Exchangable Na in Coal on Char Reactivity, Fuel, 82 (2003) 587-593.
[216] H. Wu, J.-i. Hayashi, T. Chiba, T. Takarada, C.-Z. Li, Volatilisation and catalytic effects of alkali and alkaline earth metallic species during the pyrolysis and gasification of Victorian brown coal. Part V. Combined effects of Na concentration and char structure on char reactivity, Fuel, 83 (2004) 23-30.
[217] X. Li, H. Wu, J.-i. Hayashi, C.-Z. Li, Volatilisation and catalytic effects of alkali and alkaline earth metallic species during the pyrolysis and gasification of Victorian brown coal. Part VI. Further investigation into the effects of volatile-char interactions, Fuel, 83 (2004) 1273-1279.
[218] X. Li, J. Hayashi, C. Li, Volatilisation and catalytic effects of alkali and alkaline earth metallic species during the pyrolysis and gasification of Victorian brown coal. Part VII. Raman spectroscopic study on the changes in char structure during the catalytic gasification in air, Fuel, 85 (2006) 1509-1517.
[219] X. Li, C. Li, Volatilisation and catalytic effects of alkali and alkaline earth metallic species during the pyrolysis and gasification of Victorian brown coal. Part VIII. Catalysis and changes in char structure during gasification in steam, Fuel, 85 (2006) 1518-1525.
[220] S. Zhang, J.-i. Hayashi, C.-Z. Li, Volatilisation and catalytic effects of alkali and alkaline earth metallic species during the pyrolysis and gasification of Victorian brown coal. Part IX. Effects of volatile-char interactions on char–H2O and char–O2 reactivities, Fuel, 90 (2011) 1655-1661.
[221] D.M. Quyn, J.-i. Hayashi, C.-Z. Li, Volatilisation of alkali and alkaline earth metallic species during the gasification of a Victorian brown coal in CO2, Fuel Processing Technology, 86 (2005) 1241-1251.
[222] C. Sathe, J.-i. Hayashi, C.-Z. Li, T. Chiba, Release of alkali and alkaline earth metallic species during rapid pyrolysis of a Victorian brown coal at elevated pressures ☆, Fuel, 82 (2003) 1491-1497.
[223] C.-Z. Li, C. Sathe, J.R. Kershaw, Y. Pang, Fates and roles of alkali and alkaline earth metals during the pyrolysis of a Victorian brown coal, Fuel, 79 (200) 427-438.
[224] A. Reza Manzoori, P.K. Agarwal, The fate of organically bound inorganic elements and sodium chloride during fluidized bed combustion of high sodium, high sulphur low rank coals, Fuel, 71 (1991) 513-522.
[225] M.P. Aznar, M.A. Caballero, J. Gil, J.A. Martín, J. Corella, Commercial Steam Reforming Catalysts To Improve Biomass Gasification with Steam−Oxygen Mixtures. 2. Catalytic Tar Removal, Industrial & Engineering Chemistry Research, 37 (1998) 2668-2680.
[226] Z. Abu El-Rub, E.A. Bramer, G. Brem, Experimental comparison of biomass chars with other catalysts for tar reduction, Fuel, 87 (2008) 2243-2252.
[227] R. Coll, J. Salvadó, X. Farriol, D. Montané, Steam reforming model compounds of biomass gasification tars: conversion at different operating conditions and tendency towards coke formation, Fuel Processing Technology, 74 (2001) 19-31.
[228] J. Ashok, Y. Kathiraser, M.L. Ang, S. Kawi, Bi-functional hydrotalcite-derived NiO–CaO–Al2O3 catalysts for steam reforming of biomass and/or tar model compound at low steam-to-carbon conditions, Applied Catalysis B: Environmental, 172-173 (2015) 116-128.
[229] B. Dou, J. Gao, X. Sha, S.W. Baek, Catalytic cracking of tar component from high-temperature fuel gas, Applied Thermal Engineering, 23 (2003) 2229-2239.

[230] R. Zhang, R.C. Brown, A. Suby, K. Cummer, Catalytic destruction of tar in biomass derived producer gas, Energy Conversion and Management, 45 (2004) 995-1014.
[231] P. Simell, E. Kurkela, P. Stahlberg, J. Hepola, Catalytic hot gas cleaning of gasification gas, Catalysis Today, 27 (1996) 52-62.
[232] M. Koike, C. Ishikawa, D. Li, L. Wang, Y. Nakagawa, K. Tomishige, Catalytic performance of manganese-promoted nickel catalysts for the steam reforming of tar from biomass pyrolysis to synthesis gas, Fuel, 103 (2013) 122-129.
[233] A. Jess, Catalytic upgrading of tarry fuel gases: A kinetic study with model components, Chemical Engineering and Processing, 35 (1996) 487-494.
[234] T. Furusawa, A. Tsutsumi, Comparison of Co/MgO and Ni/MgO catalysts for the steam reforming of naphthalene as a model compound of tar derived from biomass gasification, Applied Catalysis A: General, 278 (2005) 207-212.
[235] C. Pfeifer, H. Hofbauer, Development of catalytic tar decomposition downstream from a dual fluidized bed biomass steam gasifier, Powder Technology, 180 (2008) 9-16.
[236] N. Laosiripojana, W. Sutthisripok, S. Charojrochkul, S. Assabumrungrat, Development of Ni–Fe bimetallic based catalysts for biomass tar cracking/reforming: Effects of catalyst support and co-fed reactants on tar conversion characteristics, Fuel Processing Technology, 127 (2014) 26-32.
[237] C. Pfeifer, R. Rauch, H. Hofbauer, In-Bed Catalytic Tar Reduction in a Dual Fluidized Bed Biomass Steam Gasifier, Ind. Eng. Chem. Res., 43 (2004) 1643-1640.
[238] G. Oh, S.Y. Park, M.W. Seo, Y.K. Kim, H.W. Ra, J.-G. Lee, S.J. Yoon, Ni/Ru–Mn/Al2O3 catalysts for steam reforming of toluene as model biomass tar, Renewable Energy, 86 (2016) 841-847.
[239] A. Di Carlo, D. Borello, M. Sisinni, E. Savuto, P. Venturini, E. Bocci, K. Kuramoto, Reforming of tar contained in a raw fuel gas from biomass gasification using nickel-mayenite catalyst, International Journal of Hydrogen Energy, 40 (2015) 9088-9095.
[240] J. Ashok, S. Kawi, Steam reforming of biomass tar model compound at relatively low steam-to-carbon condition over CaO-doped nickel–iron alloy supported over iron–alumina catalysts, Applied Catalysis A: General, 490 (2015) 24-35.
[241] F.M. Josuinkas, C.P.B. Quitete, N.F.P. Ribeiro, M.M.V.M. Souza, Steam reforming of model gasification tar compounds over nickel catalysts prepared from hydrotalcite precursors, Fuel Processing Technology, 121 (2014) 76-82.
[242] D. Świerczyński, S. Libs, C. Courson, A. Kiennemann, Steam reforming of tar from a biomass gasification process over Ni/olivine catalyst using toluene as a model compound, Applied Catalysis B: Environmental, 74 (2007) 211-222.
[243] B. Zhao, X. Zhang, L. Chen, R. Qu, G. Meng, X. Yi, L. Sun, Steam reforming of toluene as model compound of biomass pyrolysis tar for hydrogen, Biomass and Bioenergy, 34 (2010) 140-144.
[244] M. Azharuddin, H. Tsuda, S. Wu, E. Sasaoka, Catalytic decomposition of biomass tars with iron oxide catalysts, Fuel, 87 (2008) 451-459.
[245] T. Nordgreen, T. Liliedahl, K. Sjostrom, Metallic iron as a tar breakdown catalyst related to atmospheric, fluidised bed gasification of biomass, Fuel, 85 (2006) 689-694.
[246] L. Devi, K.J. Ptasinski, F.J.J.G. Janssen, Pretreated olivine as tar removal catalyst for biomass gasifiers: investigation using naphthalene as model biomass tar, Fuel Processing Technology, 86 (2005) 707-730.

[247] A. Larsson, M. Israelsson, F. Lind, M. Seemann, H. Thunman, Using Ilmenite To Reduce the Tar Yield in a Dual Fluidized Bed Gasification System, Energy & Fuels, 28 (2014) 2632-2644.
[248] C. Christodoulou, D. Grimekis, K.D. Panopoulos, E.P. Pachatouridou, E.F. Iliopoulou, E. Kakaras, Comparing calcined and un-treated olivine as bed materials for tar reduction in fluidized bed gasification, Fuel Processing Technology, 124 (2014) 275-285.
[249] J. Delgado, M.P. Aznar, J. Corella, Calcined Dolomite, Magnesite, and Calcite for Cleaning Hot Gas from a Fluidized Bed Biomass Gasifier with Steam: Life and Usefulness, Ind. Eng. Chem. Res., 35 (1996) 3637-3643.
[250] L. Devi, K.J. Ptasinski, F.J.J.G. Janssen, S.V.B. van Paasen, P.C.A. Bergman, J.H.A. Kiel, Catalytic decomposition of biomass tars: use of dolomite and untreated olivine, Renewable Energy, 30 (2005) 565-587.
[251] P. Simell, J. Leppalahti, J. Brendenberg, Catalytic purification of tarry fuel gas with carbonate rock and ferrous materials, Fuel, 71 (1991) 211-218.
[252] Q.Z. Yu, C. Brage, T. Nordgreen, K. Sjöström, Effects of Chinese dolomites on tar cracking in gasification of birch, Fuel, 88 (2009) 1922-1926.
[253] T. Furusawa, A. Tsutsumi, Development of cobalt catalysts for the steam reforming of naphthalene as a model compound of tar derived from biomass gasification, Applied Catalysis A: General, 278 (2005) 195-205.
[254] H. Rönkkönen, E. Rikkinen, J. Linnekoski, P. Simell, M. Reinikainen, O. Krause, Effect of gasification gas components on naphthalene decomposition over ZrO2, Catalysis Today, 147 (2009) S230-S236.
[255] N. Alarcón, X. García, M.A. Centeno, P. Ruiz, A. Gordon, New effects during steam gasification of naphthalene: the synergy between CaO and MgO during the catalytic reaction, Applied Catalysis A: General, 267 (2004) 251-265.
[256] F. Ferella, J. Stoehr, I.D. Michelis, A. Hornung, Zirconia and alumina based catalysts for steam reforming of naphthalene, Fuel, 105 (2013) 614-629.
[257] G. Akay, C.A. Jordan, A.H. Mohamed, Syngas cleaning with nano-structured micro-porous ion exchange polymers in biomass gasification using a novel downdraft gasifier, Journal of Energy Chemistry, 22 (2013) 426-435.
[258] C.P.B. Quitete, R.C.P. Bittencourt, M.M.V.M. Souza, Coking resistance evaluation of tar removal catalysts, Catalysis Communications, 71 (2015) 79-83.
[259] S. Teir, S. Eloneva, R. Zevenhoven, Production of precipitated calcium carbonate from calcium silicates and carbon dioxide, Energy Conversion and Management, 46 (2005) 2954-2979.
[260] H. Gupta, L.-S. Fan, Carbonation−Calcination Cycle Using High Reactivity Calcium Oxide for Carbon Dioxide Separation from Flue Gas, Industrial & Engineering Chemistry Research, 41 (2002) 4035-4042.
[261] Z. Min, P. Yimsiri, M. Asadullah, S. Zhang, C.-Z. Li, Catalytic reforming of tar during gasification. Part II. Char as a catalyst or as a catalyst support for tar reforming, Fuel, 90 (2011) 2545-2552.
[262] S. Hosokai, K. Kumabe, M. Ohshita, K. Norinaga, C. Li, J. Hayashi, Mechanism of decomposition of aromatics over charcoal and necessary condition for maintaining its activity, Fuel, 87 (2008) 2914-2922.
[263] S. Mani, J.R. Kastner, A. Juneja, Catalytic decomposition of toluene using a biomass derived catalyst, Fuel Processing Technology, 114 (2013) 118-125.
[264] L. Burhenne, T. Aicher, Benzene removal over a fixed bed of wood char: The effect of pyrolysis temperature and activation with CO2 on the char reactivity, Fuel Processing Technology, 127 (2014) 140-148.

[265] S. Zhang, M. Asadullah, L. Dong, H.-L. Tay, C.-Z. Li, An advanced biomass gasification technology with integrated catalytic hot gas cleaning. Part II: Tar reforming using char as a catalyst or as a catalyst support, Fuel, 112 (2013) 646-653.
[266] D. Fuentes-Cano, A. Gómez-Barea, S. Nilsson, P. Ollero, Decomposition kinetics of model tar compounds over chars with different internal structure to model hot tar removal in biomass gasification, Chemical Engineering Journal, 228 (2013) 1223-1233.
[267] D. Wang, W. Yuan, W. Ji, Char and char-supported nickel catalysts for secondary syngas cleanup and conditioning, Applied Energy, 88 (2011) 1656-1663.
[268] X. Nitsch, J.-M. Commandré, J. Valette, G. Volle, E. Martin, Conversion of Phenol-Based Tars over Biomass Char under H2and H2O Atmospheres, Energy & Fuels, 28 (2014) 6936-6940.
[269] Y.-l. Zhang, Y.-h. Luo, W.-g. Wu, S.-h. Zhao, Y.-f. Long, Heterogeneous Cracking Reaction of Tar over Biomass Char, Using Naphthalene as Model Biomass Tar, Energy & Fuels, 28 (2014) 3129-3137.
[270] Y.-l. Zhang, W.-g. Wu, S.-h. Zhao, Y.-f. Long, Y.-h. Luo, Experimental study on pyrolysis tar removal over rice straw char and inner pore structure evolution of char, Fuel Processing Technology, 134 (2015) 333-344.
[271] J. Han, X. Wang, J. Yue, S. Gao, G. Xu, Catalytic upgrading of coal pyrolysis tar over char-based catalysts, Fuel Processing Technology, 122 (2014) 98-106.
[272] S.C. Peterson, M.A. Jackson, S. Kim, D.E. Palmquist, Increasing biochar surface area: Optimization of ball milling parameters, Powder Technology, 228 (2012) 115-120.
[273] Z. Min, S. Zhang, P. Yimsiri, Y. Wang, M. Asadullah, C.-Z. Li, Catalytic reforming of tar during gasification. Part IV. Changes in the structure of char in the char-supported iron catalyst during reforming, Fuel, 106 (2013) 858-863.
[274] C. Sheng, Char structure characterised by Raman spectroscopy and its correlations with combustion reactivity, Fuel, 86 (2007) 2316-2324.
[275] Z. Kong, S.B. Liaw, X. Gao, Y. Yu, H. Wu, Leaching characteristics of inherent inorganic nutrients in biochars from the slow and fast pyrolysis of mallee biomass, Fuel, 128 (2014) 433-441.
[276] Y.-S. Ho, Second-order kinetic model for the sorption of cadmium onto tree fern: A comparison of linear and non-linear methods, Water Research, 40 (2006) 119-125.
[277] Y.-S. Ho, Removal of copper ions from aqueous solution by tree fern, Water Research, 37 (2003) 2323-2330.
[278] Y.-S. Ho, H.A. Harouna-Oumarou, H. Fauduet, C. Porte, Kinetics and model building of leaching of water-soluble compounds of Tilia sapwood, Separation and Purification Technology, 45 (2005) 169-173.
[279] G.E. Rayment, D.J. Lyons, Soil chemical methods : Australasia Collingwood, Vic. : CSIRO Pub., Collingwood, Vic., 2011.
[280] H. Abdullah, D. Mourant, C.-Z. Li, H. Wu, Bioslurry as a Fuel. 3. Fuel and Rheological Properties of Bioslurry Prepared from the Bio-oil and Biochar of Mallee Biomass Fast Pyrolysis, Energy & Fuels, 24 (2010) 5669-5676.
[281] Economic Indicators, Chemical Engineering, 124 (2017) 104.
[282] D.W. Green, R.H. Perry, Perry's Chemical Engineers' Handbook, 8th ed. / prepared by a staff of specialists under the editorial direction of editor-in-chief, Don W. Green, and late editor, Robert H. Perry.. ed., New York : McGraw-Hill, New York, 2000.

[283] M.M. Wright, R.C. Brown, A.A. Boateng, Distributed processing of biomass to bio-oil for subsequent production of Fischer-Tropsch liquids, Biofuels, Bioproducts and Biorefining, 2 (2008) 229-238.
[284] A. Standard, Coal and coke - Chlorine - High-temperature combustion method, in, Standrads Australia, 2003.
[285] Coal and coke - Analysis and testing in: Higher rank coal and coke - Ultimate analysis - Total sulfur - Eschka method, 1997.
[286] S. Brunauer, P.H. Emmett, E. Teller, Adsorption of Gases in Multimolecular Layers, Journal of American Chemical Society, 1799 (1938) 309-319.
[287] D. Burevski, The application of the Dubinin-Astakhov equation to the characterization of microporous carbons, Colloid and Polymer Science, 260 (1982) 623-627.
[288] H. Zhao, D.J. Draelants, G.V. Baron, Performance of a Nickel-Activated Candle Filter for Naphthalene Cracking, Industrial & Engineering Chemistry Research, 39 (2000) 3195-3201.
[289] H. Liu, T. Chen, D. Chang, D. Chen, H. He, P. Yuan, J. Xie, R.L. Frost, Characterization and catalytic performance of Fe3Ni8/palygorskite for catalytic cracking of benzene, Applied Clay Science, 74 (2013) 135-140.
[290] G. Duman, T. Watanabe, M.A. Uddin, J. Yanik, Steam gasification of safflower seed cake and catalytic tar decomposition over ceria modified iron oxide catalysts, Fuel Processing Technology, 126 (2014) 276-283.
[291] P.N. Bhandari, A. Kumar, D.D. Bellmer, R.L. Huhnke, Synthesis and evaluation of biochar-derived catalysts for removal of toluene (model tar) from biomass-generated producer gas, Renewable Energy, 66 (2014) 346-353.
[292] J. Yu, F.-J. Tian, M.C. Chow, L.J. McKenzie, C.-Z. Li, Effect of iron on the gasification of Victorian brown coal with steam:enhancement of hydrogen production, Fuel, 85 (2006) 127-133.
[293] N. Abdoulmoumine, S. Adhikari, A. Kulkarni, S. Chattanathan, A review on biomass gasification syngas cleanup, Applied Energy, 155 (2015) 294-307.
[294] K. Mimura, T. Madono, S. Toyama, K. Sugitani, R. Sugisaki, S.-i. Iwamatsu, S. Murata, Shock-induced pyrolysis of naphthalene and related polycyclic aromatic hydrocarbons (anthracene, pyrene, and fluoranthene) at pressures of 12–33.7GPa, Journal of Analytical and Applied Pyrolysis, 72 (2004) 273-278.
[295] T.A. Milne, R.J. Evans, N. Abatzoglou, Biomass Gasifier Tars: Their Nature, Formation and Conversion, in, National Renewable Energy Laboratory, 1998.
[296] L. Devi, K. Ptasinski, F. Janssen, A review of the primary measures for tar elimination in biomass gasification processes, Biomass and Bioenergy, 24 (2003) 125-140.
[297] Y. Zhang, S. Kajitani, M. Ashizawa, Y. Oki, Tar destruction and coke formation during rapid pyrolysis and gasification of biomass in a drop-tube furnace, Fuel, 89 (2010) 302-309.
[298] D.C. Elliott, E.G. Baker, The Effect of Catalysis on Wodd-Gasification Tar Composition, Biomass, 9 (1986) 195-203.
[299] J. Han, H. Kim, The reduction and control technology of tar during biomass gasification/pyrolysis: An overview, Renewable and Sustainable Energy Reviews, 12 (2008) 397-416.
[300] L. Devi, K.J. Ptasinski, F.J.J.G. Janssen, Decomposition of Naphthalene as a Biomass Tar over Pretreated Olivine: Effect of Gas Composition, Kinetic Approach, and Reaction Scheme, Ind. Eng. Chem. Res., 44 (2005) 9096-9104.

[301] T. Furusawa, Y. Miura, Y. Kori, M. Sato, N. Suzuki, The cycle usage test of Ni/MgO catalyst for the steam reforming of naphthalene/benzene as model tar compounds of biomass gasification, Catalysis Communications, 10 (2009) 552-556.
[302] Z. Abu El-Rub, G. Brem, E.A. Bramer, Single char particle model for naphthalene reduction in a biomass gasification system, Biomass and Bioenergy, 72 (2015) 19-27.
[303] Y. Tamai, H. Watanabe, A. Tomita, Catalytic Gasification of Carbon with Steam, Carbon Dioxide and Hydrogen, Carbon, 15 (1977) 103-106.
[304] B. Liang, J. Lehmann, D. Solomon, J. Kinyangi, J. Grossman, B. O'Neill, J.O. Skjemstad, J. Thies, F.J. Luizao, J. Petersen, E.G. Neves, Black Carbon Increases Cation Exchange Capacity in Soils, Soil Scr. Soc. Am. Journal, 70 (2006) 1719-1730.
[305] D. Sutton, B. Kelleher, J. Ross, Review of literature on catalysts for biomass catalysts, Fuel Processing Technology, 73 (2001) 155-173.
[306] S. Liu, Y. Wang, R. Wu, X. Zeng, S. Gao, G. Xu, Fundamentals of Catalytic Tar Removal overin Situandex SituChars in Two-Stage Gasification of Coal, Energy & Fuels, 28 (2014) 58-66.
[307] N. Couto, A. Rouboa, V. Silva, E. Monteiro, K. Bouziane, Influence of the Biomass Gasification Processes on the Final Composition of Syngas, Energy Procedia, 36 (2013) 596-606.
[308] L. Emami Taba, M.F. Irfan, W.A.M. Wan Daud, M.H. Chakrabarti, The effect of temperature on various parameters in coal, biomass and CO-gasification: A review, Renewable and Sustainable Energy Reviews, 16 (2012) 5584-5596.
[309] J. Lehmann, Biochar for Environmental Management : Science and Technology, Hoboken : Taylor and Francis, Hoboken, 2012.
[310] Y. Shen, J. Wang, X. Ge, M. Chen, By-products recycling for syngas cleanup in biomass pyrolysis: An overview, Renewable & sustainable energy reviews., 59 (2016) 1246-1268.
[311] M.M. Wright, J.A. Satrio, R.C. Brown, D.E. Daugaard, D.D. Hsu, Techno-Economic Analysis of Biomass Fast Pyrolysis to Transportation Fuels, in, National Renewable Energy Laboratory, 2010.
[312] M.M. Wright, D.E. Daugaard, J.A. Satrio, R.C. Brown, Techno-economic analysis of biomass fast pyrolysis to transportation fuels, Fuel, 89 (2010) S2-S10.
[313] Carbon Credits (Carbon Farming Initiative) Act 2011, in: A. Government (Ed.), 2017.
[314] M. Jahirul, M. Rasul, A. Chowdhury, N. Ashwath, Biofuels Production through Biomass Pyrolysis —A Technological Review, Energies, 5 (2012) 4952.
[315] W. Department of the Environment, Heritage and the Arts, Energy Use in the Australian Residential Sector 1986-2020, in: C.o. Australia (Ed.), 2008.
[316] M.S. Peters, Plant design and economics for chemical engineers, 5th ed. / Max S. Peters, Klaus D. Timmerhaus, Ronald E. West.. ed., New York : McGraw-Hill, New York, 2003.
[317] Synergy, Synergy Home Plan (A1) tariff, in, https://www.synergy.net.au/Your-home/Energy-plans/Home-Plan-A1, 2017.
[318] Synergy, Important information about changes to electricity rates, in, https://www.synergy.net.au/Global/ARP17-Price-changes, 2017.
[319] The Facts of Electricity Prices, in: D.o. Industry (Ed.), Australian Bureau of Statistics, 2016.
[320] L. Parisot, Retail electricity price history and projected trends, in, Jacobs, 2017.

[321] K. Ravindra, A.K. Mittal, R. Van Drieken, Health Risk Assessment of Urban Suspended Particulate Matter with Special Reference to Polycyclic Aromatic Hydrocarbons: A Review, Review on Environmental Health, 16 (2001) 169-189.
[322] B.A. Mohamed, N. Ellis, C.S. Kim, X. Bi, A.E.-r. Emam, Engineered biochar from microwave-assisted catalytic pyrolysis of switchgrass for increasing water-holding capacity and fertility of sandy soil, Science of The Total Environment, 566 (2016) 387-397.
[323] D.A. Laird, P. Fleming, D.D. Davis, R. Horton, B. Wang, D.L. Karlen, Impact of biochar amendments on the quality of a typical Midwestern agricultural soil, Geoderma, 158 (2010) 443-449.
[324] W. Song, M. Guo, Quality variations of poultry litter biochar generated at different pyrolysis temperatures, Journal of Analytical and Applied Pyrolysis, 94 (2012) 138-145.
[325] S. Abel, A. Peters, S. Trinks, H. Schonsky, M. Facklam, G. Wessolek, Impact of biochar and hydrochar addition on water retention and water repellency of sandy soil, Geoderma, 202 (2013) 183-191.
[326] O.-Y. Yu, B. Raichle, S. Sink, Impact of biochar on the water holding capacity of loamy sandy soil, International Journal of Energy and Environmental Engineering, (2013).
[327] J.M. Novak, I. Lima, B. Xing, J.W. Gaskin, C. Steiner, K.C. Das, M. Ahmedna, D. Rehrah, D.W. Watts, W.J. Busscher, H. Schomberg, CHARACTERIZATION OF DESIGNER BIOCHAR PRODUCED AT DIFFERENT TEMPERATURES AND THEIR EFFECTS ON A LOAMY SAND, Annals of Environmental Science, 3 (2009).
[328] G. Fellet, L. Marchiol, G. Delle Vedove, A. Peressotti, Application of biochar on mine tailings: Effects and perspectives for land reclamation, Chemosphere, 83 (2011) 1262-1267.
[329] Z. Tan, C.S.K. Lin, X. Ji, T.J. Rainey, Returning biochar to fields: A review, Applied Soil Ecology, 116 (2017) 1-11.
[330] M. Gray, M.G. Johnson, M.I. Dragila, M. Kleber, Water uptake in biochars: The roles of porosity and hydrophobicity, Biomass and Bioenergy, 61 (2014) 196-205.